

20  
21  
22  
23  
24  
25  
26  
27  
28  
29  
30  
31  
32  
33  
34  
35  
36  
37  
38  
39  
40  
41  
42  
43  
44  
45  
46  
47  
48  
49  
50  
51  
52  
53  
54  
55  
56  
57  
58  
59  
60  
61  
62  
63  
64  
65  
66  
67  
68  
69  
70  
71  
72  
73  
74  
75  
76  
77  
78  
79  
80  
81  
82  
83  
84  
85  
86  
87  
88  
89  
90  
91  
92  
93  
94  
95  
96  
97  
98  
99  
100

**SPACE  
DIVISION**

**NASA CR-130178**

72SD4262  
28 NOVEMBER 1972

**ERTS 1 FLIGHT EVALUATION REPORT  
23 JULY TO 23 OCTOBER 1972**

(NASA-CR-130178) ERTS 1 FLIGHT  
EVALUATION Quarterly Report, 23 Jul. -  
23 Oct. 1972 (General Electric Co.)  
232 p HC \$13.75

N73-20435

CSCL 22C

Unclass

G3/13 66836

Prepared for  
**NATIONAL AERONAUTICS AND SPACE ADMINISTRATION**  
Goddard Space Flight Center  
Greenbelt, Maryland 20771



**GENERAL  ELECTRIC**

Contract NAS 5 21808

72SD4262  
28 NOVEMBER 1972

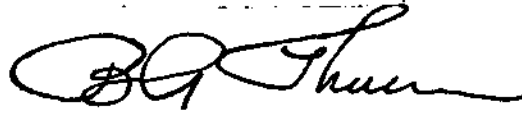
# ERTS 1 FLIGHT EVALUATION REPORT

## 23 JULY TO 23 OCTOBER 1972

Prepared for  
**NATIONAL AERONAUTICS AND SPACE ADMINISTRATION**  
Goddard Space Flight Center  
Greenbelt, Maryland 20771

Contract NAS 5 21808

Approved:



B. Phucas



Prepared by  
**SPACE DIVISION**  
Valley Forge Space Center  
P. O. Box 8555 • Philadelphia, Penna. 19101

**GENERAL**  **ELECTRIC**

PRECEDING PAGE BLANK NOT FILMED

TABLE OF CONTENTS

<u>Section</u>		<u>Page</u>
	INTRODUCTION . . . . .	
2	ORBITAL PARAMETERS . . . . .	2-1
3	POWER SUBSYSTEM . . . . .	3-1
4	ATTITUDE CONTROL SUBSYSTEM . . . . .	4-1
5	COMMAND/CLOCK SUBSYSTEM . . . . .	5-1
6	TELEMETRY SUBSYSTEM . . . . .	6-1
7	ORBIT ADJUST SUBSYSTEM . . . . .	7-1
8	MAGNETIC MOMENT COMPENSATING ASSEMBLY (MMCA) . . . . .	8-1
9	UNIFIED "S" BAND/PREMODULATION PROCESSOR . . . . .	9-1
10	ELECTRICAL INTERFACE SUBSYSTEM . . . . .	10-1
11	THERMAL CONTROL SUBSYSTEM . . . . .	11-1
12	NARROWBAND TAPE RECORDER (NBTR) . . . . .	12-1
13	WIDEBAND TELEMETRY SUBSYSTEM . . . . .	13-1
14	ATTITUDE MEASUREMENT SENSOR (AMS) . . . . .	14-1
15	WIDEBAND VIDEO TAPE RECORDERS (WBVTR) . . . . .	15-1
16	RETURN BEAM VIDICON SUBSYSTEM (RBV) . . . . .	16-1
17	MULTISPECTRAL SCANNER SUBSYSTEM (MSS) . . . . .	17-1
18	DATA COLLECTION SYSTEM (DCS) . . . . .	18-1
	APPENDIX A ERTS-1 ISSUED DOCUMENTS . . . . .	A-1
	APPENDIX B ERTS-1 ANOMALY LIST/REPORTS . . . . .	B-1
	APPENDIX C IMAGE ASSESSMENT REPORTS . . . . .	C-1
	APPENDIX D ERTS-1 GROUND TRACE REPEAT CYCLE PREDICTIONS TABLE . . . . .	D-1

## LIST OF ILLUSTRATIONS

<u>Figure</u>		<u>Page</u>
2-1	Typical Subsatellite Plot of the ERTS-1 Spacecraft . . . . .	2-2
3-1	I <sub>A</sub> Degradation vs Days . . . . .	3-2
3-2	I <sub>A</sub> Degradation vs Days . . . . .	3-3
3-3	I <sub>A</sub> and I <sub>A</sub> Degradation vs Orbits . . . . .	3-3
3-4	I <sub>A</sub> (Midday Degradation vs Days . . . . .	3-4
3-5	I <sub>A</sub> (Midday) Degradation vs Orbits . . . . .	3-5
3-6	Predicted High Noon Solar Array Current . . . . .	3-6
3-7	Actual and Predicted $\beta$ and Paddle Sun Angles. . . . .	3-7
3-8	Seasonal Solar Intensity Variation. . . . .	3-8
4-1	Separation and Acquisition, Attitude Control System . . . . .	4-3
4-2	Typical Orbit, Attitude Control System . . . . .	4-5
4-3	Cumulative Gate History - ERTS-1 . . . . .	4-7
4-4	ACS Gate Distribution to First MMCA Correction (Orbit 0-73) . . . . .	4-8
4-5	ACS Gate Distribution to Second MMCA Correction (Orbit 74-85) . . . . .	4-8
4-6	ACS Gate Distribution to Third MMCA Correction (Orbit 86-110) . . . . .	4-9
4-7	ACS Gate Distribution to Fourth MMCA Correction (Orbit 111-220) . . . . .	4-9
4-8	ACS Gate Distribution to after MMCA Corrections (Orbit 221-1300) . . . . .	4-10
5-1	Clock Drift Summary . . . . .	5-1
5-2	Command/Clock System . . . . .	5-5
7-1	Orbit Adjust Subsystem Performance Characteristics . . . . .	7-3
7-2	Orbit Adjust Subsystem Performance Characteristics . . . . .	7-5
7-3	Orbit Adjust Subsystem Performance Characteristics . . . . .	7-7
7-4	Orbit Adjust Subsystem Performance Characteristics . . . . .	7-11
9-1	USB Calibration Curves (Original and Revised) . . . . .	9-4
9-2	USB Power Output (Corrected) . . . . .	9-4
9-3	USB Performance Characteristics . . . . .	9-5
9-4	Maximum AGC Values for Use Power Output vs Distance . . . . .	9-7
11-1	Left Solar Paddle Temperature (Function 6044) . . . . .	11-3
11-2	Right Solar Paddle Temperature (Function 6040) . . . . .	11-4
11-3	Location of Solar Array Temperature Sensors . . . . .	11-5
13-1	WPA-2 Helix Current (MA) (Function 12102) . . . . .	13-2
13-2	Ground Station (ULA) AGC Readings for WPA-2 . . . . .	13-4
13-3	Ground Station (ULA) AGC Reports . . . . .	13-5



## LIST OF ILLUSTRATIONS (Cont)

<u>Figure</u>		<u>Page</u>
14-1	Attitude Measurement Sensor Performance Characteristics . . . . .	14-3
15-1	Last RBV Triplet Exposed in Orbit 148. . . . .	15-6
15-2	Last RBV Triplet Exposed in Orbit 148. . . . .	15-7
15-3	Last RBV Triplet Exposed in Orbit 148. . . . .	15-8
15-4	Strip Chart for Orbit 149 WBVTR 2 Anomaly . . . . .	15-9
15-5	Average Values of MSS Minor Frame Sync Errors (MFSF) over 10 Second Intervals for Randomly Selected Orbits. . . . .	15-13
15-6	Strip Chart for WBVTR-1 Orbit 913 . . . . .	15-15
17-1	MSS Calibration Wedge . . . . .	17-4
17-2	MSS Orbital Sensors Response . . . . .	17-5
17-3	MSS Signal Path . . . . .	17-13
18-1	DCS Non-Redundant Message Frequency . . . . .	18-11

## LIST OF TABLES

<u>Table</u>		<u>Page</u>
2-1	Orbital Parameters . . . . .	2-1
3-1	Major Power Subsystems Parameters . . . . .	3-11
3-2	Power Subsystem Analog Telemetry . . . . .	3-13
4-1	Impulse Usage ERTS-1 . . . . .	4-11
4-2	ACS Temperature and Pressure Telemetry Summary . . . . .	4-12
5-1	Command/Clock Telemetry Summary . . . . .	5-3
6-1	TLM Telemetry Summary . . . . .	6-2
7-1	OAS Telemetry Values . . . . .	7-9
7-2	Orbit Adjust Performance . . . . .	7-9
8-1	MMCA Telemetry Before and After Adjustment . . . . .	8-2
8-2	MMCA Telemetry Summary . . . . .	8-2
9-1	USB/PMP Telemetry Values . . . . .	9-1
9-2	USB Transmitter A Power Output Function 11002 . . . . .	9-3
10-1	APU Telemetry Functions . . . . .	10-1
11-1	Thermal Subsystem Analog Telemetry . . . . .	11-2
11-2	Compensation Load History . . . . .	11-6
12-1	Narrowband Tape Recorder Telemetry Values . . . . .	12-2
13-1	Wideband Modulator Telemetry Values . . . . .	13-3
14-1	AMS Temperature Telemetry Summary . . . . .	14-1
15-1	WBVTR Telemetry Values . . . . .	15-4
15-2	Function Values by Mode in Orbit 913 . . . . .	15-5
16-1	RBV Telemetry Values . . . . .	16-2
17-1	MSS Telemetry Values . . . . .	17-2
17-2	Sampled Tabulation of Line Length Code (LLC) . . . . .	17-3
17-3	MSS, T/V vs. Orbit 548 Calibration Wedge Comparison . . . . .	17-11
17-4	MSS, T/V vs. Orbital Sensor Response Comparison . . . . .	17-12
17-5	Sun Calibration Measurements . . . . .	17-15

# LIST OF TABLES (Cont)

<u>Table</u>		<u>Page</u>
17-6	MSS Sun Calibration Data . . . . .	17-17
17-7	MSS Sun Calibration Orbits . . . . .	17-18
18-1	DCS Telemetry Values . . . . .	18-1
18-2	DCS Data Mailing Addresses . . . . .	18-3
18-3	153 Platforms, 27 Users 10/24/72 . . . . .	18-9
18-4	DCP Locations . . . . .	18-10
18-5	DCS Range . . . . .	18-12
18-6	Reception Probability . . . . .	18-13
18-7	DCS Data-Quality and Quantity . . . . .	18-15
18-8	DCS Interference . . . . .	18-16
18-9	Performance of Geog-Adjacent DCP's . . . . .	18-17
18-10	Summary Performance . . . . .	18-19

## INTRODUCTION

This is the second in a series of documents issued periodically to present flight performance analysis of the ERTS-1 Spacecraft. The first, ERTS-1 Launch and Flight Activation Evaluation Report dated 18 October 1972 (72SD4255), gives a summary of each subsystem, the spacecraft configuration, a table of command matrix, telemetry matrix and the launch configuration.

This report contains analyses of performance for the first three months of operation, i.e., orbits 0 to 1300.

Future ERTS-1 reports are scheduled on a quarterly basis.

## SECTION 1

### SUMMARY - ORBITS 0-1300

The ERTS-1 spacecraft was launched from the Western Test Range on 23 July, 1972 at 18:06:06.508Z. The launch and orbital injection phase of the space flight were nominal and deployment of the spacecraft followed predictions. Orbital operations of the spacecraft and payload subsystems were satisfactory through orbit 147 after which a power transient disabled one of the Wideband Video Tape Recorders. Operations resumed until orbit 196 when the Return Beam Vidicon failed to respond when commanded off. The RBV was commanded off via alternate commands and since that time ERTS-1 has performed its mission with the Multispectral Scanner and the remaining Wideband Video Tape Recorder providing image data.

### ORBITAL PARAMETERS

The launch and injection of ERTS-1 required some correction at orbit 44 and 59 to achieve the desired 18 day repeat cycle. These corrections were made as noted in Section 7. During orbit 938 it was necessary to execute another 13 second burn of the -X thruster to maintain the ground trace in the desired 18 day repeat pattern of +10 miles.

### POWER SUBSYSTEM (PWR)

Following orbital injection the solar paddles deployed properly and began providing power for the spacecraft and payload subsystems at about 1 percent higher than ground predictions. The solar array output had little or no degradation until the occurrence of three major solar flares between 2 August and 7 August 1972 which degraded the solar array 2.6 percent. Future predictions of the solar array show that sufficient power should be available for normal operation through all of 1973. An electrical failure of the WBVTR-2 (orbit 148, 149) and the RBV power circuit (orbit 196) put heavy current transients on the power system. Performance remained excellent during and after the failures. Battery temperature rose and the temperature spread increased due to increase in sun intensity but performance of each battery remained good.

### ATTITUDE CONTROL SUBSYSTEM (ACS)

From the initial acquisition, the ACS performance has been excellent. All functions are active and well within specifications. Perturbations due to sun glint in the IR horizon scanners are not disruptive enough to necessitate single scanner mode. The magnetic moment compensating assembly corrected the + Roll gating to permit flywheel unloading during darkness when payloads are disabled. There is a tendency for the gating frequency to increase slightly but during this period only 3 percent of the impulse available at launch has been used. The ACS responded well to orbit adjust maneuvers.

### COMMAND/CLOCK SUBSYSTEM

All stored commands have executed and all real time commands except the expected one in approximately 5,000, associated with the logic race in the design. No serious problems have resulted from these few commands failing to execute. A minor anomaly has occurred in Comstor B; cell 12 which on five occasions verified with a delta of 256 seconds added to the desired execute time. Each time, a second try verified correctly. No explanation has yet been found for this condition. During periods the S/C is near the USSR, the VHF Command Receiver AGC telemetry consistently shows strong interrogating signals.

### TELEMETRY SUBSYSTEM

The telemetry subsystem has consistently performed in an excellent manner. All data was very noisy during the orbit 148, 149 power transient but no permanent effects were noted. Memory Section 0,0 has been in use since launch and no alternates have been required. All dropouts have been associated with known link or ground problems.

### ORBIT ADJUST SUBSYSTEM

The orbit adjust subsystem has been fired four times all from the -X thruster. The four second burn gave 60 percent of computed thrust but longer burns gave very near computed thrust. All components functioned as predicted.

### MAGNETIC MOMENT COMPENSATING ASSEMBLY

The Magnetic Moment Compensating Assembly has been operated six times during this period and performance has been reasonably close to nominal. The hysteresis loop associated with the MMCA requires trial and error after the first charge and dump. The attained performance of the unit is considered excellent. It has responded and held the Pole-Cm values commanded.

### UNIFIED 'S' BAND/PREMODULATION PROCESSOR

The Unified S-Band Receiver, Transmitter and Premodulation Processor have all operated satisfactorily throughout this entire reporting period providing telemetry information, ranging signals and relay of the DCS signals on demand without fail. Only the A sections of the transmitter and Receiver have been used, and they have operated continuously since separation for 2245 hours. The transmitter has shown a power decline from 1.58 watts at launch to 1.03 watts, but is still well within safe operating limits.

### ELECTRICAL INTERFACE SUBSYSTEM

The Auxiliary Processing Unit (APU) and Interface Switching Module (ISM) performed normally in this report period. The Power Switching Module (PSM) performed normally except for the RBV power circuit. In orbit 196 a failure of the RBV power circuit within the PSM caused a high momentary transient current on the payload regulator as the RBV relay closed. Subsequently, the RBV power relay would not execute "OFF" commands. This led to shutdown of the RBV throughout the remainder of this report period. An investigation of the failure is being performed.

### THERMAL SUBSYSTEM

The thermal subsystem performed normally throughout this report period. Solar panels have higher and lower temperatures than Nimbus, which currently are unexplained after factoring the differences between the spacecraft. The solar array is performing satisfactorily.

## NARROW BAND TAPE RECORDER

The Narrow Band Tape Recorder Subsystem operated satisfactorily. Each recorder in turn sequenced through its modes of record, standby, playback and off for a total On time of 1171 hours.

## WIDE BAND TELEMETRY SUBSYSTEM

The Wideband Telemetry Subsystem has operated satisfactorily since initial turn-on in orbit 12. WPA-1 has been inactive since orbit 196, when its associated RBV developed input power problems. Up to that time, WPA-1 had operated for 8 hours, 50 minutes and 21 seconds in the 20 watt mode.

WPA-2 after initially operating in the 10-watt mode, was switched to the 20-watt mode in orbit 30, and has accumulated a total flight on time of 99 hours, 3 minutes and 23 seconds.

## ATTITUDE MEASUREMENT SENSOR (AMS)

The AMS continues to function in all respects. Derived values are being used in image processing and effort is continuing to improve correlation relationship between spacecraft attitude, the ACS and the AMS.

## WIDEBAND VIDEO TAPE RECORDERS (WBVTR)

Both WBVTR's operated normally through orbit 147 where a transient attributed to a short in the power lead to ground of the WBVTR coursed through all subsystems of the vehicle disrupting the attitude and telemetry. Exhaustive investigations concluded that the ground noise currents were generated by a short in WBVTR No. 2. (See Appendix B) WBVTR No. 2 had a total on time of 124 hours, 57 minutes and 54 seconds. MSS Video, MSS Bit Error Rate, search track, control track and spacecraft time are nominal.

## RETURN BEAM VIDICON

After a satisfactory test of the RBV in orbit 26, the subsystem was used operationally in 65 percent of the orbits until orbit 196. 1690 scenes were photographed in 91 periods of activity. The total earth surface photographed was 14.7 million square nautical miles. During orbit 196, a short to ground occurred in the primary power on-off switch located in



the Power Switching Module external to the RBV subsystem. The RBV has not since been turned on, but alternate means of RBV power switching are available for later turn On when desired.

#### MULTISPECTRAL SCANNER SUBSYSTEM

The MSS subsystem was activated during orbit 20 and a sun calibration was obtained during orbit 21. The subsystem operated in 73 percent of the orbits imaging over 18,000 scenes covering over 158 million square nautical miles of earth surface without a single malfunction. The only performances below expectation are low sun cal outputs in all bands (especially Band 1) and a decrease in the cal wedge in Bands 1 and 2 with time in orbit. These points are under investigation.

#### DATA COLLECTION SYSTEM

The DCS has operated flawlessly since initial turn-on in orbit 5. 45,261 messages were received in OCC. 95 percent of these were without error. Messages are received at Greenbelt and Goldstone from seven orbits per day. The number of platforms from which messages have been received have steadily increased to a total of 153 with as many as 43 per orbit, without discernible mutual interference. Only Receiver No. 1 has been operated to date. Some of these platforms have not yet entered operational status.

# PAYLOAD OPERATION SUMMARY

Launch through Orbit 1300

SUB SYSTEM	ON-TIME			OPERATIONAL SUMMARY	
	H	M	S		
RBV	13	59	09	Total scenes photographed	1690
				Average scenes per day	139
				Total area photographed square	
				nautical mile	$14.7 \times 10^6$
				On-Off cycles	91
				% Real Time scenes	57
				% Recorded scenes	43
MSS	173	41	49	Total scenes photographed	18,194
				Average scenes per day	199
				Total area photographed square	
				nautical mile	$158.6 \times 10^6$
				On-Off cycles	947
				% Real Time scenes	54
				% Recorded scenes	46
DCS	2237	00	00	Message received at OCC	45,261
				Non perfect message	2,178
				Ground platforms active	153
				Ground platforms active/orbit	43
				Users	27
				Average message per orbit	93
WBVTR-1	127	57	54	% Record Mode	35
				% Playback Mode	44
				% Rewind Mode	19
				Minor Frace Sync Error Count:	
				Real Time	0
				Playback	under 10
WBVTR-2	9	26	33	% USAGE SAME AS WBVTR-1	
				FAILED IN ORBIT 148/9	

---

WPA-1	8 50 21	% Real Time Mode	70
		% Playback Mode	30
		Not used after Orbit 185	

---

WPA-2	99 03 23	% Real Time Mode	66
		% Playback Mode	34

---

## SECTION 2

### ORBITAL PARAMETERS

The ERTS-1 launch and injection was satisfactory and required only a minor orbit adjust to achieve nominal parameters. These adjustments were made in orbit 38, 44 and 59. After three repeat cycles an orbit maintenance burn was made (Orbit 938).

The orbital parameters are given in Table 2-1. Figure 2-1 shows the subsatellite plot and Appendix D gives a table of repeat cycles.

Table 2-1. Orbital Parameters

Element			Planned	25 Oct 1972
(1)	Apogee	KM	917	917.3
(2)	Perigee	KM	917	898.1
(3)	Inclination	deg	99.0919	99.103
(4)	Semimajor Axis	KM	7,294.662	7,285.850
(5)	Eccentricity	--	0.0001	0.00132
(6)	Anomalistic Period	min	103.341	103.152
(7)	Nodal Period	min	--	103.268
(8)	Argument of Perigee	deg	0	93.721
(9)	18 Day Repeat Cycle	NM	<u>+5</u>	+1.25

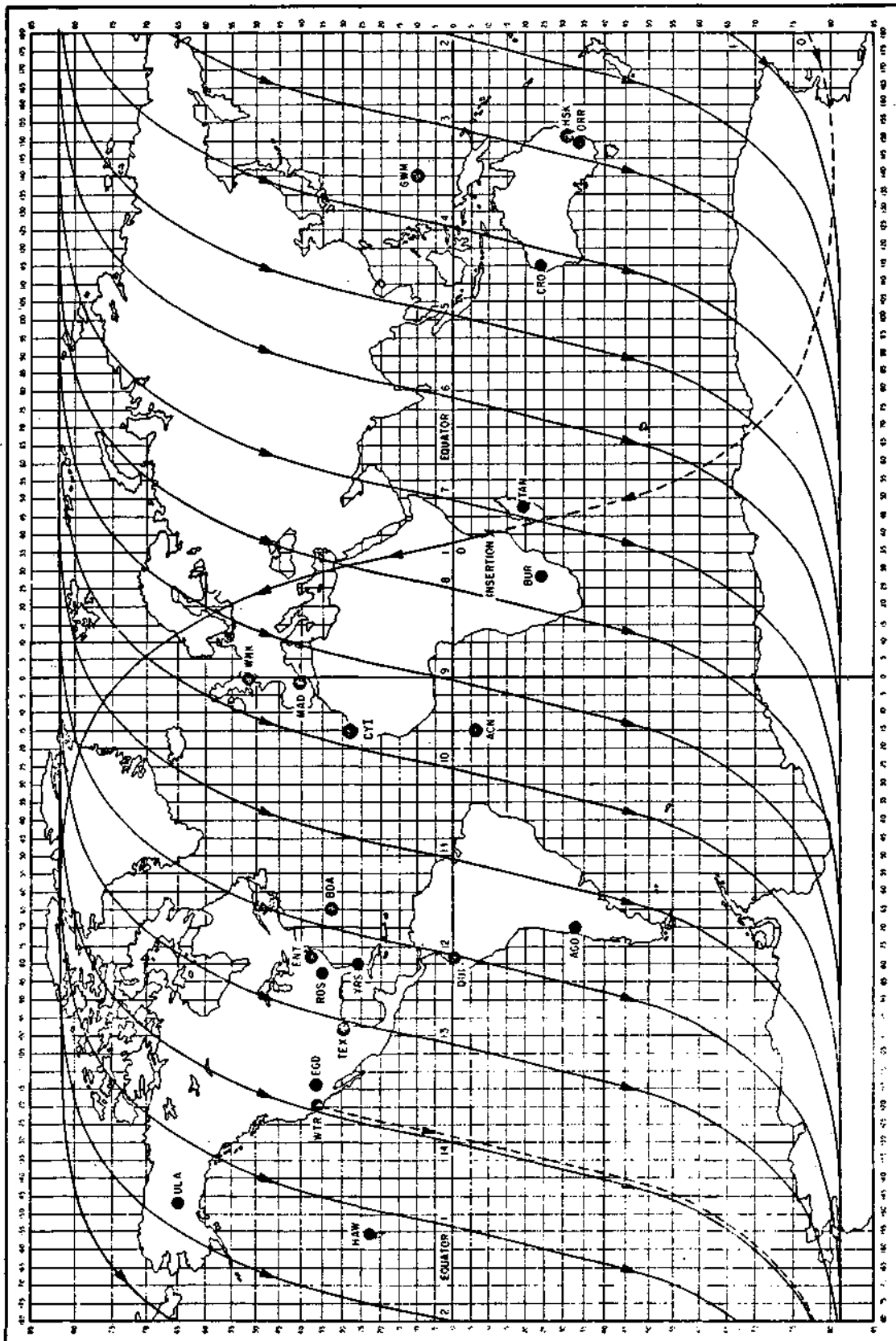


Figure 2-1. Typical Subsatellite Plot of the ERTS-1 Spacecraft

### SECTION 3

#### POWER SUBSYSTEM (PWR)

The power subsystem has performed well throughout this report period. The solar paddles were exposed to solar flare radiation and two electrical failures applied heavy transient loads to the subsystem, but the power subsystem operation remained good. Solar array current has been remaining approximately constant and will continue the present level until late December 1972 when it will decrease due to the combination of sun angle, solar intensity, and solar array degradation. The decreasing solar array output will bottom out in the summer of 1973 and then increase toward the end of 1973. There will be sufficient power generated to meet load requirements through the end of 1973. Batteries are performing well, with depth of discharge averaging about 12-14%. Regulator voltages are stable and are unchanged from initial launch values. Compensation loads are on to help maintain better sensory ring temperature balance. They are using excess solar array power which would otherwise be dissipated in auxiliary loads.

The solar array has provided excess energy for the payload and spacecraft load throughout this report period. Excess power above that required to charge the battery packs and operate the loads was dissipated in auxiliary and compensation loads per ERTS-1 power management procedures. The solar array showed no degradation to the tenth orbital day (August 2, 1972). It suddenly decreased 2.6% in the next four days due to solar flare activity and then began following a normal solar cell radiation degradation curve. This is shown in Figure 3-1. Since the array was not degrading per the normal curve before the solar flare, it is difficult to predict what radiation dosage it received; however, it did receive at least the amount equivalent to 70 days of operation or  $6.4 \times 10^{13}$  DENI's (Damage Equivalent, Normal Incident, 1 Mev Electrons). The solar array degradation is also shown plotted versus semi-log orbits in Figure 3-2 and in a linear orbit plot in Figure 3-3. Figure 3-1, 3-2, and 3-3 plot normalized value of array current adjusted to 35 VDC, 35°C, 1 AU and sun angle normal. This value is keyed to the paddle temperature as it passes through 35°C. At this temperature the spacecraft is in an orbital position where the paddle still receives about 3% estimated albedo contribution. Variation of albedo as well as spacecraft loading cause some scattering of data.

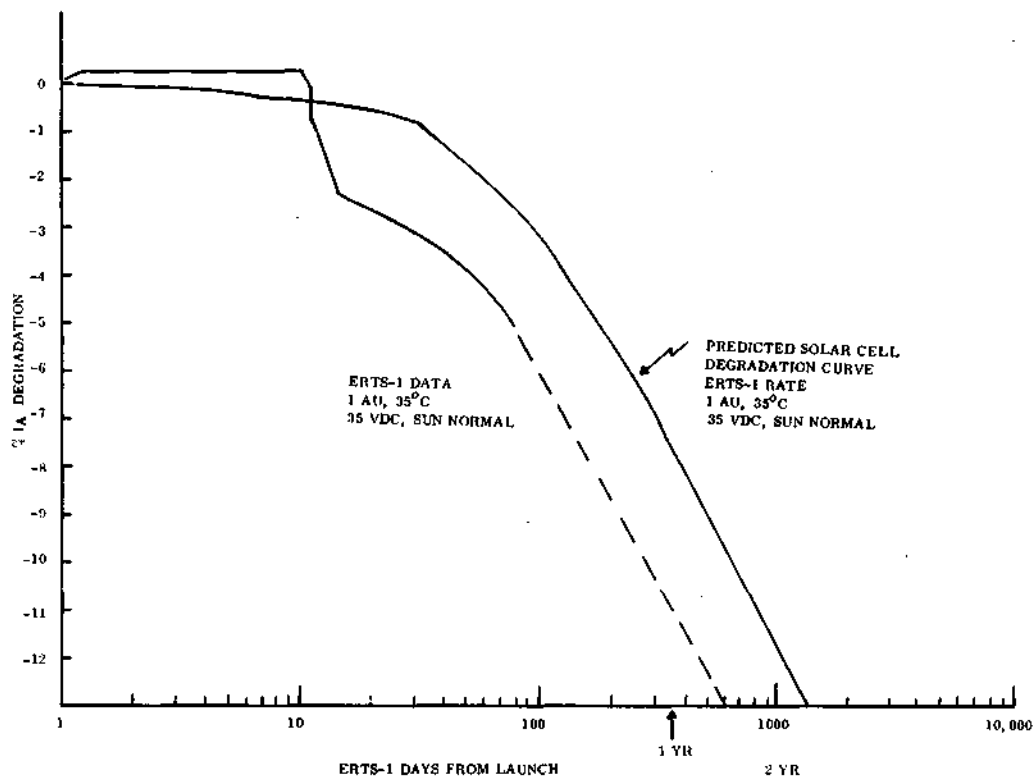


Figure 3-1.  $I_A$  Degradation vs Days

As a cross check, the value of solar array current at high noon (where there is no albedo contribution and the solar array is near temperature stabilization) was adjusted to 1 AU, sun angle normal. No temperature or voltage adjustments were made as these are approximately constant from orbit to orbit.

High noon solar array degradation is plotted versus semi-log days on Figure 3-4, and semi-log orbits on Figure 3-5. It correlates closely to the previous graphs.

Using the previous degradation curves, knowledge of the sun angle to the orbit plane, and knowledge of the seasonal sun intensity, the power output of the solar panels can be projected ahead as shown in Figure 3-6. Seasonal variations of the sun angle to the paddle normal is shown in Figure 3-7. Seasonal variations of the sun intensity is shown in Figure 3-8. It can be observed that as the solar array degraded the sun intensity and paddle sun angle changed so as to compensate for the degradation and keep the solar array output approximately constant. Beginning in late December 1972 this trend is reversed and the paddle sun angle

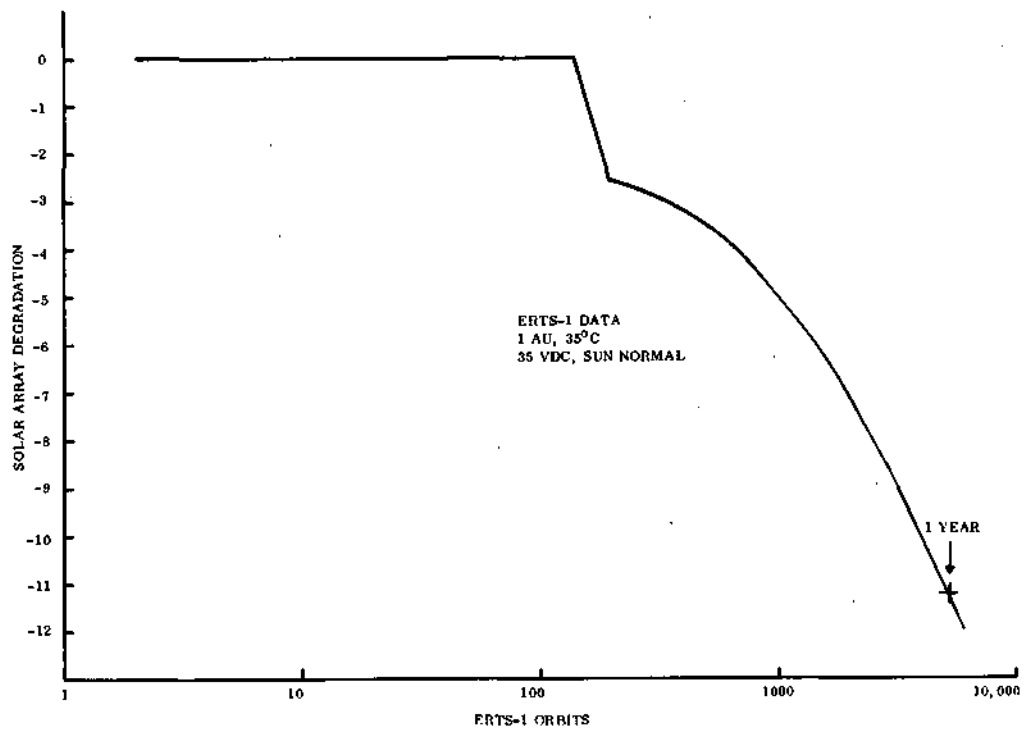


Figure 3-2.  $I_A$  Degradation vs Days

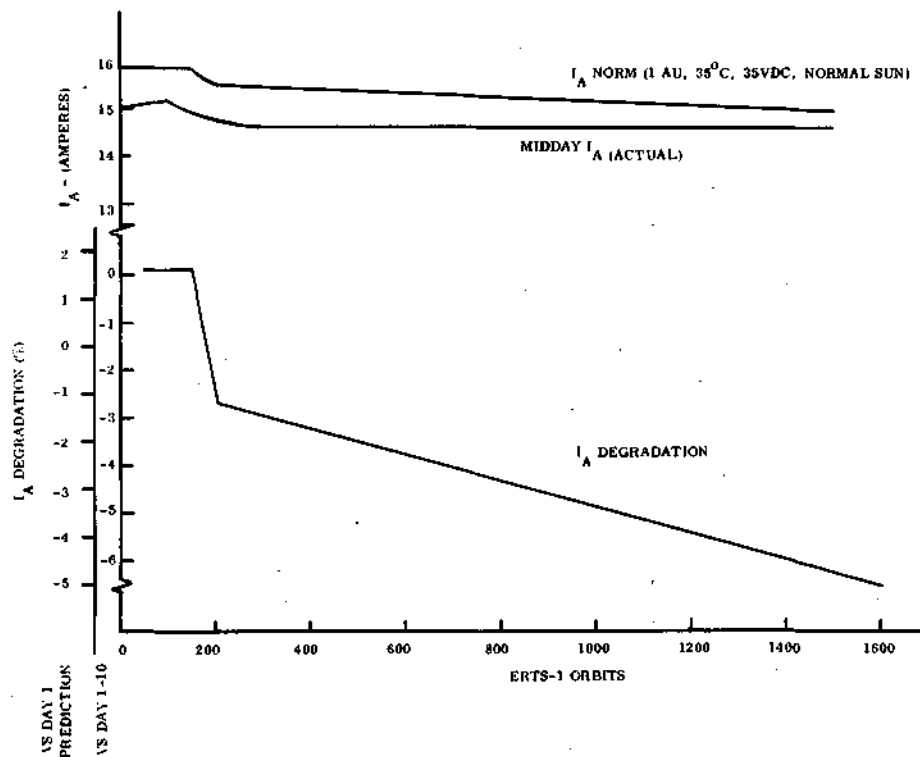


Figure 3-3.  $I_A$  and  $I_A$  Degradation vs Orbits



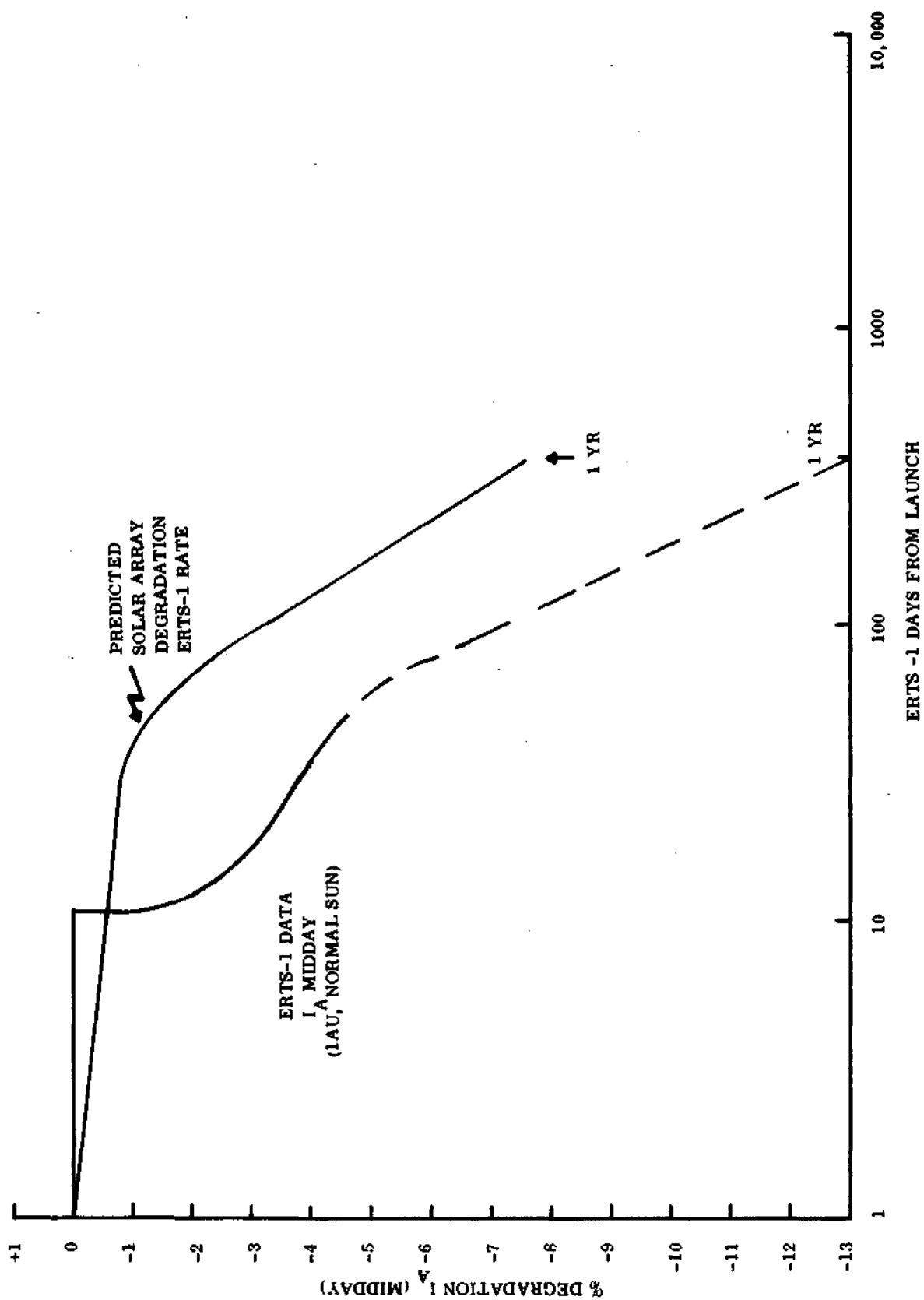


Figure 3-4.  $I_A$  (Midday) Degradation vs Days

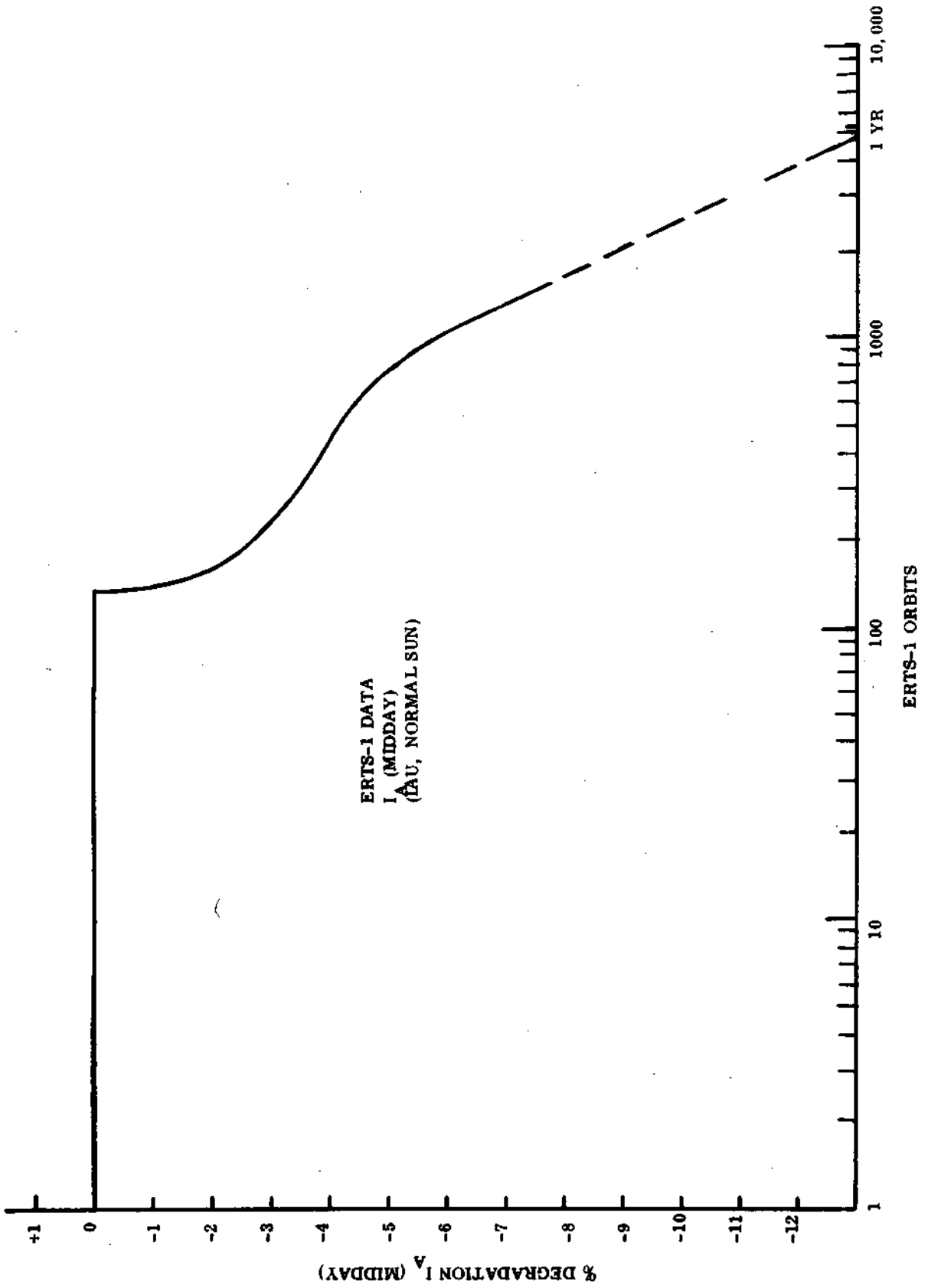


Figure 3-5.  $I_A$  (Midday) Degradation vs Orbits

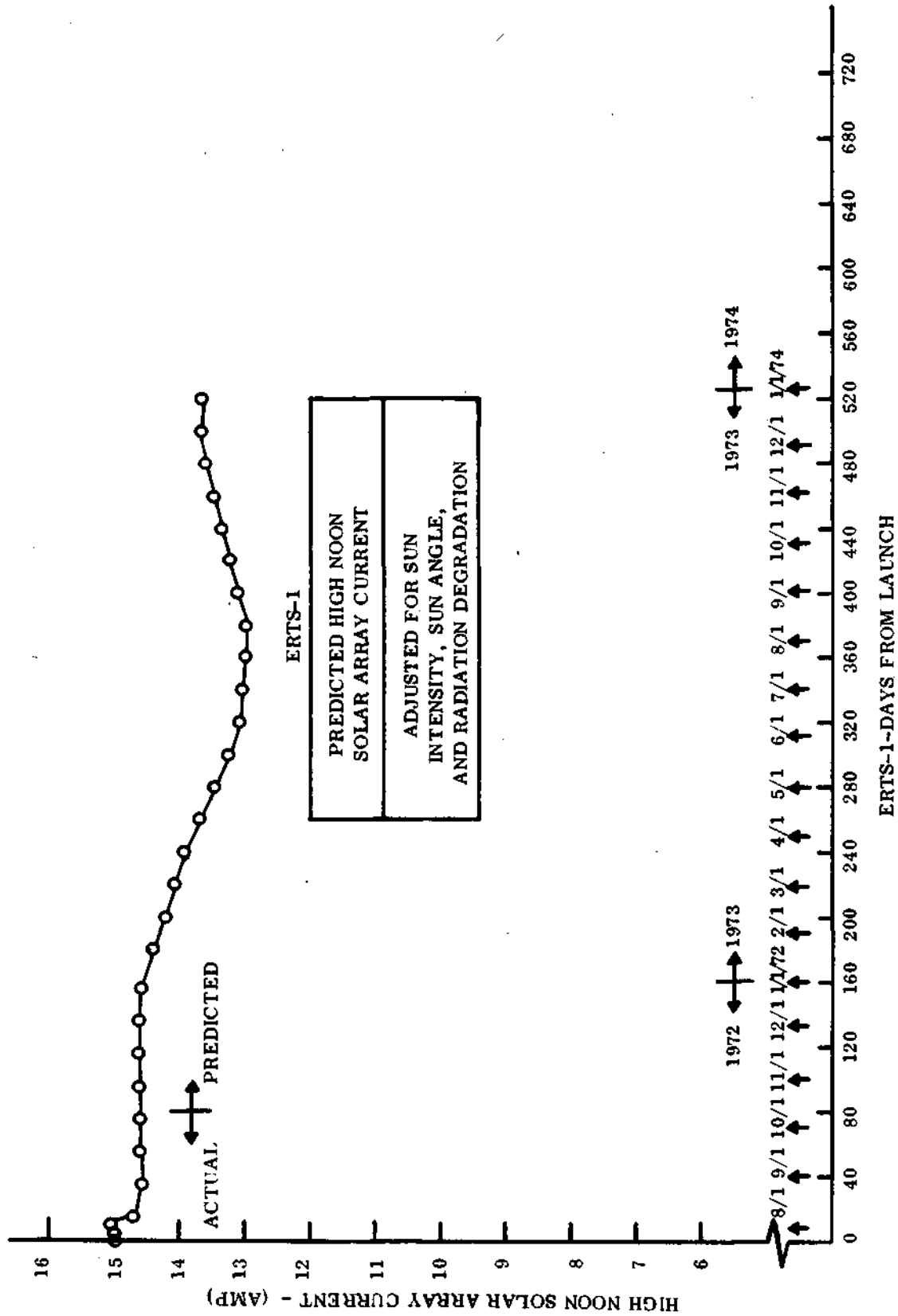


Figure 3-6. Predicted High Noon Solar Array Current

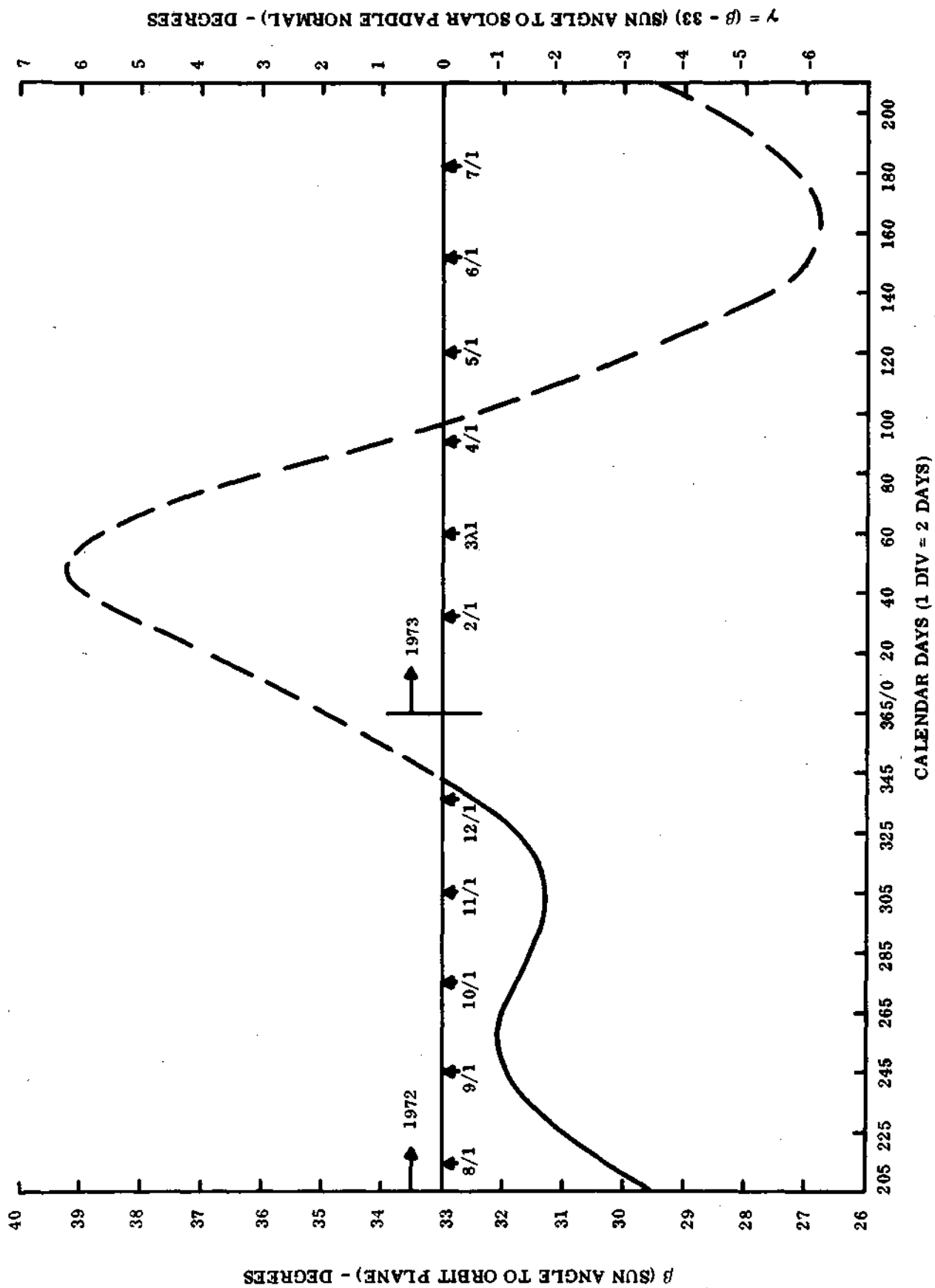


Figure 3-7. Actual and Predicted  $\beta$  and Paddle Sun Angles

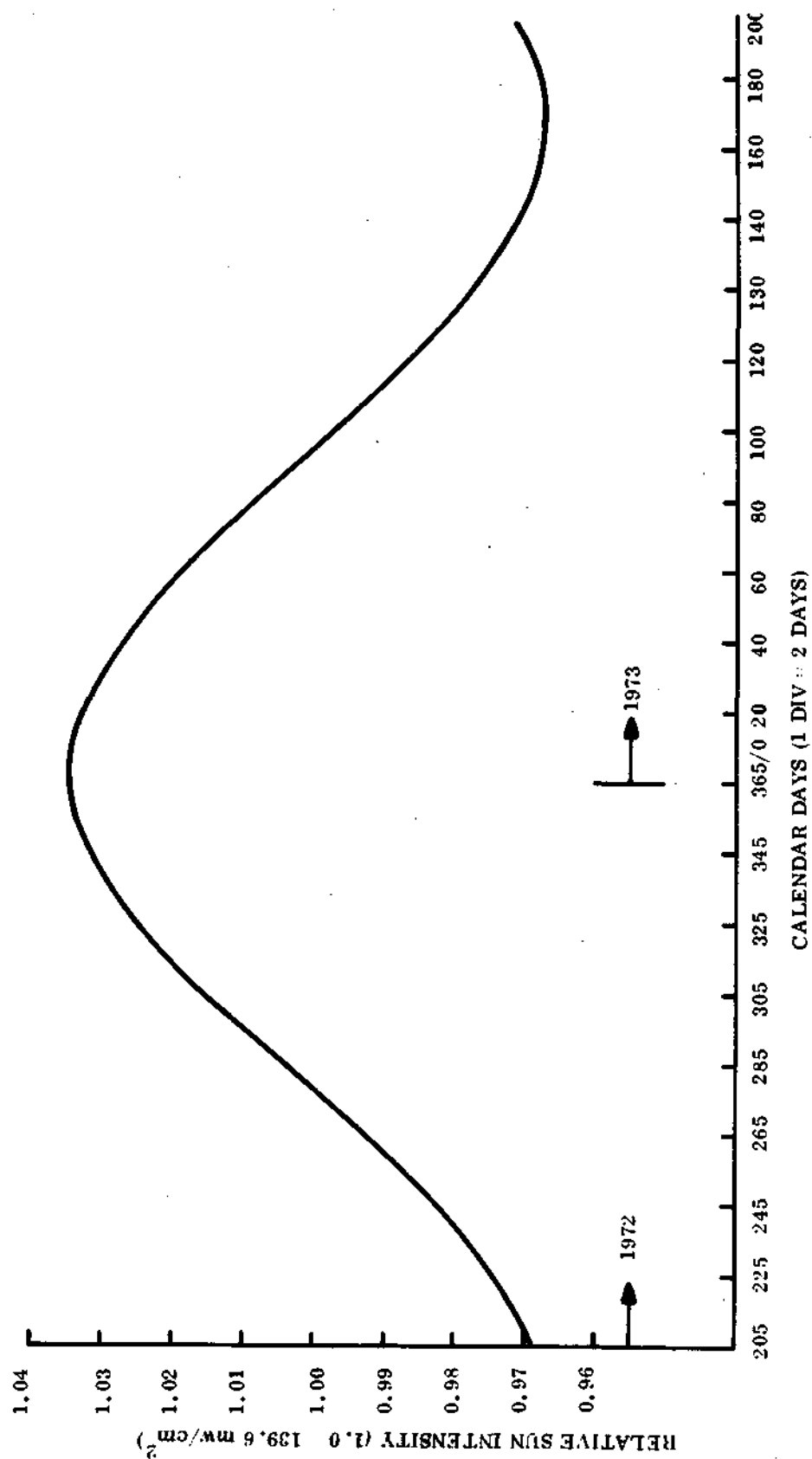


Figure 3-8. Seasonal Solar Intensity Variation

and sun intensity change (major factor) so that the solar array output decreases until mid June when it begins to rise again. The solar array will generate sufficient power to meet load requirements through all of 1973.

On July 18 it was postulated that a flare erupted on the far side of the sun as noted by an increase in charged particle count on 18 July and 22 July. On 2 August, 3 August and 7 August there was intense sun activity in sun spots facing the earth. The shock front of these flares hit the earth approximately  $07:30 \pm 00:15$  on 2 August 1972,  $01:30 \pm 00:30$  on 3 August 1972, and  $15:30 \pm 00:15$  on 7 August 1972. At the time of a solar flare, there is electro-magnetic radiation of X-rays, and Gamma rays, transmitted with the speed of light to the earth, arriving in seconds. Additionally charged particles, i.e., electrons, protons, and alpha particles, are emitted with a wide range of energy levels (or velocities). These arrive at the earth, or 1 AU, approximately one hour later. This shock front or wave distorts the magnetic field in interplanetary space and of earth as it travels. Past flares have given magnetic changes of 500 gamas with the rate of change undefined. Protons and alpha particles cause most of the degradation to the solar cells as their large mass causes damage centers in the silicon which upset the balance of the semi-conductor action at the N/P junction. Dosage of radiation is converted to an equivalent of a single type of radiation particle by various empirically determined factors. The unit is called a DENI or Damage Equivalent Normal Incidence 1 Mev electrons. As reported under the Solar Array section, a flux dosage of approximately  $6.4 \times 10^{13}$  DENI is estimated to have been received during the four-day period in which the solar flares occurred. Though no direct correlation has been made, it is interesting to note that the WBVTR 2 failure occurred on orbit 148 and 149 or 3 August 1972; and the RBV power circuit failure occurred on orbit 196 or 6 August 1972. Both events are in the solar flare activity period.

Auxiliary loads are switched nearly every orbit to maintain proper energy balance in the power subsystem. Power management auxiliary load plans are calculated each day following definition of the days operation activities. Temperature of the batteries and battery voltages have been held quite easily to satisfactory operating limits. The power subsystem has not limited desired spacecraft operation in any way during this report period.

Battery packs have been ranging from 10 to 15 percent depth of discharge over a 24-hour period of normal spacecraft operation. In early orbits battery temperatures were averaging approximately  $21^{\circ}\text{C}$  with a temperature spread of  $3 - 4^{\circ}\text{C}$ . In later orbits increased payload activity and increasing sun intensity caused a rise of the temperature average to approximately  $23.5^{\circ}\text{C}$  with a temperature spread of about  $5^{\circ}\text{C}$ . Charge and load sharing were satisfactory at the higher temperatures spread so no special effort was made to hold the spread any lower. Table 3-1 shows the battery and major power subsystem parameter for typical power management orbits in this report period. Power management orbits are a complete night followed by a complete day.

The power system electronics continued to perform well in this report period. All regulator voltages were stable without drift. During orbits 148 and 149, Wide Band Video Tape Recorder 2 failed. The failure caused erratic telemetry readings so that analyses during the operation of the WBVTR after failure was difficult. After the WBVTR was turned off, normal operation of the power subsystem was observed. In orbit 196 a failure in the RBV power circuit caused a heavy current in payload regulator number 3 before the short cleared. However, there was good operation after the transient. It was necessary to turn off payload regulator number 3 in order to turn off the RBV. When the payload regulator was turned on again, regulator number 4 came on line. It has performed satisfactorily without drift since it began operation in orbit 201. Table 3-2 shows power subsystem telemetry (average over telemetry period recorded on NBTR) for various orbits. Some parameters in Table 3-2 may be slightly different from Table 3-1 because Table 3-1 uses a time span for power management different from the time span used in Figure 3-4, which is the playback period from NBTR.

Table 3-1. Major Power Subsystems Parameters

ORBIT	NO	7	26	500	899	1291
BATT 1	MAX	32.91	32.48	32.99	32.91	32.99
2	CHGE	32.91	32.48	32.99	32.82	32.99
3	VOLTS	32.91	32.48	33.08	32.91	32.99
4		32.91	32.48	33.08	32.91	32.99
5		32.91	32.48	33.08	32.99	32.08
6		32.82	32.31	33.08	32.91	32.99
7		32.82	32.22	33.08	32.91	32.99
8		32.82	32.14	33.08	32.91	32.99
AVERAGE		32.87	32.38	33.06	32.91	33.00
BATT 1	END-	29.32	28.81	29.23	28.21	28.55
2	of-	29.32	28.81	29.32	28.30	28.55
3	NIGHT	29.23	28.81	29.23	28.21	28.55
4	VOLTS	29.32	28.89	29.32	28.30	28.55
5		29.41	28.89	29.32	28.30	28.64
6		29.23	28.81	29.23	28.21	28.55
7		29.32	28.89	29.32	28.30	28.55
8		29.23	28.81	29.23	28.21	28.55
AVERAGE		29.30	28.84	29.28	28.25	28.56
BATT 1	CHGE	13.51	13.11	13.54	13.12	13.29
2	SHARE	12.80	12.93	12.87	13.17	12.95
3	(%)	10.82	11.38	11.10	11.55	11.23
4		12.34	12.39	12.21	12.32	12.29
5		12.36	12.32	12.33	12.25	12.30
6		12.77	12.80	12.66	12.64	12.74
7		13.01	12.62	12.88	12.65	12.83
8		12.39	12.45	12.41	12.31	12.36
BATT 1	LOAD	12.81	12.71	12.67	12.70	12.68
2	SHARE	13.20	12.90	13.47	13.37	13.71
3	(%)	11.38	11.43	11.84	11.87	12.09
4		12.75	12.77	12.95	12.71	12.89
5		12.37	12.54	12.17	12.31	12.32
6		12.59	12.53	12.47	12.45	12.24
7		12.84	12.80	12.50	12.41	12.33
8		12.06	12.32	11.93	12.17	11.74
BATT 1	TEMP	22.15	21.11	24.02	24.19	24.63
2	in	19.27	18.74	20.53	21.92	21.37
3	(°C)	19.14	18.77	19.85	20.49	20.36
4		22.14	21.57	22.88	22.75	23.41
5		22.86	21.82	24.17	24.15	24.67
6		22.38	21.21	24.00	24.15	24.98
7		22.80	21.41	24.76	24.85	25.64
8		22.99	21.82	24.92	25.11	25.67
AVERAGE		21.72	20.81	23.14	23.45	23.84



Table 3-1. Major Power Subsystems Parameters (Cont'd)

ORBIT NO	7	26	500	899	1291
S/C Reg Bus Pwr(w)	167.9	176.8	184.5	179.5	168.0
Comp Load Pwr(w) P/o S/C reg bus pwr	49.0	49.0	49.0	41.8	41.8
P/L Reg Bus Pwr(w)	8.1	16.2	12.0	31.9	19.6
C/D Ratio	1.41	1.06	1.15	1.10	1.17
Total Charge(A-M)	327.8	309.2	282.3	343.0	296.8
Total Discharge (A-M)	232.6	290.9	245.2	312.9	253.6
Solar Array (A-M)	1058	1044	1034	1040	1033
S.A. Peak I (A)	15.8	15.8	15.45	15.45	15.36
Beta Angle (DEG)	-3.40	-3.33	-1.17	-1.10	-1.65
MAX R PAD TEMP (°C)	+65.0	+65.0	+68.0	+69.0	+71.0
MIN R PAD TEMP (°C)	-59.0	-62.0	-59.0	-58.0	-58.0
MAX L PAD TEMP (°C)	+56.1	+57.9	+60.5	+61.4	+65.0
MIN L PAD TEMP (°C)	-66.0	-67.0	-66.0	-64.0	-64.0

**Table 3-2. Power Subsystem Analog Telemetry**  
(Average Value for Frames of Data Received in NBTR Playback)

FUNCTION	DESCRIPTION	UNIT	O R B I T S				
			7	26	500	899	1291
6001	BAT 1 DISC	AMP	0.94	0.94	0.87	0.89	0.96
6002	2		0.98	0.95	0.93	0.94	1.03
6003	3		0.83	0.84	0.80	0.83	0.91
6004	4		0.93	0.93	0.89	0.89	0.98
6005	5		0.89	0.92	0.84	0.86	0.93
6006	6		0.92	0.91	0.85	0.87	0.93
6007	7		0.93	0.94	0.86	0.87	0.95
6008	8		0.87	0.91	0.83	0.84	0.90
6011	BAT 1 CHG	AMP	0.62	0.58	0.60	0.71	0.58
6012	2		0.59	0.57	0.57	0.72	0.56
6013	3		0.50	0.50	0.49	0.63	0.49
6014	4		0.57	0.54	0.54	0.67	0.54
6015	5		0.57	0.54	0.54	0.67	0.54
6016	6		0.59	0.57	0.55	0.69	0.55
6017	7		0.60	0.55	0.56	0.69	0.56
6018	8		0.57	0.55	0.54	0.67	0.54
6021	BAT 1 VOLT	VDC	31.61	30.87	31.40	30.94	31.28
6022	2		31.62	30.87	31.41	30.94	31.28
6023	3		31.62	30.87	31.41	30.94	31.29
6024	4		31.65	30.90	31.44	30.97	31.32
6025	5		31.69	30.95	31.48	31.02	31.36
6026	6		31.60	30.86	31.39	30.92	31.27
6027	7		31.62	30.89	31.42	30.96	31.30
6028	8		31.63	30.89	31.42	30.96	31.30
6031	BAT 1 TEMP	DGC	22.49	21.17	23.89	24.18	24.61
6032	2		19.54	18.80	20.46	21.91	21.36
6033	3		19.36	18.76	19.82	20.50	20.36
6034	4		22.45	21.57	22.77	22.73	23.41
6035	5		23.09	21.84	24.10	24.09	24.64
6036	6		22.56	21.24	23.93	24.14	24.99
6037	7		23.10	21.43	24.67	24.87	26.57
6038	8		23.26	21.86	24.81	25.10	25.66
6040	RT PAD TEMP	DGC	25.94	25.82	27.12	28.00	30.33
6041	R PAD V N	VDC	34.47	33.40	34.12	33.42	33.96
6042	R PAD V M	VDC	34.28	33.29	33.67	32.89	33.59
6044	LT PAD TEMP	DGC	14.03	14.14	16.10	17.34	19.50
6045	L PAD V F	VDC	34.74	33.69	34.41	33.70	34.26
6046	L PAD V G	VDC	34.79	33.68	34.45	33.72	34.27
6050	S/C UR BUS V	VDC	32.05	31.24	31.80	31.29	31.69
6051	S/C RG BUS V	VDC	24.54	24.54	24.54	24.54	24.55
6052	AUX REG A V	VDC	23.41	23.41	23.50	23.47	23.47
6053	AUX REG B V	VDC	23.50	23.50	23.50	23.50	23.50
6054	SOLAR I	AMP	14.77	14.87	14.38	14.35	14.40
6055	S/C RG BUS I	AMP	6.86	7.11	6.99	7.17	6.86
6056	S/C RG BUS I	AMP	6.86	7.11	6.98	7.17	6.85
6058	PC MOD T 1	DGC	21.83	21.82	22.35	23.21	22.81
6059	PC MOD T 2	DGC	21.63	21.68	22.25	22.91	22.74
6070	P/L RG BUS V	VDC	24.67	24.66	24.68	24.67	24.68
6071	P/L UR BUS V	VDC	31.90	31.08	31.65	31.15	31.54
6072	P/L RG BUS I	AMP	0.33	0.57	0.41	1.13	0.79
6073	P AUS A V	VDC	23.50	23.51	23.51	23.53	23.52
6074	P AUS B V	VDC	23.50	23.51	23.51	23.53	23.52
6075	PR MOD T 1	DGC	21.52	21.50	22.38	24.00	23.15
6076	PR MOD T 2	DGC	20.38	20.34	20.88	22.07	21.47
6079	FUSE BLOW V	VDC	24.56	24.56	24.58	24.56	24.56
6080	SHUNT 1 I	AMP	0.00	0.00	0.00	0.00	0.00
6081	2		0.00	0.00	0.00	0.00	0.00
6082	3		0.00	0.00	0.00	0.00	0.00
6083	4		0.00	0.00	0.00	0.00	0.00
6084	5		0.00	0.00	0.00	0.00	0.00
6085	6		0.00	0.00	0.00	0.00	0.00
6086	7		0.00	0.00	0.00	0.00	0.00
6087	8		0.00	0.00	0.00	0.00	0.00
6100	P/L RG BUS I	AMP	0.33	0.58	0.41	1.12	0.79
TOTAL NO.	MAJOR FRAMES	FRM	385	764	783	394	390

## SECTION 4

### ATTITUDE CONTROL SUBSYSTEM (ACS)

Performance of the Attitude Control Subsystem has been excellent during acquisition and flight operations. Perturbations experienced during the WBVTR-2 and RBV power circuit anomalies did no apparent harm to the ACS and recovery of spacecraft attitude was well behaved (see Figure 15-4). Full control was achieved in 18 minutes. Additional detail of the ACS performance during orbit adjust is contained in Section 7.

ACS dynamics for acquisition and for a typical orbit are shown in Figures 4-1 and 4-2. Area 1 (Figure 4-2) is the orbital point at which the ACS forward scanner sees the sun and responds to the distorted earth pulse.

The spacecraft excursion during this perturbation is acceptable since pneumatics are disabled to prevent expulsion of gas and the local sun elevation is too low for payload sensor operation. As noted, the ACS rapidly dampens to a suitable value.

Area 2 is the orbital point at which the ACS rear scanner sees the sun and responds to the distorted earth pulse.

Area 3 shows a typical cold cloud signature and the relatively insignificant perturbations resulting.

Area 4 and 5 illustrates ACS dynamics during pitch and roll gating. Spontaneous gates last for 50 milliseconds and use an impulse of 0.017 lb-sec in pitch and 0.043 lb-sec in roll to torque the vehicle and reduce the flywheel speeds; 85 RPM (0.57 TMV) in pitch and 215 RPM (0.86 TMV) in roll. Momentary enable gates are nominally 40 MS or less in duration (the command pulse width) and about 1 in 10 gate signals from the pneumatics pulse modulator does not trigger gas flow and further reduces the average gate duration. It is estimated that a momentary enable average pitch gate uses 0.01 lb-sec impulse and roll 0.34 lb-sec impulse. Total impulse used can be calculated as follows:

From Table 4-1

Total pitch impulse

$$475 \text{ Gates} \times 0.01 \text{ lb-sec/gate} = 4.75 \text{ lb-sec.}$$

Total Roll impulse

$$525 \text{ gates} \times 0.034 \text{ lb-sec/gate} = 17.80 \text{ lb-sec.}$$

$$\text{Impulse for orbit adjust and initial acquisition} = \underline{2.00} \text{ lb-sec.}$$

$$\text{Total Impulse Used} \quad \quad \quad 23.55 \text{ lb-sec.}^*$$

\* This is well within the accuracy of telemetry used to compute and plot impulse remaining on Figure 4-3.

Gating for the ACS has been as noted in Figures 4-4, 4-5, 4-6, 4-7 and 4-8 which show the gate distribution. Since orbit 85, gates have been allowed through the use of the pneumatics momentary enable commands which permit gating during satellite night when payloads are not operated. These momentary enable commands account for the population clusters. Figure 4-3 shows the cumulative gate relationship for orbits 0 through 1300. It is apparent, from the changing slope of the curve, that a small torque is acting on both pitch and roll (yaw is corrected through cross coupling with roll) to increase the number of gates/orbit. Nozzle leakage has been investigated and no measurable leakage occurred for 15 orbits. One gate is equivalent to  $\approx 0.5$  PCM count in function 1213 manifold pressure (low). This small increase in gate frequency is continuing to be studied.

All ACS components have operated in a fully satisfactory manner throughout this period. Table 4-2 gives typical ACS telemetry values.





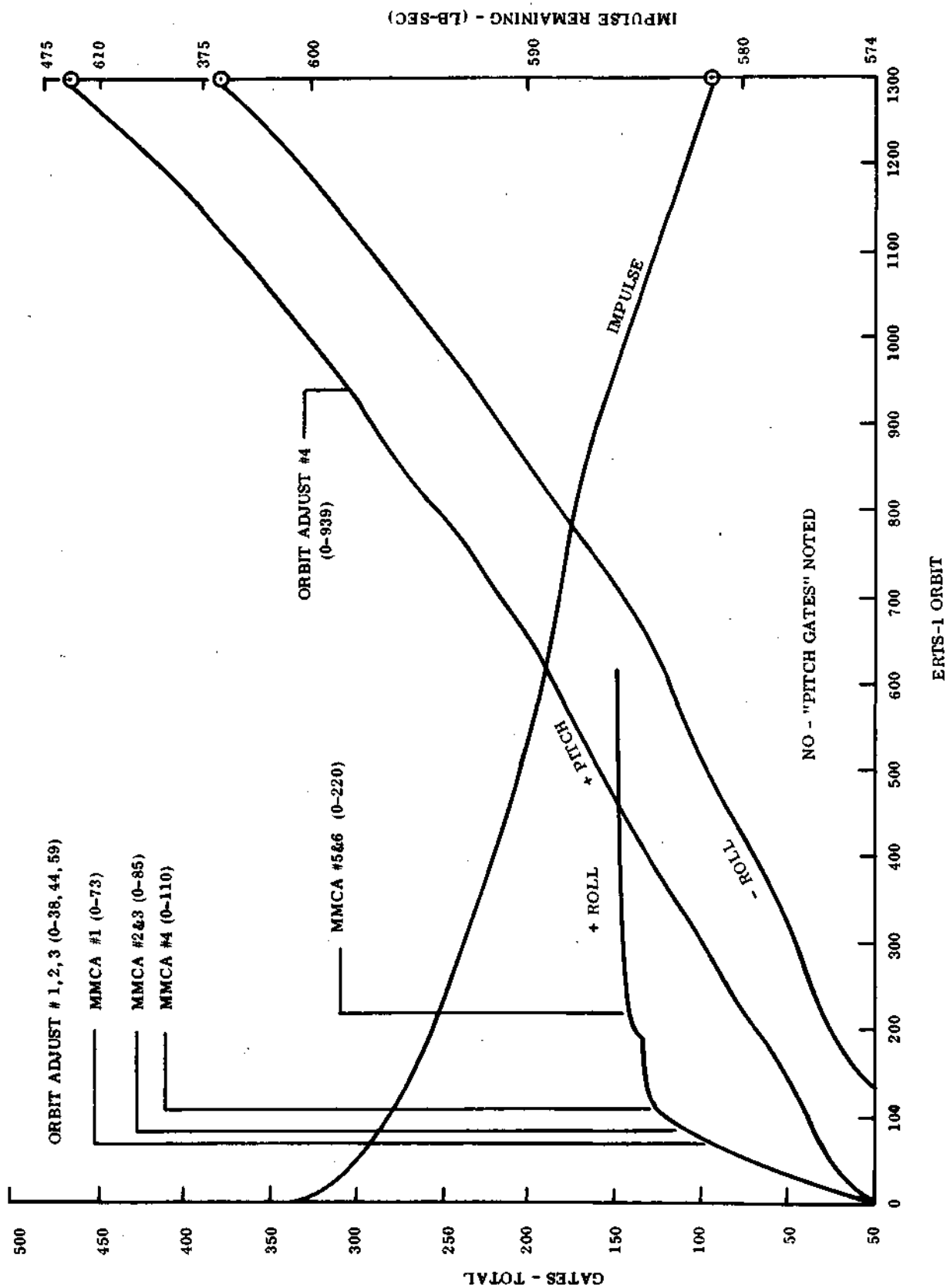


Figure 4-3. Cumulative Gate History ERTS 1

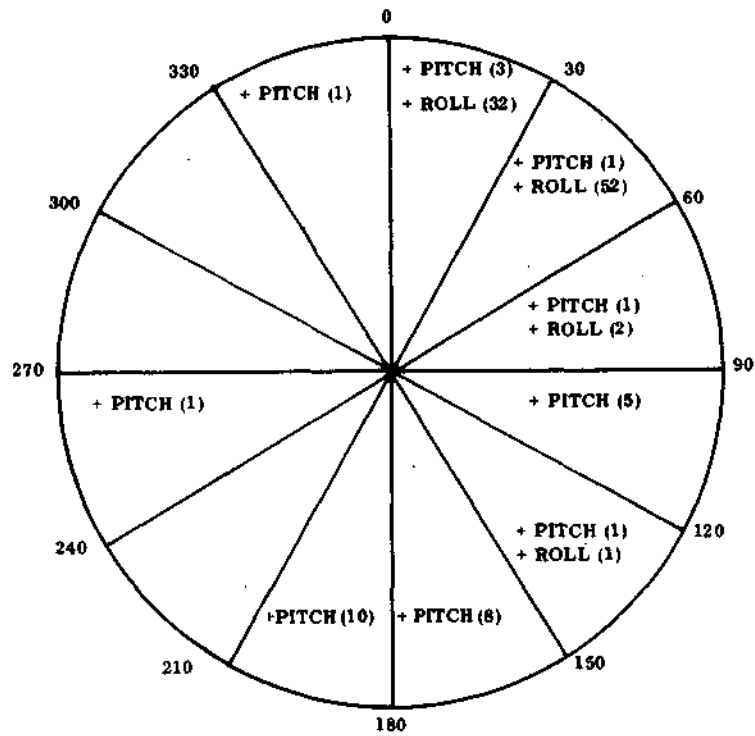


Figure 4-4. ACS Distribution to First MMCA Correction (Orbit 0-73)

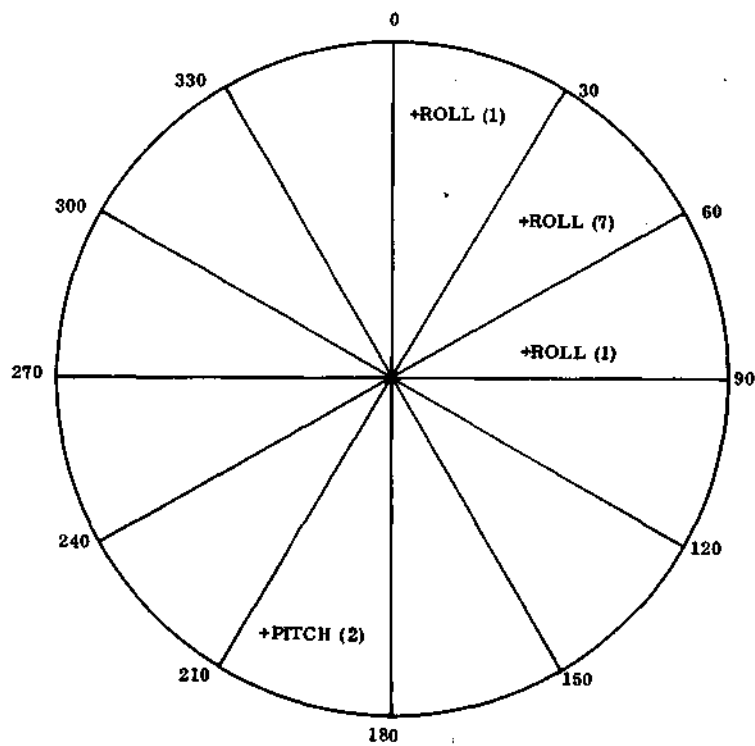


Figure 4-5. ACS Gate Distribution to Second MMCA Correction (Orbit 74-85)



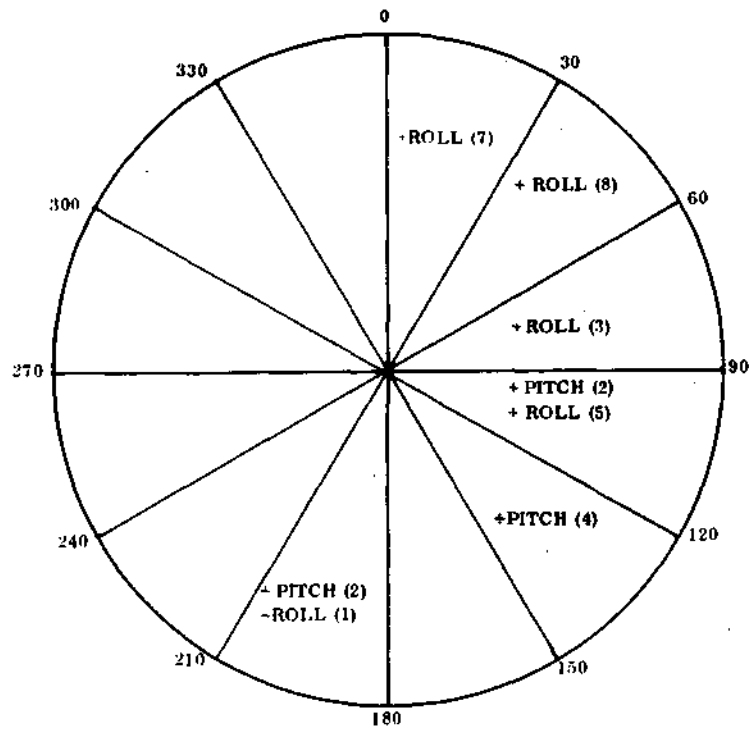


Figure 4-6. ACS Gate Distribution to Third MMCA Correction (Orbit 86-110)

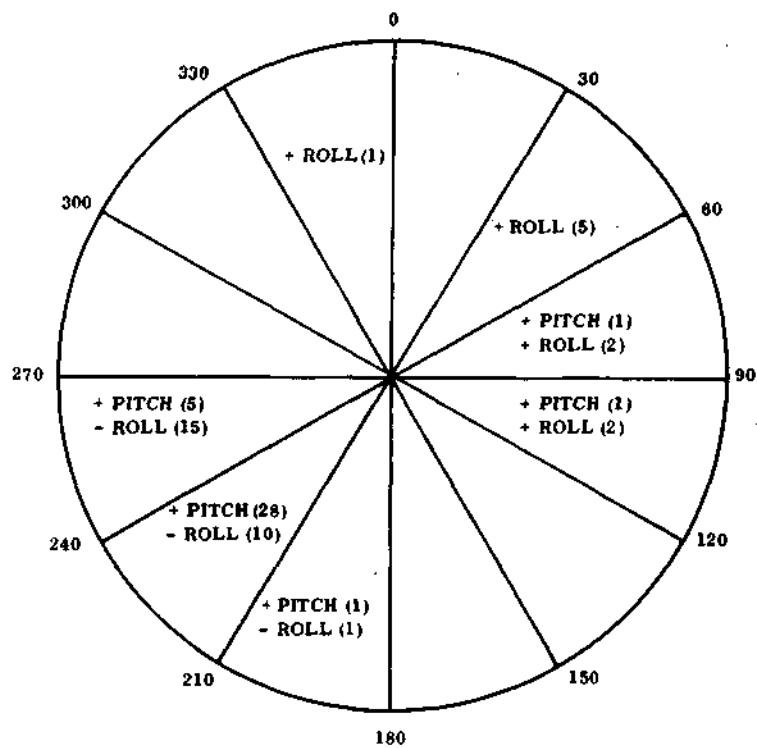


Figure 4-7. ACS Gate Distribution to Fourth MMCA Correction (Orbit 111-220)

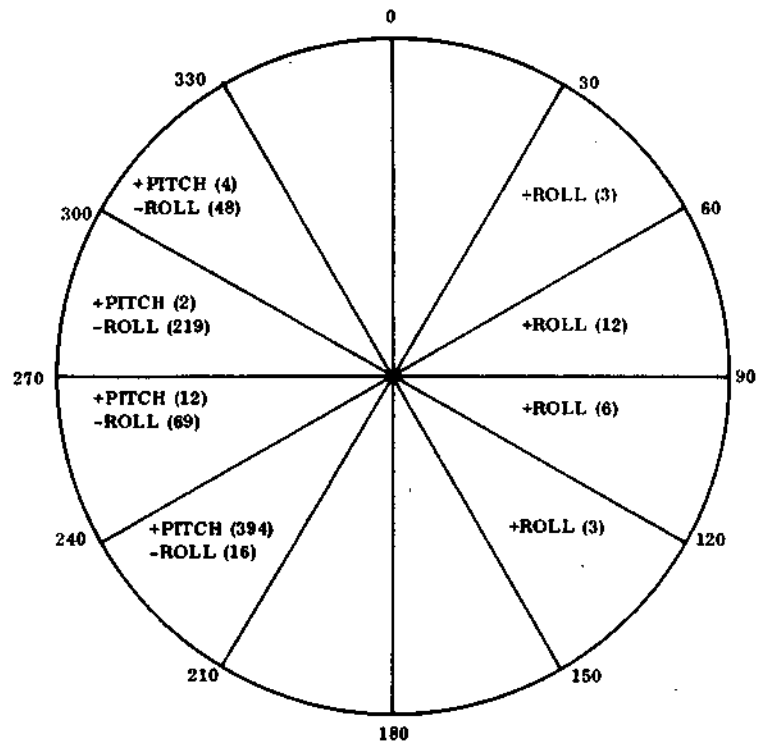


Figure 4-8. ACS Gate Distribution After MMCA Corrections (Orbit 221-1300)

Table 4-1. Impulse Useage ERTS-1

Item	Units	Orbit			
		0/ 1	500	900	1300
Gas Remaining*	Lbs	12.02	11.81	11.74	11.63
Gates	Total				
-Pitch		-	0	0	0
+Pitch		-	145	280	475
-Roll		-	90	215	375
+Roll		-	143	150	150
*Computed for Freon-14.					
$W = \frac{PV}{CRT}$					

Where:

W = Weight of Freon-14 in lbs.

P = Tank pressure in lbs/ ft<sup>3</sup>.

V = Tank volume in ft<sup>3</sup> (0.272 for ERTS-1).

C = Compressibility factor for Freon-14.

R = Universal gas constant (17.55 for Freon-14).

T = Tank temperature Degree Rankine.

Table 4-2. ACS Temperature and Pressure Telemetry Summary

Function	Units	* T/V 20°C Plateau	O R B I T			
			31	500	900	1300
1084 RMP 1 Gyro Temperature	DGC	79.0	44.5	21.49	22.14	23.33
1094 RMP 2 Gyro Temperature		73.0	74.3	75.07	75.06	75.07
1222 SAD RT MTR HSNG Temp.		28.0	21.1	20.45	21.12	22.24
1242 SAD LT MTR HSNG Temp.		27.0	27.0	28.88	29.74	30.81
1223 SAD RT MTR WNDNG Temp.		29.0	25.3	24.77	25.67	26.93
1243 SAD LT MTR WNDNG Temp.		29.0	28.7	31.35	32.46	33.50
1228 SAD RT HSG Pressure	PSI	7.57	7.6	7.59	7.59	7.59
1248 SAD LT HSG Pressure	PSI	6.91	7.0	6.99	7.10	7.10
1007 FWD Scanner MTR Temp.	DGC	17.00	19.8	19.14	19.57	20.36
1016 Rear Scanner MTR Temp.	DGC	25.00	20.5	19.03	19.55	20.28
1003 FWD Scanner Pressure	PSI	4.80	4.6	4.66	4.76	4.80
1012 Rear Scanner Pressure	PSI	5.16	7.8	7.88	7.92	7.93
1212 Gas Tank Pressure	PSI	1810.	1988.	1937.	1940.	1933.
1210 Gas Tank Temperature	DGC	20.0	22.6	22.89	23.72	24.66
1213 Manifold Pressure	PSI	57.53	56.7	57.11	57.10	56.66
1211 Manifold Temperature	DGC	24.0	21.9	21.98	22.91	24.08
1059 CLB Power Supply Card Temp.		36.0	37.1	39.41	40.00	41.07
1260 TH01 EBP		26.0	25.4	26.52	27.27	28.37

Table 4-2. ACS Temperature and Pressure Telemetry Summary (cont'd)

Function	Units	*T/V 20°C Plateau	O R B I T			
			31	500	900	1300
1081 RMP 1 MTR Volts	VDC	-30.13	Off	Off	Off	Off
1082 RMP 1 MTR Current	Amps	0.11	Off	Off	Off	Off
1080 RMP 1 Supply Volts	VDC	-23.88	Off	Off	Off	Off
1091 RMP 2 MTR Volts	VDC	-29.68	-29.7	-29.69	-29.66	-29.65
1092 RMP 2 MTR Current	Amps	0.10	0.10	0.10	0.10	0.10
1090 RMP 2 Supply Volts	VDC	-23.46	-23.4	-23.43	-23.42	-23.41
1220 SAD RT MTR WNDNG Volts	VDC	- 5.0	- 4.8	- 4.38	- 4.43	- 4.48
1240 SAD LT MTR WNDNG Volts	VDC	- 5.2	- 4.8	- 4.60	- 4.52	- 4.47
1227 SAD RT -15 VDC Conv.	VDC	-14.88	14.9	14.89	14.90	14.89
1247 SAD LT -15 VDC Conv.	VDC	-15.12	15.2	15.15	15.14	15.15
1056 CLB + 6 VDC	TMV	2.33	2.4	2.35	2.35	2.35
1055 CLB + 10 VDC TMV	TMV	2.73	2.75	2.75	2.75	2.75
1057 CLB Power Supply Volts	TMV	2.77	2.8	2.79	2.78	2.78

Table 4-2. ACS Temperature and Pressure Telemetry Summary (cont'd)

Function	Units	*T/V 20°C Plateau	O R B I T			
			31	500	900	1300
1261 TH02 EBP	DGC	23.0	22.9	23.30	23.91	25.13
1262 TH03 EBP		25.0	23.4	22.15	22.78	24.12
1263 TH01 STS		-8.0	-6.8	-2.25	-3.13	1.91
1264 TH02 STS		-11.0	-14.6	-10.92	-11.73	-8.05
1265 TH03 STS		-12.0	-3.1	4.03	3.13	7.49
1266 TH04 STS		4.0	-13.9	-7.46	-7.80	-3.47
1267 TH05 STS		-2.0	-8.9	-4.06	-5.39	3.07
1224 SAD R FSST	DGC	28.0	39.5	51.04	51.79	53.44
1244 SAD L FSST		22.0	27.1	37.36	39.31	41.90

\*Thermal Vacuum Test Data

## SECTION 5

### COMMAND/CLOCK SUBSYSTEM

Command processing for both real time and stored commands for ERTS-1 has been normal during this period except for one minor problem with one comstor cell which will be noted later.

Commanding difficulties which have been experienced have been isolated to ground transmission problems.

Several commands have been missed which were attributed to the logic race in the command clock design. This is expected for 1 in 5,000 commands. Three have been noted in approximately 26,000 commands. Whether the last command entered executed, as is normal in this case, has not been confirmed. The time base provided by the S/C clock has been well within specifications during this period. Drift has averaged -1.2 m. s. /orbit (see Figure 5-1).

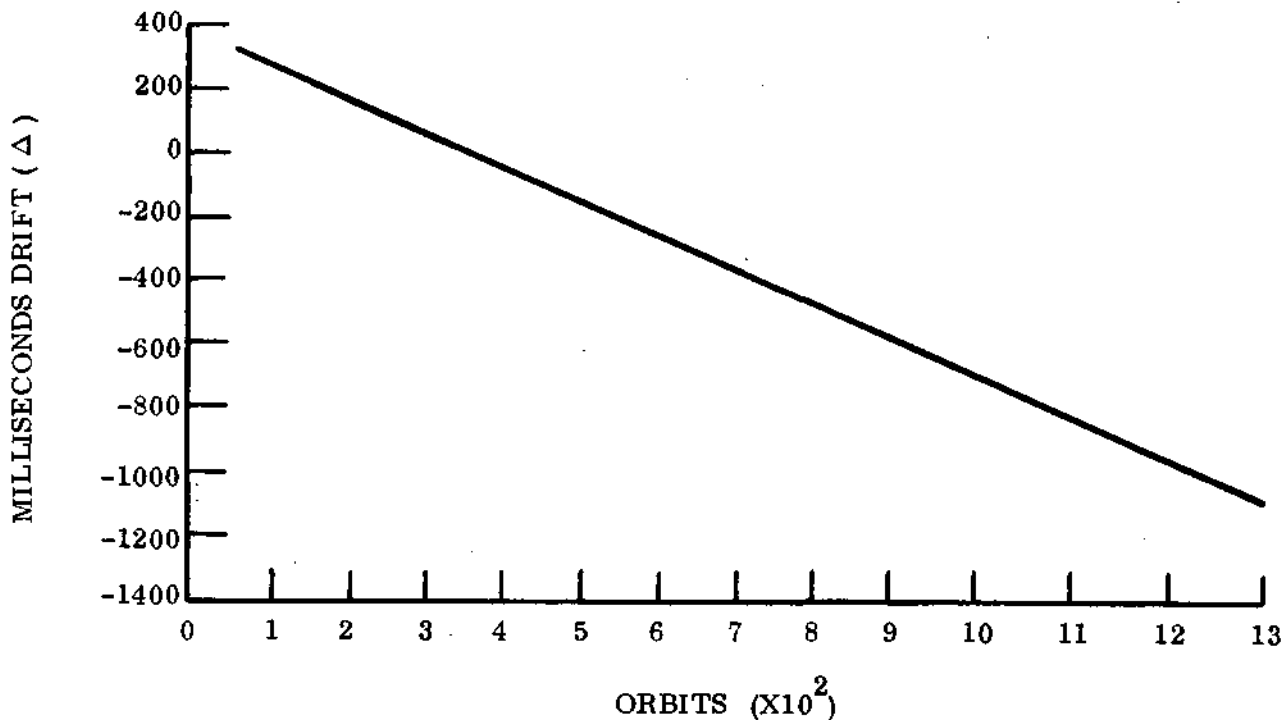


Figure 5-1. Clock Drift Summary

Spacecraft time code transmitted via RBV, MSS and Telemetry has been reliable and accurate. All frequency outputs to other subsystems have been nominal. The command clock did not upset during the power transient anomalies in orbits 148, 149 and 196.

There has been no occasion to switch to alternate units from original configuration.

In orbit 583 in the Bermuda pass during an attempted Comstor load cell 12 of Comstor B gave a return that was 256 seconds higher than entered. Cell 12 loaded with 525 "Inv A ON" for 14:57:20; verified as 525 for 15:01:36. The same  $\Delta$  time was noted in Cell 12 Comstor B at orbit 635 Alaska and again at orbits 891 Greenbelt, 1225 Greenbelt, and 1254 Greenbelt. On second try Comstor loaded normally each time. This intermittent problem is under further investigation.

Table 5-1 gives typical telemetry values.

The VHF command Receiver-B has operated flawlessly since launch. Receiver A has not yet been used. Interference has frequently been observed in strip charts and telemetry data, but this has had no impact on the operational functions. Especially noticeable is a regular and long pattern of interference for thousands of miles, generally centered about the Black Sea (see Figure 5-2).



Table 5-1. Command/Clock Telemetry Summary

Function No.	Name	Mode	Units 20°C	* T/V Plateau	Orbit 35	Orbit 500	Orbit 900	Orbit 1300
8005	Pri. Power Supply Temp.	--	°C	37.0	37.31	38.52	38.77	39.00
8006	Red. Power Supply Temp.	--	°C	41.3	35.73	37.01	37.33	37.63
8007	Pri. Osc. Temp	--	°C	31.1	31.14	31.36	31.59	31.92
8008	Red. Osc. Temp.	--	°C	30.3	30.47	30.56	30.77	31.26
8009	Pri. Osc. Output	--	TMV	1.07	0.95	0.95	.95	.96
8010	Red. Osc. Output	--	TMV	0.98	**	**	**	**
8011	100Khz	Pri. - Red.	TMV	3.10	3.11	3.11	3.11	3.10
8012	10KHz	Pri. - Red.	TMV	3.07	3.10	3.07	3.08	3.08
8013	2.5 KHz	Pri. - Red.	TMV	2.95	2.95	2.95	2.95	2.95
8014	400 Hz	Pri. - Red.	TMV	4.40	4.40	4.40	4.40	4.40
8015	Pri. #4V Power Supply	Pri. Clk ON	VDC	4.10	4.10	4.10	4.10	4.10
8016	Red. #4V Power Supply	Red. Clk ON	VDC	3.98	3.95	3.95	3.95	3.95
8017	Pri. #6V Power Supply	Pri. Clk ON	VDC	6.07	6.06	6.07	6.08	6.07
8018	Red. #6V Power Supply	Red. Clk ON	VDC	5.95	6.00	5.95	5.94	5.94
8019	Pri. -6V Power Supply	Pri. Clk ON	VDC	-6.02	-6.02	-6.02	-6.03	-6.02
8020	Red. -6V Power Supply	Red. Clk ON	VDC	-6.02	-5.99	-6.01	-6.00	-6.00
8021	Pri.-23V Power Supply	Pri. Clk ON	VDC	-22.96	-22.88	-22.89	-22.89	-22.89
8022	Red.-23V Power Supply	Red. Clk ON	VDC	-23.0	-22.98	-23.02	-23.01	-23.00
8023	Pri.-29V Power Supply	Pri. Clk ON	VDC	-29.2	-29.13	-29.15	-29.14	-29.15
8024	Red.-29V Power Supply	Red. Clk ON	VDC	-29.2	-29.07	-29.21	-29.21	-29.21
8101	CIU A -12V	CIU A ON	VDC	-12.3	-12.33	-12.33	-12.33	-12.33
8102	CIU B -12V	CIU B ON	VDC	-12.2	-12.26	-12.26	-12.26	-12.26
8103	CIU A -5V	CIU A ON	VDC	- 5.34	- 5.32	- 5.34	- 5.34	- 5.34
8104	CIU B -5V	CIU B ON	VDC	- 5.30	- 5.31	- 5.31	- 5.31	- 5.31
8105	CIU A Temp.	CIU A ON	°C	24.3	24.47	24.41	24.54	24.75
8106	CIU B Temp.	CIU B ON	°C	24.6	24.96	24.92	25.09	25.26
8201	Receiver RF-A Temp	-	°C	29.0	**	**	**	**
8202	Receiver RF-B Temp	-	°C	28.5	27.98	27.98	28.23	28.24
8203	D MOD A Temp.	-	°C	37.5	25.41	25.43	25.60	25.72
8204	D MOD B Temp	-	°C	35.4	35.03	35.22	35.33	35.38
8205	Receiver A AGC	ReceiverA ON	DBM	-70.0	**	**	**	**
8206	Receiver B AGC	ReceiverB ON	DBM	-57.0	-94.74	-89.72	-94.52	-98.37
8207	Amp. A Output	ReceiverA ON	RMV	1.50	**	**	**	**
8208	Amp. B Output	ReceiverB ON	TMV	1.54	2.81	2.90	2.78	2.62
8209	Freq. Shift Key A OUT	ReceiverA ON	TMV	1.11	**	**	**	**
8210	Freq. Shift Key B OUT	ReceiverB ON	TMV	1.10	1.10	1.11	1.10	1.10
8211	Amp. A Output	ReceiverA ON	TMV	1.11	**	**	**	**
8212	Amp. B Output	ReceiverB ON	TMV	1.13	1.13	1.13	1.13	1.13
8215	D MOC A -15V	ReceiverA ON	TMV	4.98	**	**	**	**
8216	D MOD B -15V	ReceiverB ON	TMV	4.99	5.00	5.00	5.00	5.00
8217	Regulator A-10V	ReceiverA ON	TMV	5.39	**	**	**	**
8218	Regulator B -10V	ReceiverB ON	TMV	5.50	5.50	5.50	5.50	5.50

FOLDOUT FRAME 1

FOLDOUT FRAME 2

\* Thermal Vacuum Test Data

\*\* A component not used since prelaunch



## SECTION 6

### TELEMETRY SUBSYSTEM

The Telemetry subsystem was launched on the ON mode and has been operating continuously since then providing data from the spacecraft either to ground stations, the narrow band recorders, or both. Typical telemetry values are given in Table 6-1. Only memory section 0, 0 has been used in the telemetry matrix. Total performance has been excellent.

Table 6-1. TLM Telemetry Summary

FUNCTION NO.	FUNCTION NAME	UNIT	T/V* 20°C PLATEAU	ORBIT 35	500	900	1300
9001	Memory Sequencer A Converter	VDC	6.34	6.35	6.33	6.33	6.33
9002	Memory Sequencer B Converter	VDC	6.44	**	**	**	**
9003	Memory Sequencer Temp	°C	20.1	19.59	20.78	21.07	21.05
9004	Formatter A Converter	VDC	5.99	5.99	5.99	5.99	5.99
9005	Formatter B Converter	VDC	6.02	**	**	**	**
9006	Dig. Mux A Converter	VDC	10.02	10.01	10.03	10.04	10.04
9007	Dig. Mux B Converter	VDC	10.01	**	**	**	**
9008	Formatter/Dig. Mux Temp	°C	22.2	22.50	24.23	24.75	24.85
9009	Analog Mux A Converter	VDC	26.18	26.01	26.18	26.18	26.18
9010	Analog Mux B Converter	VDC	26.21	**	**	**	**
9011	A/D Converter A Voltage	VDC	10.00	10.00	10.00	10.05	10.06
9012	A/D Converter B Voltage	VDC	10.06	**	**	**	**
9013	Analog Mux. A/D Converter Temp	°C	26.7	25.00	26.23	27.10	27.25
9014	Preregulator A Voltage	VDC	19.91	19.93	20.00	19.99	19.99
9015	Preregulator B Voltage	VDC	19.88	**	**	**	**
9016	Reprogrammer Temp	°C	19.9	22.0	22.50	22.50	22.50
9017	Memory A Converter	VDC	6.00	6.00	6.00	6.00	6.00
9018	Memory A Temp	°C	19.3	17.51	17.50	17.90	17.41
9019	Memory B Converter	VDC	6.03	**	**	**	**
9020	Memory B Temp	°C	17.4	17.68	17.50	18.55	17.71

\* Thermal Vacuum Test Data

\*\* Units not used since prelaunch.

Table 6-1. TLM Telemetry Summary (Cont)

FUNCTION NO.	FUNCTION NAME	UNIT	T/V* 20°C PLATEAU	ORBIT 35	500	900	1300
9100	Reflected Power (Xmtr A)	dBm	0	11.95	12.35	12.27	12.33
9101	Xmtr A -20 VDC	VDC	-19.76	-19.75	-19.75	-19.76	-19.76
9102	Xmtr B -20 VDC	VDC	-19.79	**	**	**	**
9103	Xmtr A Temp	°C	20.5	20.95	21.45	21.55	21.51
9104	Xmtr B Temp	°C	20.0	21.69	22.20	22.31	22.26
9105	Xmtr A Power Output	dBm	25.48	25.12	25.33	25.36	25.36
9106	Xmtr B Power Output	dBm	25.84	**	**	**	**

\* Thermal Vacuum Test Data  
 \*\* Units not used since prelaunch

## SECTION 7

### ORBIT ADJUST SUBSYSTEM (OAS)

An orbit adjust sequence for ERTS-1 was initiated during orbit 38 to assess the OAS in preparation for an in-plane correction of the launch-injection orbital semi-major axis from 7281.461 K. M. (18-day ground track repeat cycle 651.51 K. M. ) to the mean nominal value of 7285.816 K. M. (Error for 18-day ground track repeat cycle of 0.0 K. M. )

The OAS thruster heaters were turned on and verified at 09:04:16 in orbit 37 (before each burn the heaters were turned off). In orbit 38, after spacecraft telemetry values were confirmed to be normal for orbit adjust, the OAS and -X solenoid were turned on at 11:25:01 and off at 11:25:06 (backup off commands were in the Comstor). Due to spacecraft timing only four seconds of burn was achieved which is within timing constraints on the command system. Figure 7-1 shows dynamic response of the ACS and OAS parameters. An analysis of data and tracking of the spacecraft showed the firing to be normal in all respects. The semi-major axis was increased to 7281.484 K. M. (Error for 18-day ground track repeat cycle 648.36 K. M. ) and the initial orbital correction sequence was planned.

In orbit 43 the OAS heaters were turned on at 19:50:26 and in orbit 44 the OAS and -X solenoid were turned on at 21:44:35 and off at 21:48:46 to effect a firing period of 251 seconds. Again the performance was normal. Figure 7-2 shows performance characteristics. Tracking data confirmed that the semimajor axis was increased to 7283.456 K. M. (Error for 18-day ground track repeat cycle 353.18 K. M. )

A third burn was performed in orbit 59. The OAS heaters were turned on during orbit 58 at 21:37:21 and the OAS and -X thruster were turned on, at 23:34:40 and off at 23:39:58. All off commands were backed up in Comstor, for a firing period of 318 seconds. Figure 7-3 shows performance characteristics. Tracking data confirmed that the semimajor increased to 7285.838 K. M. (Error for 18-day ground track repeat cycle 2.4 K. M. ) which was considered satisfactory for the initial ERTS-1 orbit correction.

FOLDOUT FRAME

FOLDOUT FRAME

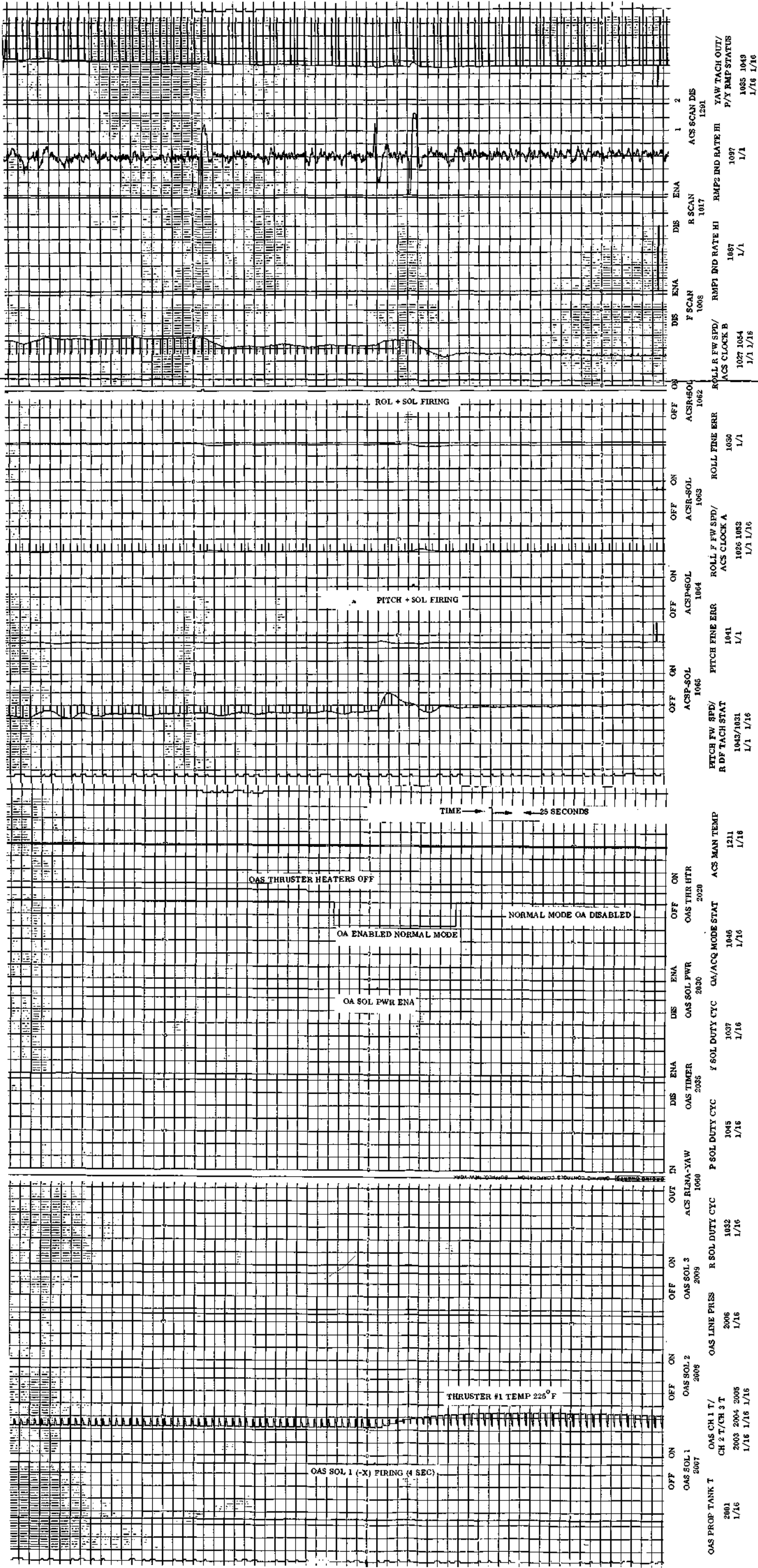


Figure 7-1. Orbit Adjust Subsystem Performance Characteristics







FOLDOUT FRAME

FOLDOUT FRAME

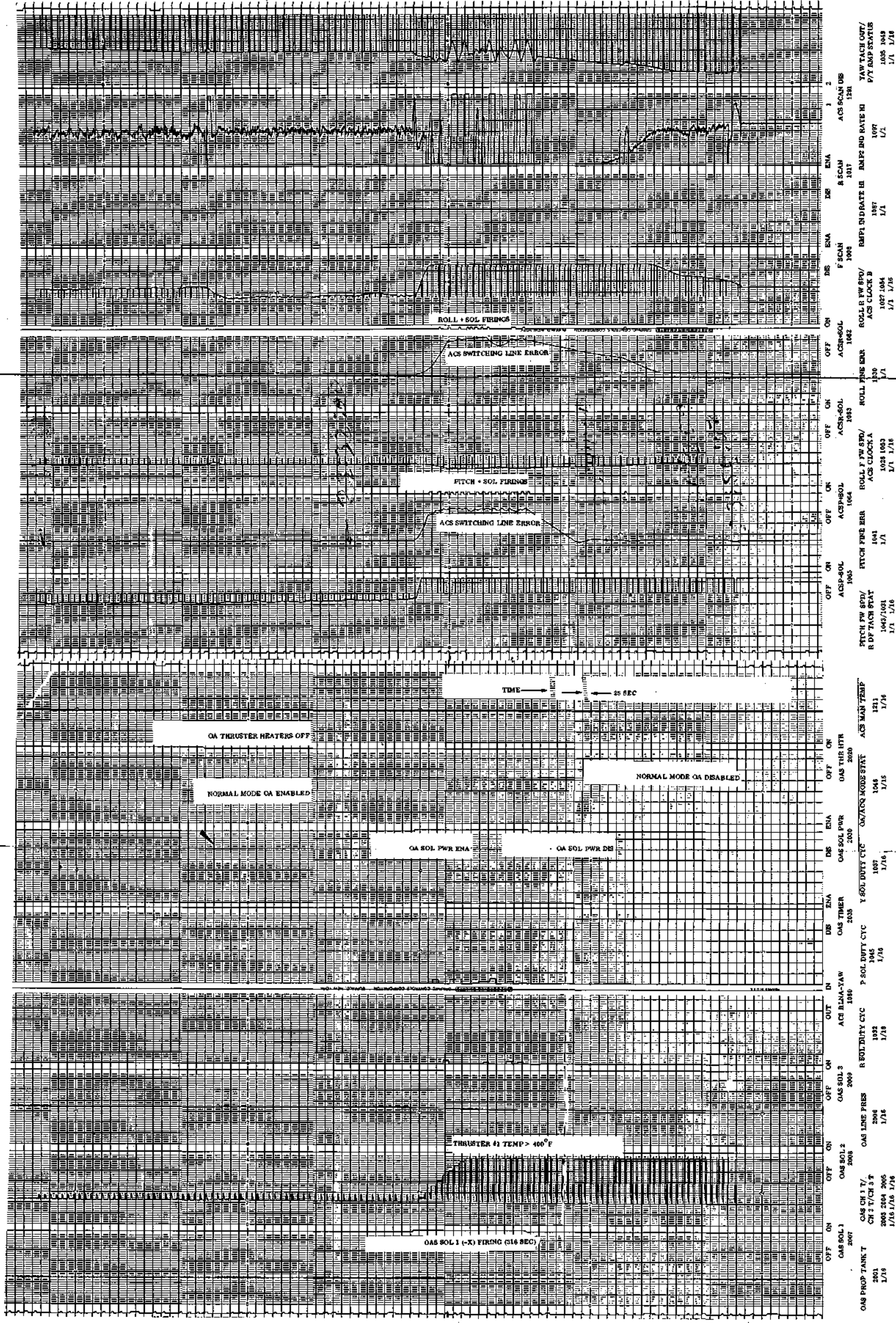


Figure 7-3. Orbit Adjust Subsystem Performance Characteristics

A fourth burn was performed in orbit 939 for the purpose of maintaining a satisfactory ground track. The OAS heaters were turned on during orbit 937 at 22:33:25 and the OAS and the -X thruster were turned on at 00:30:01 and off at 00:30:14. All commands were backed up in Comstor for a firing period of 13 seconds. Figure 7-4 shows performance characteristics. Tracking data confirmed that the semimajor axis increased 0.039 K. M. (Error for 18-day ground track repeat cycle =1.3 K. M.) which allows for several cycles prior to requiring a second orbit maintenance adjustment.

During periods of inactivity the OAS parameters have had normal readings on telemetry. Table 7-1 gives average for the off quiescent state. Table 7-2 shows orbit adjust performance.

Table 7-1. OAS Telemetry Values

Function No.	Name	Units	* T/V 20°C Plateau	35	500	900	1300
2001	Prop. Tank Temp.	*C	18.2	22.03	23.29	23.28	23.69
2003	Thrust Chamber No.1 (-X) Temp.	*C	20.9	29.57	29.60	30.29	31.38
2004	Thrust Chamber No.2 (+X) Temp.	*C	19.7	38.76	39.94	38.72	39.68
2005	Thrust Chamber No.3 (-Y) Temp.	*C	18.9	34.55	37.65	37.68	37.87
2006	Line Pressure	Psi	4.0	539.29	486.86	486.86	486.84

\* Thermal Vacuum Test Data

Table 7-2. Orbit Adjust Performance

Orbit	Burn Time (sec)	Average Sma** (KM)	Performance % of Plan	N <sub>2</sub> H <sub>4</sub> Used #
-*	-	7281.461	-	-
38	4	7281.484	60.0	0.01
44	251	7283.456	103.5	0.94
59	318	7285.838	101.5	1.10
938	13	7285.877	110.0	0.02
Average Force 0.81 LB <sub>f</sub>				

\* After Injection

\*\* Semi-Major Axis



## SECTION 8

### MAGNETIC MOMENT COMPENSATING ASSEMBLY (MMCA)

The ACS gating frequency during the early orbits of ERTS-1 was considerably higher than desired, + Pitch and + Roll in the ratio of 1 +P to 3 +R for an average of 1.7 gates/orbit was noted until orbit 73. At that time a MMCA correction was executed. The following conditions were commanded:

Pitch Positive Coil	23:39:04
Capacitor High	23:39:05
Power On	23:39:05
Capacitor Charge	23:43:00 TT
Capacitor Charge	23:43:01
Capacitor Dump	23:43:13 TT
Capacitor Dump	23:43:14
MMCA OFF	23:44:28

This charge of 13 seconds gave a dipole of the +pitch magnetic rod of 1200 pole -Cm. See Table 8-1 for telemetry confirmation. As noted in Graph 4-1 the +R gating improved. In Orbit 85 a 16-second charge/dump of +Pitch was executed. Due to command timing of difficulties the executed time was only 11 seconds and no change was observed. (The threshold for charge time to overcome hysteresis in the +Pitch rod is 11 seconds.) A second charge (20:21:09)/dump (20:21:25) of 16 seconds was executed changing the +Pitch dipole 600 pole-Cm for a total of 1800 pole-Cm. During orbit 110 another adjustment was made. Once a charge is put into a magnetic rod additional charges are by trial and error. The +Pitch charge (14:29:09)/dump (14:29:25) of 16 seconds gave a change of 550 Pole-Cm for a total of 2350 Pole-Cm. During orbit 220 two additional charge (13:31:00, 13:34:01)/dump (13:31:22, 13:34:23) sequences of 22 seconds each were executed.

A delta change of 600 pole-Cm was obtained and the +Pitch rod was charged to a total of 2950 Pole-Cm. Figure 4-3 shows the resulting reduction in roll gating frequency. No magnetic change has been noted in the MMCA, except as commanded in Table 8-1.

Table 8-2 gives typical telemetry values for the MMCA.

Table 8-1. MMCA Telemetry Before and After Adjustment

FUNCTION	72	75	83	88	106	115	218	224
4003	3.49	3.48	3.48	3.48	3.47	3.49	3.50	3.50
4004	3.11	3.11	3.11	3.11	3.11	3.11	3.11	3.11
4005	3.13	2.87	2.87	2.77	2.77	2.65	2.65	2.52
4006	3.18	3.20	3.20	3.20	3.18	3.18	3.18	3.18

Table 8-2. MMCA Telemetry Summary

Number	Name	Units	T/V 20°C*	Orbit			
			Plateau	35	500	900	1300
4001	A1 Board Temp	°C	19.8	19.77	19.33	19.55	19.54
4002	A2 Board Temp	°C	23.6	23.58	23.15	23.57	23.36
4003	Hall Current	TMV	3.50	3.48	3.50	3.50	3.50
4004	Yaw Flux Density	TMV	3.07	3.11	3.11	3.11	3.08
4005	Pitch Flux Density	TMV	3.12	3.13	2.50	2.50	2.52
4006	Roll Flux Density	TMV	3.22	3.19	3.17	3.17	3.17

\* Thermal Vacuum Test Data

**SECTION 9**  
**UNIFIED S-BAND SUBSYSTEM (USB)**

The USB equipment was turned on initially after separation, late in orbit zero as described in the ERTS-1 Launch and Flight Activation Report.

Since separation, the USB has operated continuously for 2245 hours through orbit 1300.

As shown in Table 9-1, all functions for USB have in general maintained their original values, except the USB transmitter power, function 11002. Only Transmitter A has been in use as of Orbit 1300.

**Table 9-1. USB/PMP Telemetry Values**

Function			Telemetry Value				
No.	Name		*TV	35	334	961	1256
11001	USB Revr. AGC	DBM	-127.24	-122.78	-126.84	-125.81	-124.34
11002	USB Trans. Pwr.	WTS	2.21	3.11	3.20	2.04	1.24
11003	Receiver Error	KHZ	-24.33	-21.79	-21.22	-21.32	-21.33
11004	Transp. Temp.	DGC	20.37	22.92	22.38	23.10	23.47
11005	Transp. Pressure	PSI	15.68	15.91	15.92	15.97	15.96
11007	Trans A-15VDC	VDC	-15.16	-15.20	-15.20	-15.20	-15.20
11009	Ranging -15VDC	VDC	-14.76	-14.76	-14.76	-14.76	-14.76
11101	PMP A Volt	VDC	-15.21	-15.12	-15.15	-15.17	-15.13
11003	PMP A Temp.	DGC	23.14	30.44	29.63	30.87	31.22

\*Thermal Vacuum Test Data

NOTE: Only A Unit of Transmitter and PMP have been turned on.

The telemetry values for function 11002 USB Transmitter A Power Output, show a steady decline and include three sharp step-downs (orbits 808, 988, 1258). The original calibration curve for the USB, which is used to compute the values in tables in this section has been revised.

Figure 9-1 shows the original and revised calibration curves. Using this, Table 9-2 was prepared showing the true values for USB Transmitter Power output. Figure 9-2 shows the power decline and the three step-downs. (See Figure 9-3 for Strip Chart Display).

In order to determine the effects of the power decline shown in Figure 9-2, the AGC voltage levels at ground stations were examined. The three prime stations, Greenbelt, Goldstone, and Alaska each regularly report after each pass the maximum AGC level observed. In Figure 9-4, these readings are plotted against distance from the ground stations for the early orbits, and again for the late orbits. Alaska uses an 85 foot receiving antenna and an uncooled receiver. Goldstone and Greenbelt use 35 foot antennas and cooled receivers. This yields a net advantage to Alaska of about 7 dB as is apparent in Figure 9-4. Figure 9-4 also shows a real decline of about 1.4 dB. This result is in good conformity with the 29.5% power decline as computed from an average corrected telemetry value of 1.58 watts for the early orbits and 1.03 watts for the late orbits. This power decline with use is within expected limits. The step-downs, however, are more indicative of sudden physical changes. The possibility has been explored that a connector resistance has been changed slightly due to vibration of the nearby MSS scan mirror, but no conclusion is yet possible.

The USB transmitter can operate satisfactorily with 0.5 watts for DCS relay and probably as low as 0.3 watts for telemetry transmissions and ranging functions.

Table 9-2. USB Transmitter A Power Out Function 11002

Orbit No.	SCEST Value From Old Curve (watts)	Value From New Curve (watts)
83	3.41	1.58
174	3.33	1.56
334	3.20	1.52
533	2.87	1.47
741	2.81	1.46
780	2.80	1.45
804	2.69	1.43
807	2.73	1.44
808	2.35	1.37
809	2.00	1.27
815	2.05	1.30
961	2.04	1.29
982	2.01	1.27
985	1.91	1.25
988	1.31	1.19
989	1.24	1.17
993	1.32	1.19
1020	1.25	1.17
1030	1.28	1.18
1256	1.24	1.17
1258	1.17	1.16
1259	0.93	1.04
1260	0.91	1.03
1296	0.91	1.03



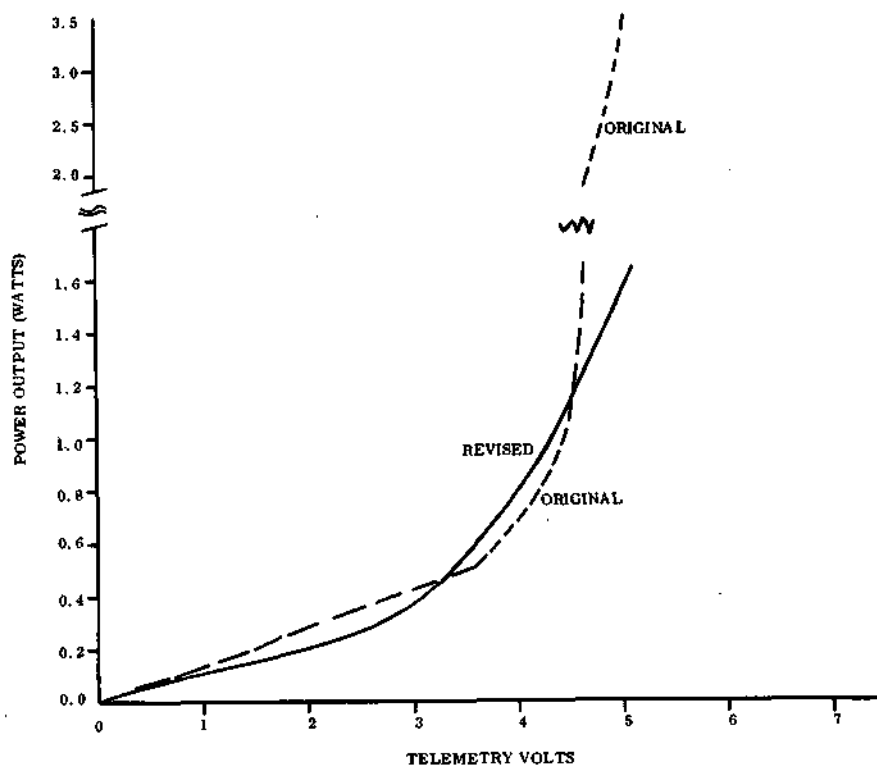


Figure 9-1. USB Calibration Curves (Original and Revised)

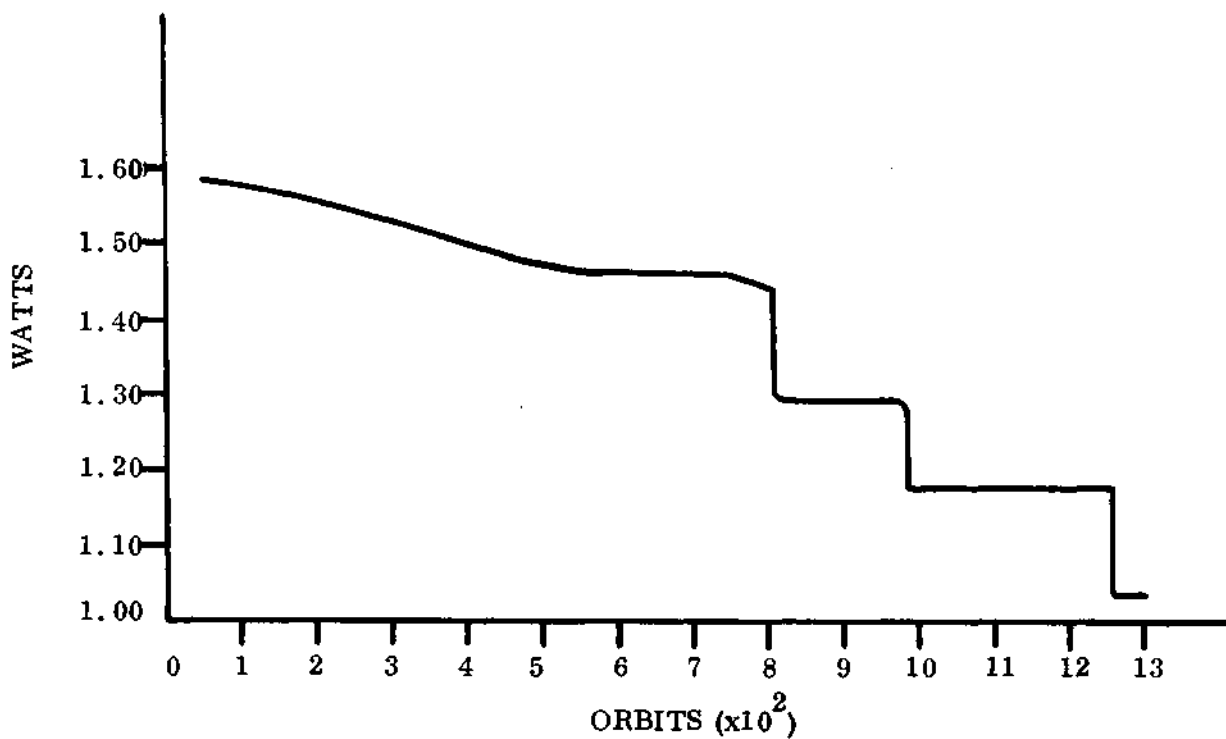


Figure 9-2. USB Power Output (Corrected)

FOLDOUT FRAME

FOLDOUT FRAME

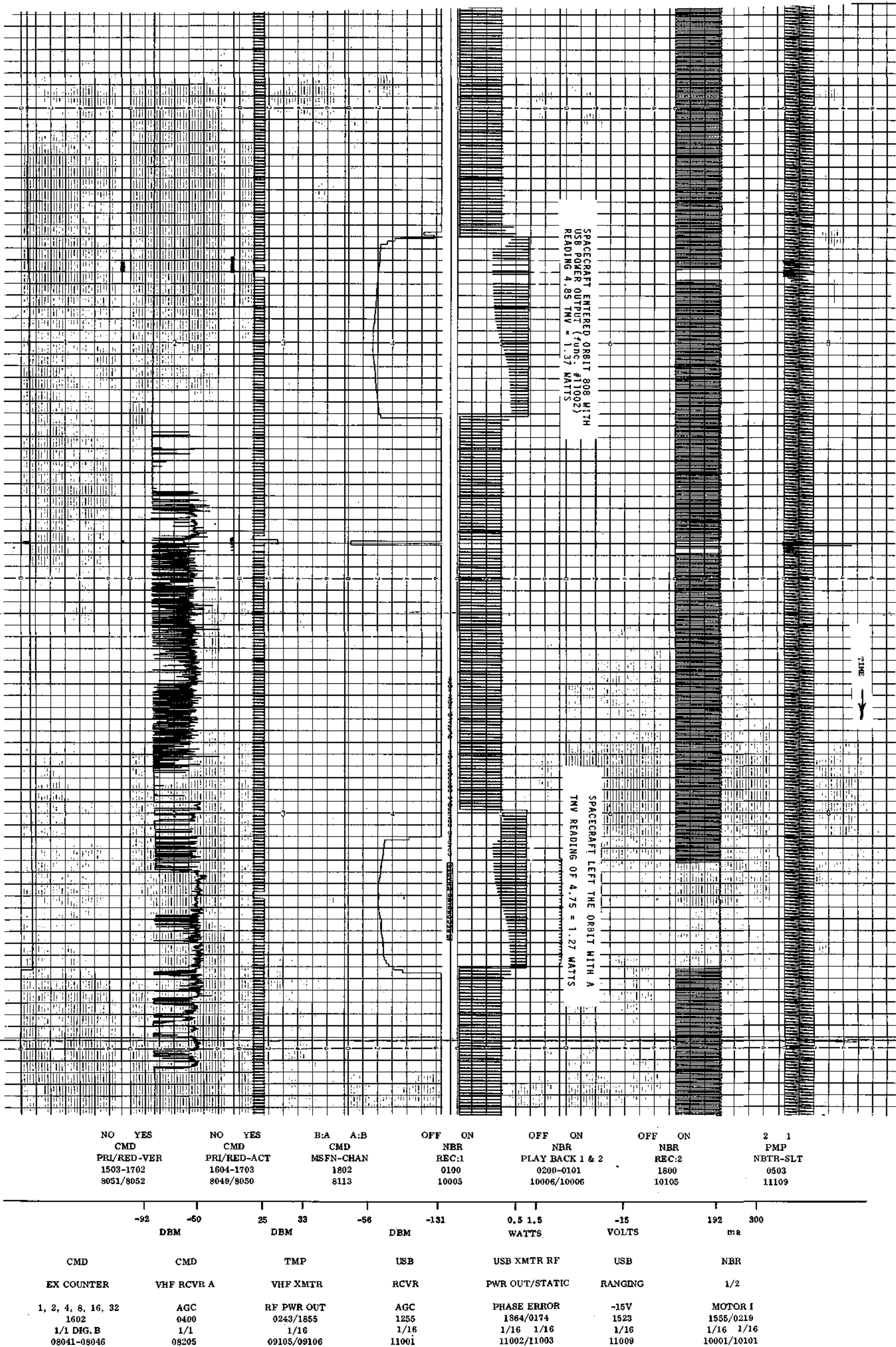


Figure 9-3. USB Performance Characteristics

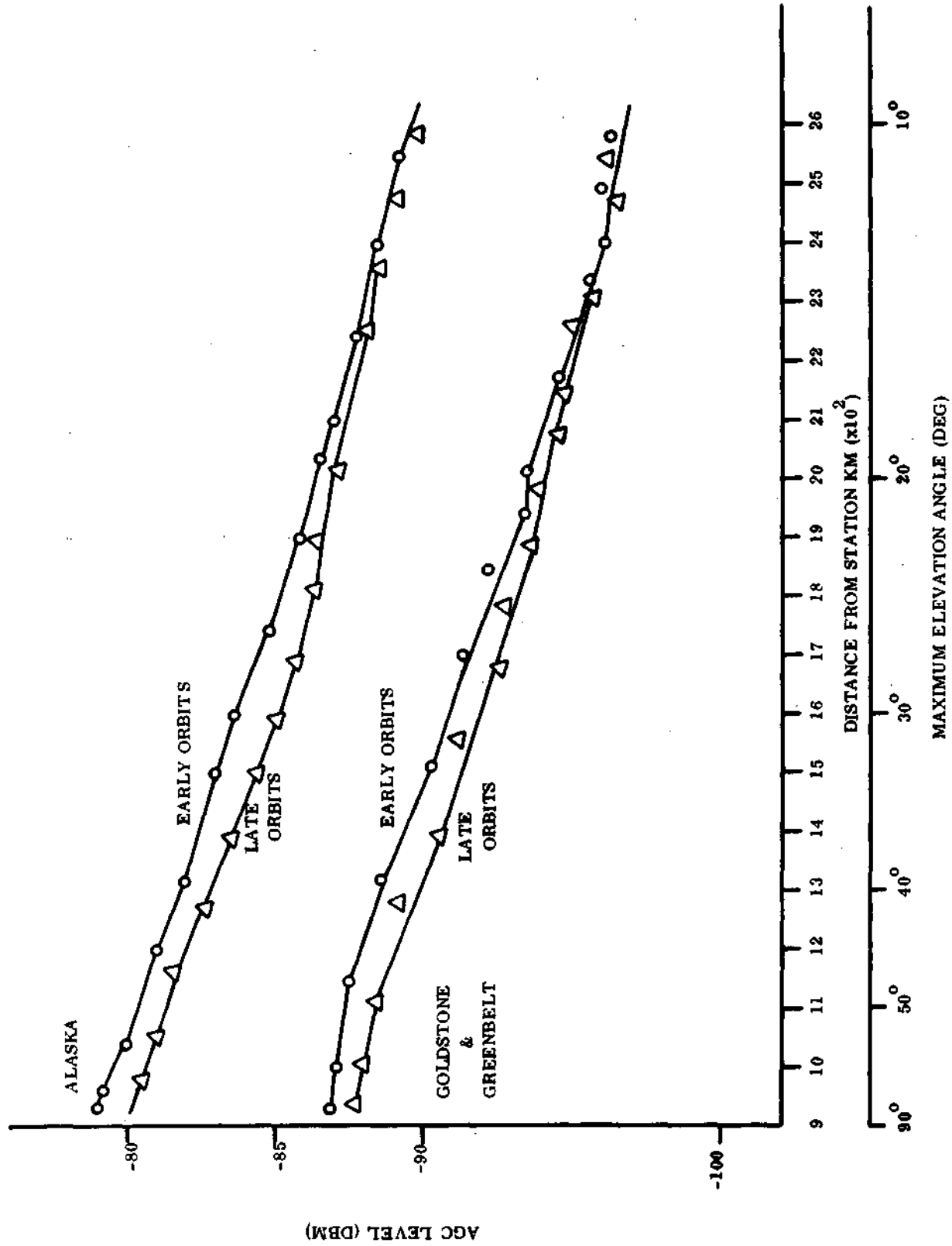


Figure 9-4. Maximum AGC Values for Use Power Output vs Distance

## SECTION 10

### ELECTRICAL INTERFACE SYSTEM

Auxiliary Processing Unit, (APU) consists of Search Track Data, Time Code Data, and Back Up Timers which operated satisfactorily throughout this report period. Telemetry for the APU is shown in Table 10-1. The APU was launched in the STANDBY mode and commanded to Normal mode in orbit 5 where it remained throughout this report period. Interface Switching Module (ISM) performed all switching normally during this report period. AMS power On, Payload Regulator Switchover, Orbit Adjust Heater, and Compensation Loads were exercised within this report period.

Table 10-1. APU Telemetry Functions

Function	Description	Unit	Orbit 7	Orbit 26	Orbit 500	Orbit 899	Orbit 1291
13200	APU, -24.5 VDC	VDC	24.90	24.90	24.91	24.91	24.91
13201	APU, -12 volts	VDC	12.08	12.08	12.08	12.08	12.08
13202	APU Temp	DGC	25.49	25.72	26.30	26.72	26.98

The Power Switching Module (PSM) contains the switching relays for power to the Orbit Adjust, MSS, WBVTR #1 and #2, RBV, and PRM. The Orbit Adjust power circuit was powered for the duration of the Orbit Adjust maneuver in orbits 38, 44, 59, and 939. The MSS power circuits have been operated on a regular basis throughout this report period. WBVTR #1 power circuit was exercised regularly throughout this report period. WBVTR #2 power circuit was exercised regularly until its failure in orbit 148 and 149 when it was switched off. The RBV power circuit was exercised regularly until a failure in the power circuit occurred in orbit 196. An investigation committee reached the following conclusions: (See Appendix B3.)

1. Turn on of the RBV was accompanied by a current transient of approximately 200 amperes for from 430 to 520 milliseconds and subsequent failure of the normal RBV turn off function.

2. A simple relay contact weld is not probable.
3. The failure was a short circuit from the payload power bus to the chassis.
4. The short circuit has cleared.
5. The failure was a short circuit internal to the PSM between the relay and the RBV fuses.
6. The RBV was not the cause of or affected by the failure.
7. Alternate modes of RBV power switching are available.

It is to be noted that the failed relay is the one operated by the payload back up timer signal supplied by the APU. Therefore the RBV will not be protected by the back up timer in future operation. The PRM and its fuse tap was turned off in orbit 196 after the failure. In orbit 201 the PRM and fuse tap was activated. PRM regulator 4 came on where PRM 3 was on previously. Since PRM 4 was operating normally it remained on throughout the rest of this report period.

The separation subsystem performed as expected. The 2.5 second timer caused paddle unfold. Before separation the subsystem properly restrained the paddles, disabled the primary and redundant matrix A drivers, provided - 24.5 VDC to the Attitude Control reset line and provided telemetry signals indicating that the spacecraft was still mated to the Delta Vehicle. After separation all circuits were activated, separation was confirmed by Function 5002 Spacecraft Separation Switch changing from 0 to 1 state at 19:06:35 and subsequent readings from all subsystems activated by the separation event.

**SECTION 11**  
**THERMAL CONTROL SUBSYSTEM**

11-1

## SECTION 11

### THERMAL SUBSYSTEM

The thermal subsystem has maintained spacecraft temperature control over a satisfactory range during this report period. Table 11-1 shows average analog telemetry values from data recorded on the NBTR. During this report period the sun intensity increased 3.2% due to seasonal variations (shown in Figure 3-8). This caused a gradual rise in average temperatures of about  $1^{\circ}$  to  $2^{\circ}$  C around the spacecraft. No detrimental effects were observed from the solar flares activity which exposed the thermal control surfaces to charged particle radiation.

A plot of the left and right solar paddle temperatures over an orbit are shown in Figures 11-1 and 11-2. The location of the temperature sensors are shown in Figure 11-3. The increase in temperature from orbit 10 to 995 is due to the 3.2% seasonal increase of sun intensity. The upper temperature on the left solar paddle is about  $+10^{\circ}$  C higher than orbital experience on Nimbus 4; and the lower temperature is about  $19^{\circ}$  C lower than Nimbus 4 for orbit 10. The right solar panel has similar differences from Nimbus 4. The difference after taking into account ERTS-1 albedo are not fully understood and are under investigation. One difference (which has not fully been evaluated) is the ERTS-1 sensing thermistors were lightly bonded to the surface of the backside skin rather than potted with a large mass of adhesive to the backside surface as on Nimbus 4. Because of the 9.42Z equator crossing and a  $33^{\circ}$  cant on the paddles the thermal prediction and analysis is quite complex and different from Nimbus 4.

Table 11-1. Thermal Subsystem Analog Telemetry  
(Average Value for Frames of Data Received in NSTR Playback)

FUNCTION	DESCRIPTION	UNIT	O R B I T S				
			7	26	500	899	1291
7001	TMM TH0 1ST I	DGC	19.31	19.52	20.91	21.59	21.47
7002	TMM TH0 2 SBO	DGC	18.48	18.60	19.28	20.24	20.01
7003	TMM TH0 3ST I	DGC	18.24	18.24	19.59	20.12	20.28
7004	TMM TH0 3 SBI	DGC	19.24	19.47	19.85	20.73	20.46
7005	TMM TH0 4ST I	DGC	18.25	18.39	19.18	20.73	19.81
7006	TMM TH0 5 SBO	DGC	17.69	17.57	18.04	18.83	18.53
7007	OA - X THRUSTER	DGC	21.73	21.95	22.30	22.54	23.04
7008	TMM TH0 7 STO	DGC	15.89	15.95	16.44	17.01	16.87
7009	TMM TH0 6 SBI	DGC	19.41	19.38	20.07	20.73	20.62
7010	TMM TH0 7 STI	DGC	18.36	18.38	19.17	19.61	19.71
7011	TMM TH0 8 STO	DGC	21.60	21.78	22.22	22.52	22.87
7012	TMM TH0 9 SBI	DGC	21.62	21.81	22.37	22.62	23.07
7013	TMM TH10 SBO	DGC	18.76	18.73	19.19	19.37	19.82
7014	TMM TH11 ST I	DGC	22.09	22.37	23.02	23.32	23.62
7015	TMM TH12 SBO	DGC	22.03	22.37	22.74	23.27	23.37
7016	TMM TH13 STI	DGC	20.75	20.95	21.80	22.22	22.68
7017	RBV BEAM CTR LN	DGC	21.25	21.53	22.19	22.47	22.85
7018	TMM TH14 STO	DGC	20.52	20.38	21.56	22.10	22.10
7019	NBR RAD OUTBDB4	DGC	4.88	5.09	5.51	5.96	6.08
7020	TMM TH15 SBI	DGC	21.39	21.14	22.87	23.33	23.78
7021	TMM TH16 STI	DGC	20.87	20.73	22.65	23.23	23.68
7022	TMM TH17 SBI	DGC	20.70	20.22	22.39	23.06	23.46
7023	TMM TH18 SBO	DGC	22.01	21.90	23.87	24.40	24.86
7030	TMM TH03 BUR	DGC	16.01	16.50	17.82	17.09	17.39
7031	TMM TH06 BUR	DGC	13.54	13.59	13.98	14.42	14.39
7032	TMM TH09 BUR	DGC	19.77	19.92	20.26	20.44	20.89
7033	TMM TH12 BUR	DGC	21.25	21.51	21.94	22.42	22.49
7034	TMM TH15 BUR	DGC	19.92	19.70	21.40	21.85	22.44
7035	TMM TH18 BUR	DGC	19.95	20.11	21.46	21.91	22.12
7040	TMM TH01 TCB	DGC	18.97	19.27	20.16	20.93	20.80
7041	TMM TH02 TCB	DGC	17.93	17.99	18.80	19.34	19.72
7042	TMM TH03 TCB	DGC	18.22	18.34	19.00	19.72	19.93
7043	TMM TH04 TCB	DGC	19.03	18.95	19.42	20.46	19.93
7044	TMM TH05 TCB	DGC	16.38	16.27	16.79	17.33	17.13
7045	TMM TH07 TCB	DGC	18.23	18.41	18.89	19.23	19.37
7046	TMM TH09 TCB	DGC	19.64	19.38	20.04	20.15	20.60
7048	TMM TH11 TCB	DGC	21.77	21.98	22.51	22.85	23.16
7049	TMM TH12 -TCB	DGC	21.60	21.92	22.15	22.69	22.58
7050	TMM TH13 TCB	DGC	21.10	21.21	22.00	22.35	22.51
7051	TMM TH14 TCB	DGC	21.94	21.38	23.02	23.23	23.65
7052	TMM TH16 TCB	DGC	21.71	21.30	23.59	24.53	25.11
7053	TMM TH17 TCB	DGC	22.43	21.73	23.91	24.28	24.81
7054	TMM TH18 TCB	DGC	20.54	20.02	21.83	22.22	22.51
7060	TMM SHUTTER BY1	DGC	23.56	25.85	31.62	37.08	36.21
7061	TMM SHUTTER BY2	DGC	0.00	6.62	12.69	13.07	16.89
7062	TMM SHUTTER BY3	DGC	6.09	10.96	18.70	33.53	25.96
7063	TMM SHUTTER BY4	DGC	26.32	30.60	33.35	38.24	36.27
7064	TMM SHUTTER BY5	DGC	15.00	15.03	10.46	12.26	14.42
7065	TMM SHUTTER BY7	DGC	10.66	17.14	17.30	18.21	20.98
7067	TMM SHUTTER BY9	DGC	33.31	33.26	34.40	37.97	39.15
7068	TMM SHUTTER BY10DEG	DGC	19.76	24.68	26.03	27.32	29.54
7069	TMM SHUTTER BY11DEG	DGC	38.13	39.66	44.55	46.04	48.48
7070	TMM SHUTTER BY12DEG	DGC	43.46	43.81	44.91	47.64	47.05
7071	TMM SHUTTERBY13 DEG	DGC	39.75	40.39	47.54	47.88	47.96
7072	TMM SHUTTERBY14 DEG	DGC	35.29	34.20	38.50	41.42	42.85
7073	TMM SHUTTERBY15 DEG	DGC	47.45	45.40	55.67	59.35	63.42
7074	TMM SHUTTERBY16 DEG	DGC	31.69	24.50	39.62	47.22	51.25
7075	TMM SHUTTERBY17 DEG	DGC	43.96	39.06	54.02	56.48	60.34
7076	TMM SHUTTERBY18 DEG	DGC	33.88	29.60	39.90	41.98	43.14
7080	TMM Q1 T ZENERV	VDC	8.19	8.19	8.19	8.19	8.19
7081	TMM Q2T ZENER V	VDC	8.40	8.40	8.40	8.40	8.40
7082	TMM Q3T ZENER V	VDC	8.31	8.31	8.31	8.32	8.35
7083	TMM Q1S ZENER V	VDC	8.31	8.31	8.33	8.35	8.35
7084	TMM Q2S ZENER V	VDC	8.19	8.19	8.10	8.20	8.20
7085	TMM Q3S ZENER V	VDC	8.15	8.15	8.15	8.15	8.15
7090	TMM PSM MOUNT	DGC	20.82	21.60	22.25	22.84	23.14
7091	TMM IND ATTITUDEGDC	DGC	19.15	19.40	20.05	20.71	20.69
7092	TMM RBV RADIAORDC	DGC	15.33	15.65	16.42	16.78	17.31
7093	TMM RBVC CTR BM	DGC	19.84	20.30	21.06	21.36	21.81
7094	TMM WBVTR ROOT	DGC	12.85	12.96	14.44	15.51	15.64
7095	TMM WBVTR RAD CT	DGC	4.82	4.81	6.14	7.08	7.50
7096	TMM WBVTR STRAP	DGC	16.46	16.62	18.18	19.54	19.39
7097	TMM WB MT BAY 1	DGC	19.41	20.56	22.69	22.90	21.59
7098	TMM WB MAT BAY1	DGC	19.21	20.22	22.30	22.42	21.93
7099	TMM WBVTR SEP 3	DGC	18.40	18.60	19.88	21.53	20.69
7100	TMM WBVTR SEP17	DGC	21.43	21.31	23.35	24.38	24.41
7101	TMM WBVTR IDENT	DGC	21.26	21.49	23.16	24.67	24.19
7102	TMM WBVTR 2 BAY	DGC	17.35	17.46	18.34	19.51	19.07
7103	TMM WBVTR2 BY15	DGC	21.08	21.00	22.80	23.43	23.75
7104	TMM WBVTR2 CTR	DGC	19.05	19.35	20.88	21.94	21.86
7105	TMM NBR B SEP6	DGC	17.90	18.06	18.85	19.69	19.71
7106	TMM NBRB SEP 1	DGC	20.75	20.82	22.16	22.59	22.89
7107	TMM NBR BM CTR	DGC	18.95	19.37	20.48	21.12	21.34
7108	TMM MSS MOUNT14	DGC	19.21	19.18	20.77	21.26	21.59
7109	TMM OA - Y THRUSTER	DGC	22.27	22.21	24.00	24.43	24.85
7110	TMM MSS WBVTRRM	DGC	17.94	18.14	19.30	20.17	20.27
7111	TMM OA + X THRUSTER	DGC	19.44	20.30	22.03	22.24	21.82
7130	TMM AUX P 1 T	DGC	18.69	15.60	16.99	7.94	14.42
7131	TMM AUX P 2 T	DGC	6.81	10.63	2.56	1.15	19.10

FOLDOUT FRAME

FOLDOUT FRAME

2



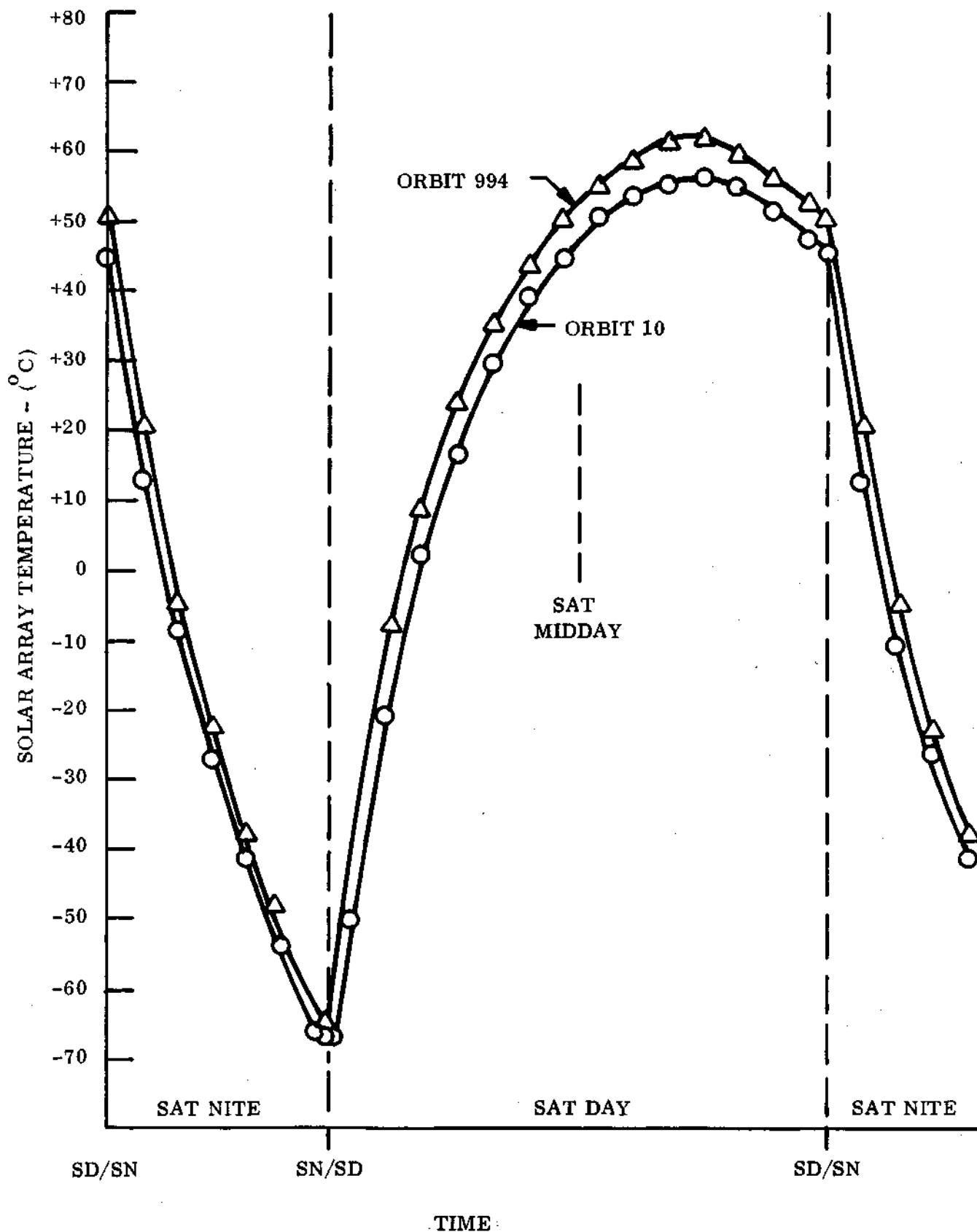


Figure 11-1. Left Solar Paddle Temperature (Function 6044)

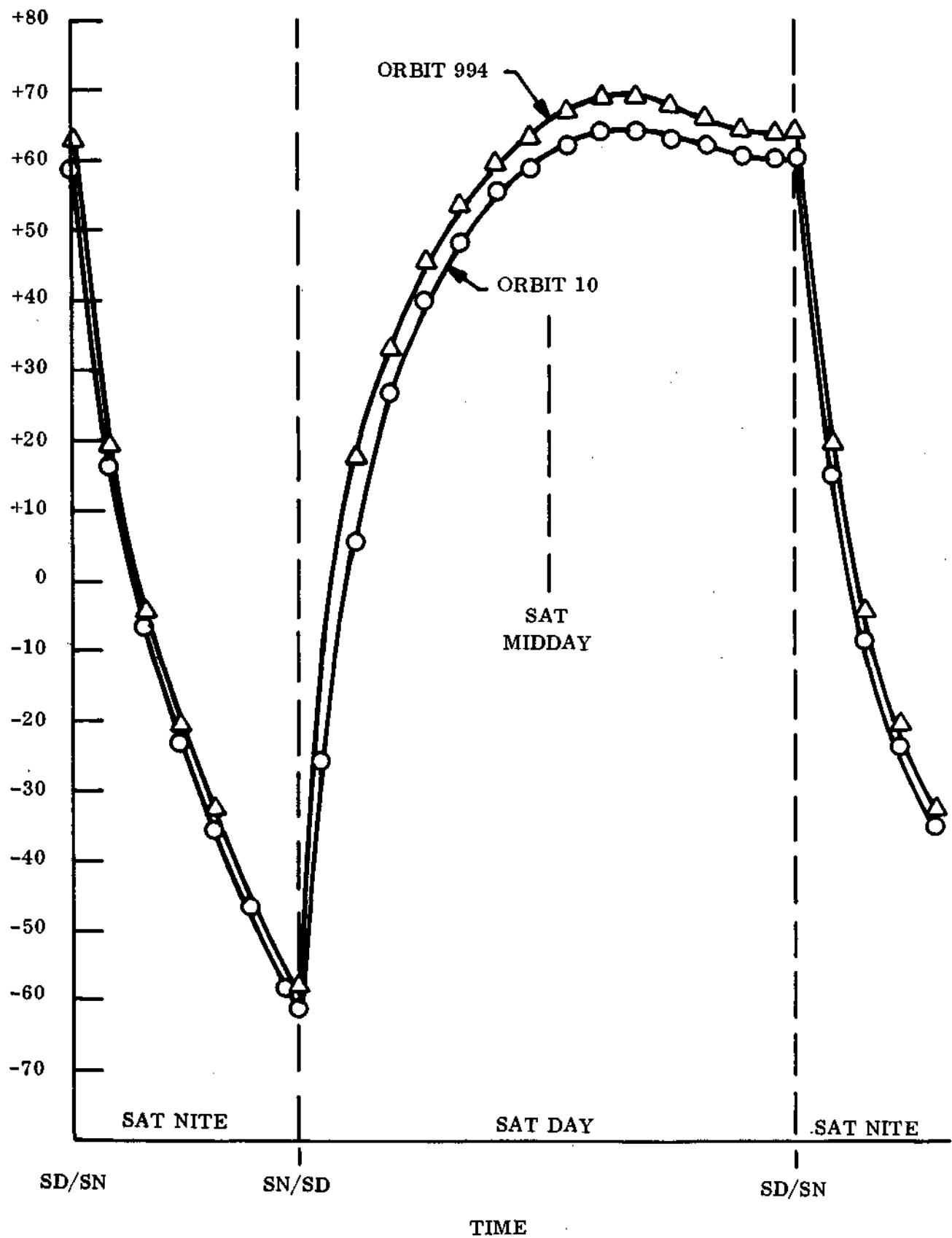


Figure 11-2. Right Solar Paddle Temperature (Function 6040)

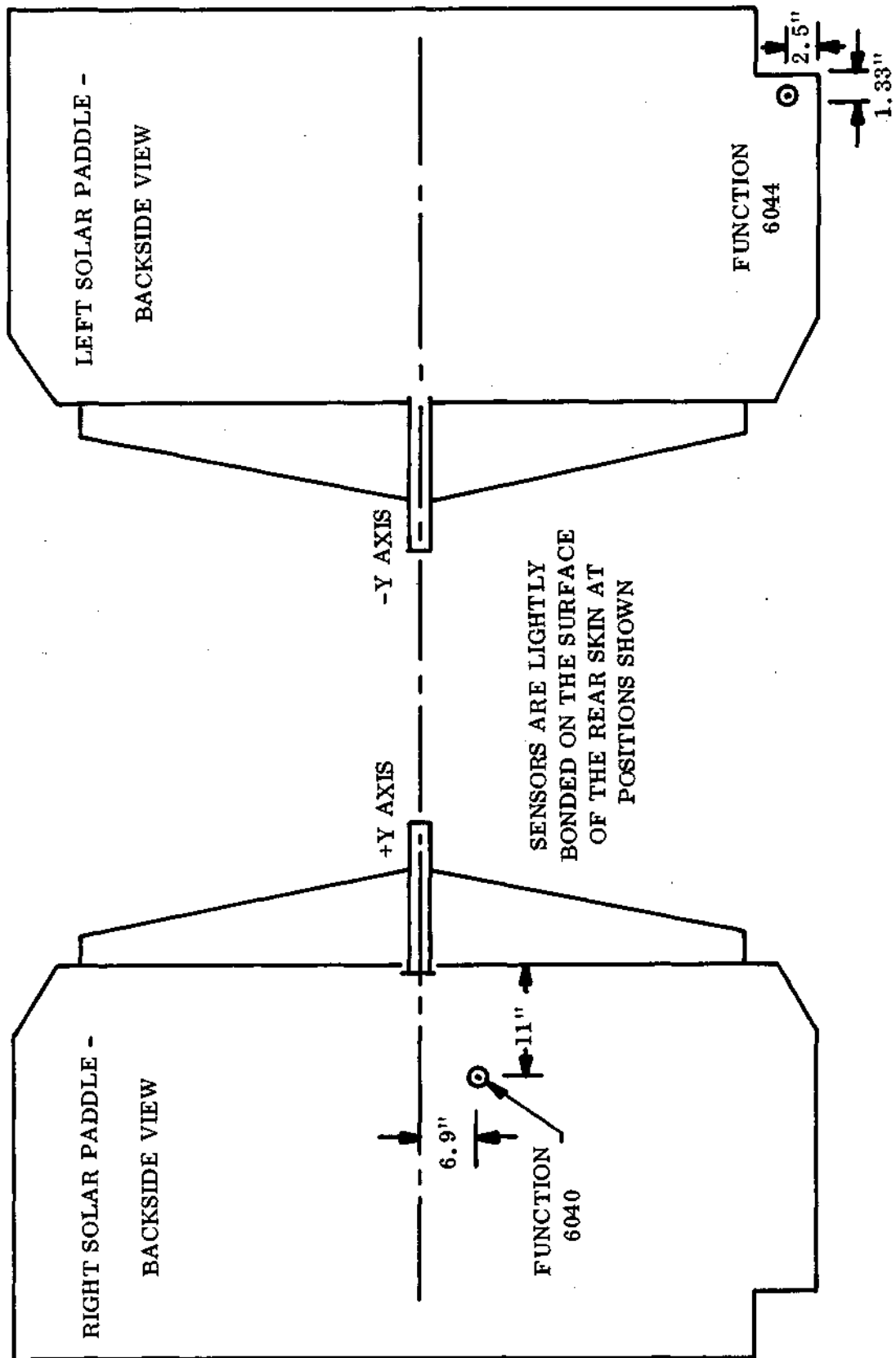


Figure 11-3. Location of Solar Array Temperature Sensors

## COMPENSATION LOADS

Compensation loads were off at launch. On orbit 2 loads 3, 4, 5, 7, and 8 were turned on to keep the sensory ring warm while the spacecraft was undergoing initial checkout. On orbit 6 loads 1 and 2 were turned on in addition to those already on. The additional loads provide more heat to the sensory ring facing away from the sun and help maintain a smaller temperature spread between batteries. After payload operation began it was decided to leave the compensation loads on as long as the temperatures remained satisfactory. On orbit 118 the loads were turned off and remained off until orbit 156. After orbit 149 normal spacecraft operation was discontinued while the failure analysis and investigation was underway. The compensation loads maintained sensory ring temperatures until operation was resumed. On orbit 194 the loads were again turned off and remained off until the RBV power failure on orbit 196. The loads were turned on in orbit 197 and a decision was made to keep them on after payload operation resumed. At orbit 701 compensation load 3 was turned off to lower the operating temperature range of the wide band tape recorder electronic unit 1 which had risen in temperature due to heavy use and the increased seasonal sun intensity. The compensation load history is shown in Table 11-2.

Table 11-2 Compensation Load History

ORBITS	COMPENSATION LOADS							
	1	2	3	4	5	6	7	8
0-1	0	0	0	0	0	0	0	0
2-5	0	0	X	X	X	0	X	X
6-117	X	X	X	X	X	0	X	X
118-155	0	0	0	0	0	0	0	0
152-193	X	X	X	X	X	0	X	X
194-196	0	0	0	0	0	0	0	0
197-700	X	X	X	X	X	0	X	X
701-1300	X	X	0	X	X	0	X	X

KEY: 0 = OFF ; X = ON

## SECTION 12

### NARROWBAND TAPE RECORDER SUBSYSTEM (NBTR)

The initial operations of the NBTR Subsystem were reported in the ERTS-1 Launch and Flight Activation Report. Since Orbit 1 the two NBTR's have alternated in Record and Playback modes in a completely satisfactory manner, with a nominal one minute overlap.

Table 12-1 lists the telemetry values for initial orbits and late orbits, showing no significant change during the period of this report.

Since launch, each recorder operated for a period of 1171 hours (including record and playback) during this reporting period.

Table 12-1. Narrowband Tape Recorder Telemetry Values

Function		Typical Telemetry Values					
		Thermal Vac Values	Rec. Mode Orbit 1	P/ B Mode		Rec. Mode Orbit 1291	Rec. Mode Orbit 1292
Number	Name			Orbit 6	Orbit 13		
10001	A - Motor Cur. (ma) Record P/ B	198 185	190.10	180.0		193.41	180.10
10101	B - Motor Cur. (ma) Record P/ B	194 185	193.26		188.18	193.47	184.50
10002	A - Pwr Sup. Cur. (ma) Record P/ B	315 540	320.56	535.78		335.50	562.21
10102	B - Pwr Sup. Cur. (ma) Record P/ B	313 535	317.62	570.78		330.74	552.10
10003	A - Rec. Temp. (DGC)	25.4	25.47	24.00	23.51	23.65	24.52
10103	B - Rec. Temp. (DGC)	23.8	24.58	22.07	24.09	24.09	23.05
10004	A - Supply (VDC)	-24.55	-24.47	-24.59	-23.02	-24.61	-24.51
10104	B - Supply (VDC)	-24.49	-24.44	-24.50	-24.60	-24.57	-24.69

## SECTION 13

### WIDE BAND TELEMETRY SUBSYSTEM

Initial turn-on and checkout of the Wide Band Telemetry Subsystem were reported in the ERTS-1 Activation Report referenced in Appendix A. This activity consisted of initial turn on of the two components of the subsystem - Wide Band Power Amplifier -1 and -2 (WPA-1 and WPA-2) - in Orbit 12 in the 10 watt mode. In orbit 20 both were tested in the 20 watt mode. WPA-1 remained in that mode thereafter. WPA-2 status was reduced to the 10-watt mode until orbit 30, after which time it, too, was put in the 20-watt mode where it has since remained.

The helix current for WPA-2 (function 12102) read 6.96 ma on orbit 30. On orbit 31 it rose to 7.6 ma and has remained between 7.3 and 7.6 ma ever since, with no long-term trend either up or down, as shown in Figure 13-1.

The RBV has not been used since orbit 196 as described in Section 6, and consequently WPA-1, its transmission link to ground stations, has also been inoperative since that time. WPA-2, serving as the transmission link for MSS to ground stations has operated nominally throughout this 90-day period. All telemetry readings have been normal as shown in the typical values of Table 13-1.

WPA-1 was powered since launch for a total period of 8 hours, 50 minutes and 21 seconds. From launch through orbit 1300, WPA-2 has been powered for a total period of 99 hours, 3 minutes and 23 seconds.

The WPA's have operated with WBR input 57 percent of the time and with MSS input 43 percent of the time.

The power output of the WPA's has remained practically constant throughout these orbits. Figure 13-2 shows the reported AGC level versus distance from the ground station. The goal of the spacecraft antenna pattern design was to provide uniform field strength at all

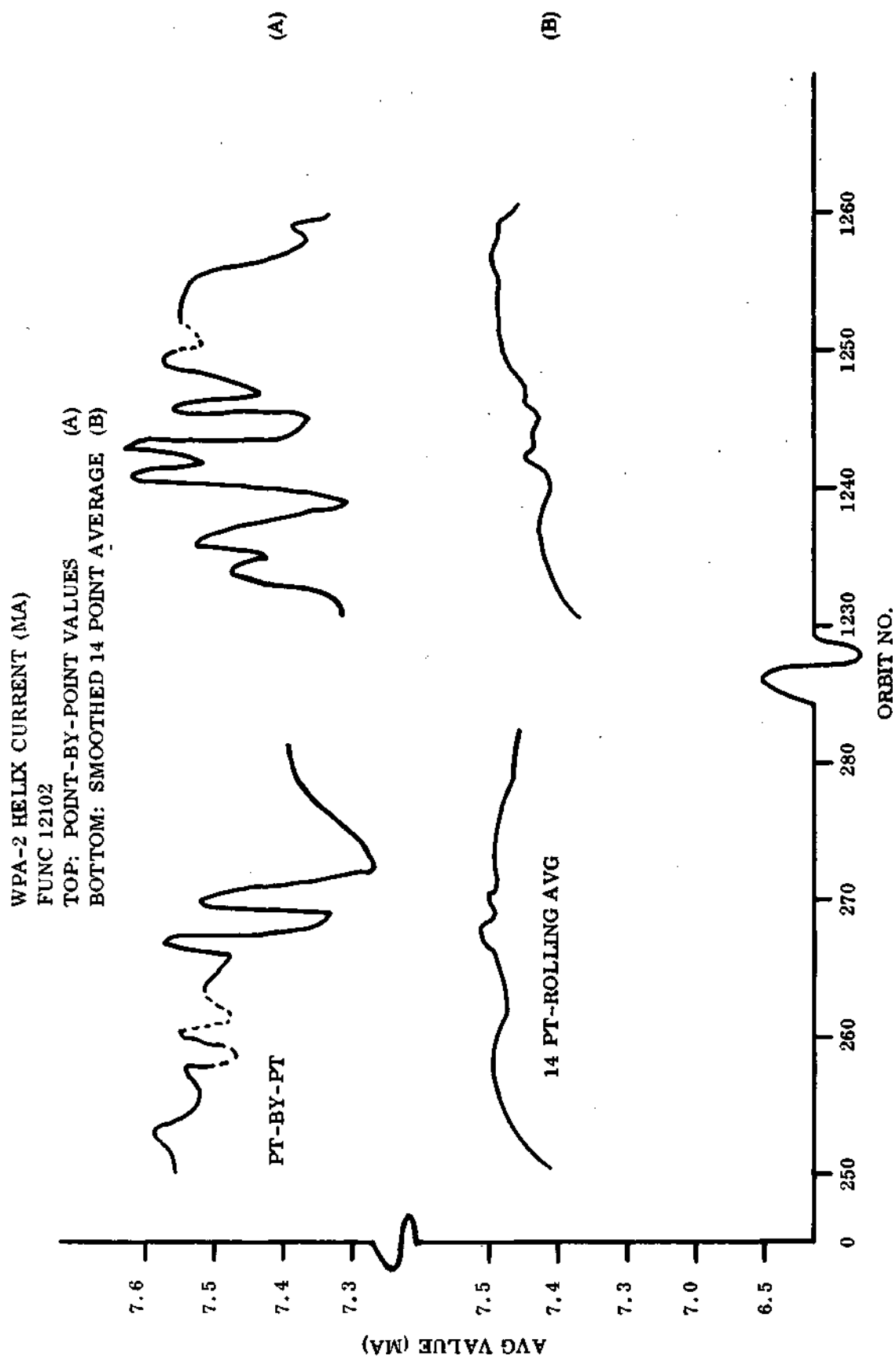


Figure 13-1. WPA-2 Helix Current (Ma) (Function 12102)



Table 13-1. Wideband Modulator Telemetry Values

WBPA-1							
Number	Function		T/ V*				
	Name		Values	26	82	144	196
12001	Temp TWT Coll.	(DgC)	38.7	35.7	35.7	35.7	37.10
12002	Helix Current	(Ma)	6.47	6.08	6.29	6.37	6.29
12003	TWT Cath. Cur.	(Ma)	45.4	45.89	45.13	45.89	45.89
12004	Forward Pwr	(DBM)	43.2	43.18	43.21	43.18	43.21
12005	Reflected Pwr	(DBM)	32.4	34.95	35.20	34.68	35.03
12227	Loop Str. AFC ConVolt	(MHZ)	(1)	-0.39	-0.49	-0.07	-0.87
12229	Mod Temp VCO	(DgC)	24.4	21.93	21.24	19.39	23.54
12232	+15VDC A <sup>(3)</sup> Pwr Sup <sup>(3)</sup>	(TMV)	2.69	2.69	2.69	2.69	2.69
12234	-15 VDC Pwr Sup A	(TMV)	5.91	5.98	5.91	5.98	5.93
12236	+5 VDC Pwr Sup A	(TMV)	4.01	3.94	4.02	4.01	3.93
12238	-5 VDC Pwr Sup A	(TMV)	5.26	5.28	5.22	5.23	5.23
12240	-24 VDC Unreg Volt A	(TMV)	5.42	5.56	5.44	5.56	5.48
12242	Inv. Temp	(DgC)	24.5	20.60	21.32	19.31	20.73
WBPA-2							
Number	Function		T/ V*				
	Name		Values <sup>(2)</sup>	33	494	911	1256
12101	Temp TWT Coll.	(DgC)	31.5	35.38	36.17	34.80	37.11
12102	Helix Current	(Ma)	5.26	7.32	7.36	7.35	7.61
12103	TWT Cath. Cur.	(Ma)	33.5	44.30	43.04	42.90	44.13
12104	Forward Pwr	(DBM)	41.2	43.57	43.48	43.50	43.57
12105	Reflected Pwr	(DBM)	30.6	31.59	32.55	32.13	32.61
12228	Loop Str HFC ConVolt	(MHZ)	(1)	1.11	0.07	-0.09	0.12
12229	Mod Temp VCO	(DgC)	24.4	21.70	23.00	23.19	21.32
12232	+15 VDC A <sup>(3)</sup> Pwr Sup	(TMV)	2.67	2.68	2.68	2.69	2.68
12234	-15 VDC Pwr Sup A	(TMV)	5.95	5.90	5.88	5.96	5.95
12236	+5 VDC Pwr Sup A	(TMV)	4.01	3.97	3.92	3.93	4.02
12238	-5 VDC Pwr Sup A	(TMV)	5.26	5.24	5.25	5.24	5.23
12240	-24.5 VDC Unreg Volt A	(TMV)	5.42	5.43	5.39	5.53	5.53
12242	Inv. Temp	(DgC)	24.5	23.03	23.00	22.24	22.69

\*Thermal Vacuum Test Data

(1) Satisfactory if not zero or -7.5.

(2) Tested T/ V in 10-watt mode; put in 20-watt mode in Orbit 30 and used in that mode since. Thermal vacuum values not representative for orbital operation, therefore.

(3) B Power Supply not used in orbit.

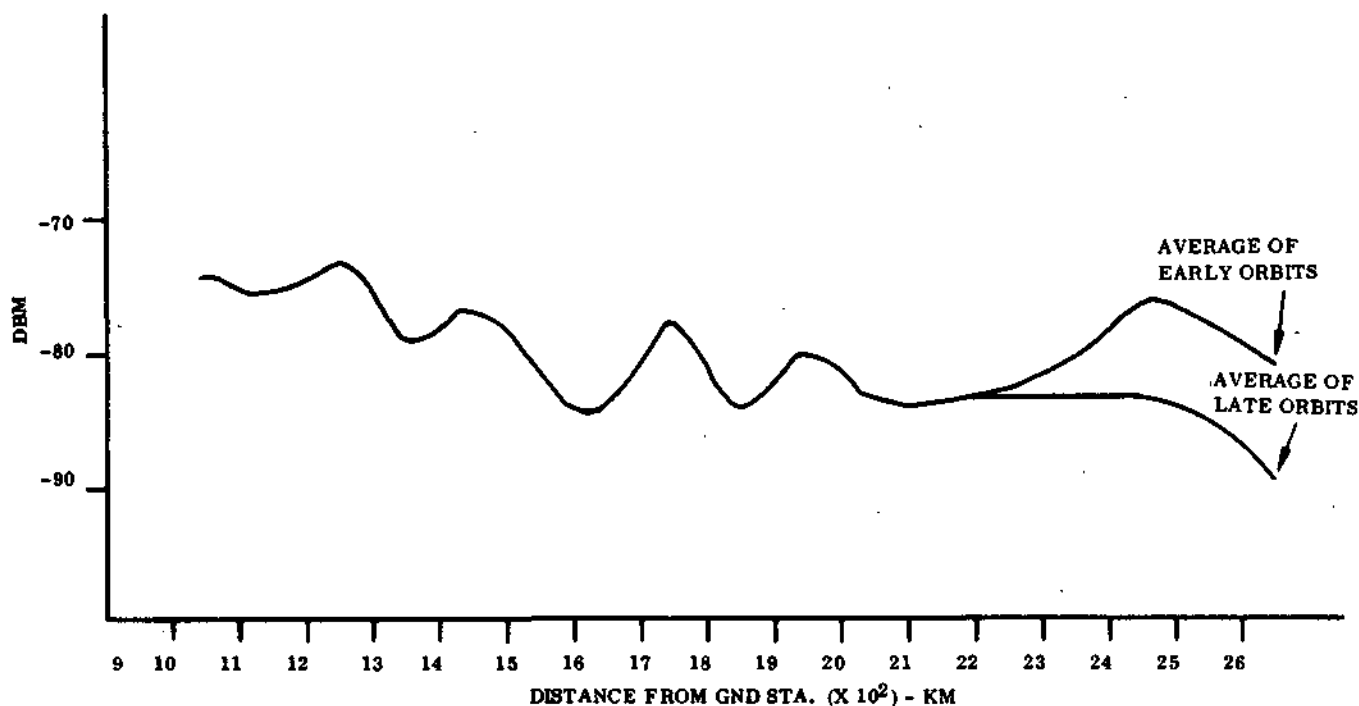


Figure 13-2. Ground Station (ULA) AGC Readings for WPA-2

points on the ground within its horizon as much as possible. The dips in Figure 13-2 represent nulls in the pattern. The field strength remains within  $\pm 5$  dB throughout its horizon. There is an apparent droop in the late orbits at maximum ranges. This aspect is explored in Figure 13-3 which plots the AGC levels at two ranges, 2000 K. M. , 2500 K. M. as a function of time. On the same time scale (orbit numbers) is plotted the telemetry power output measurement, function 12104, Forward Power for WPA-2. No decrease in power is apparent.

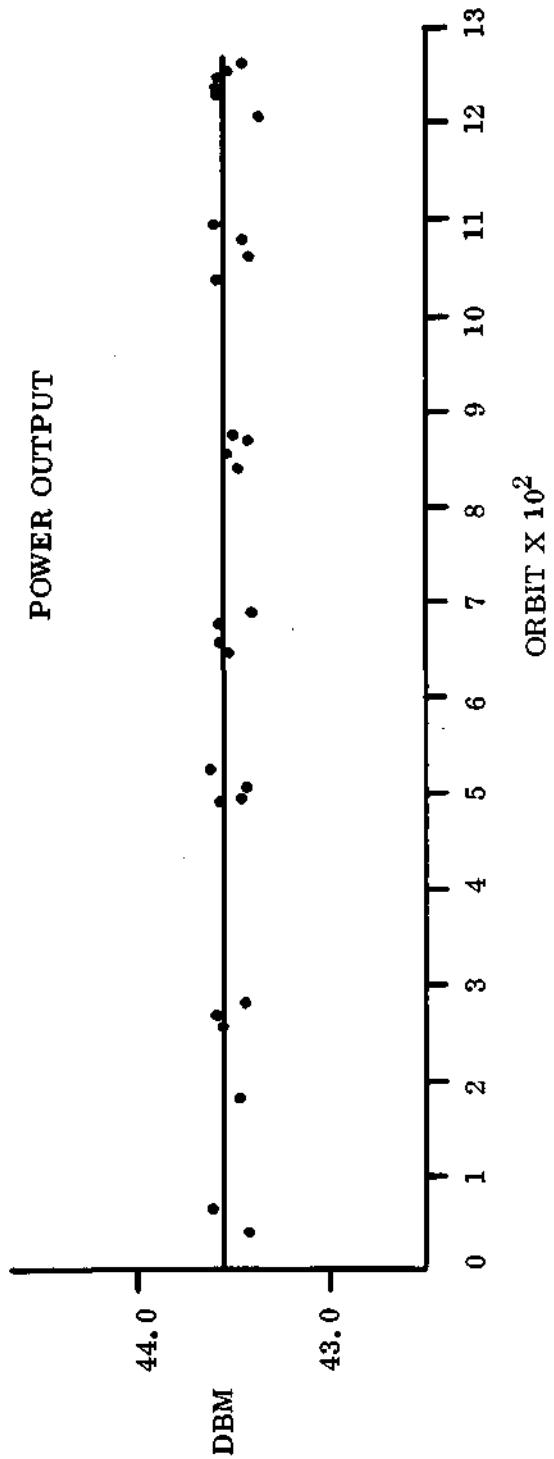
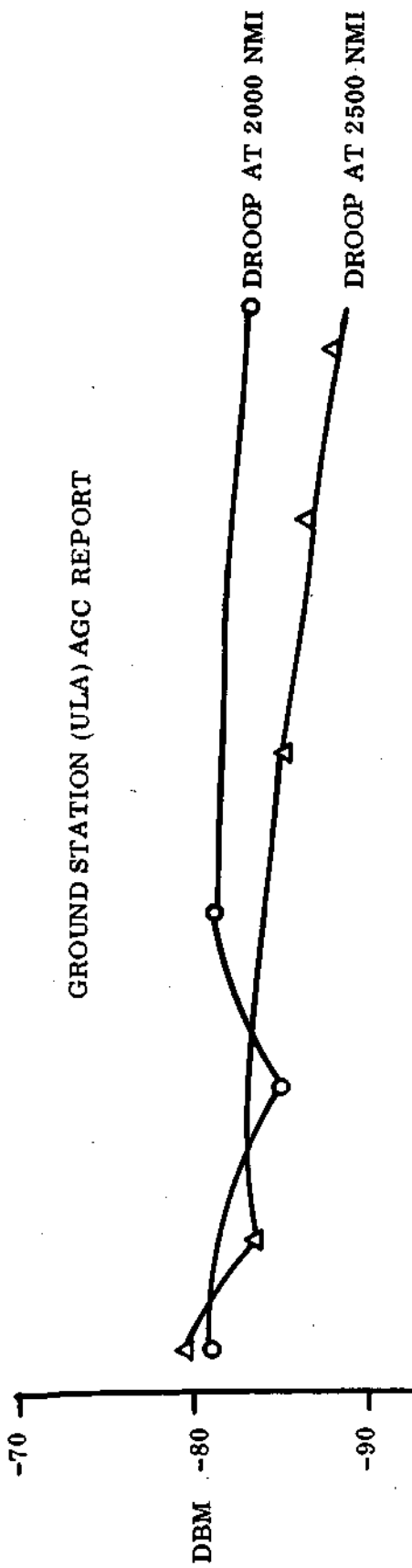


Figure 13-3. WPA 2 Power Measurement at S/C and Ground Stations

## SECTION 14

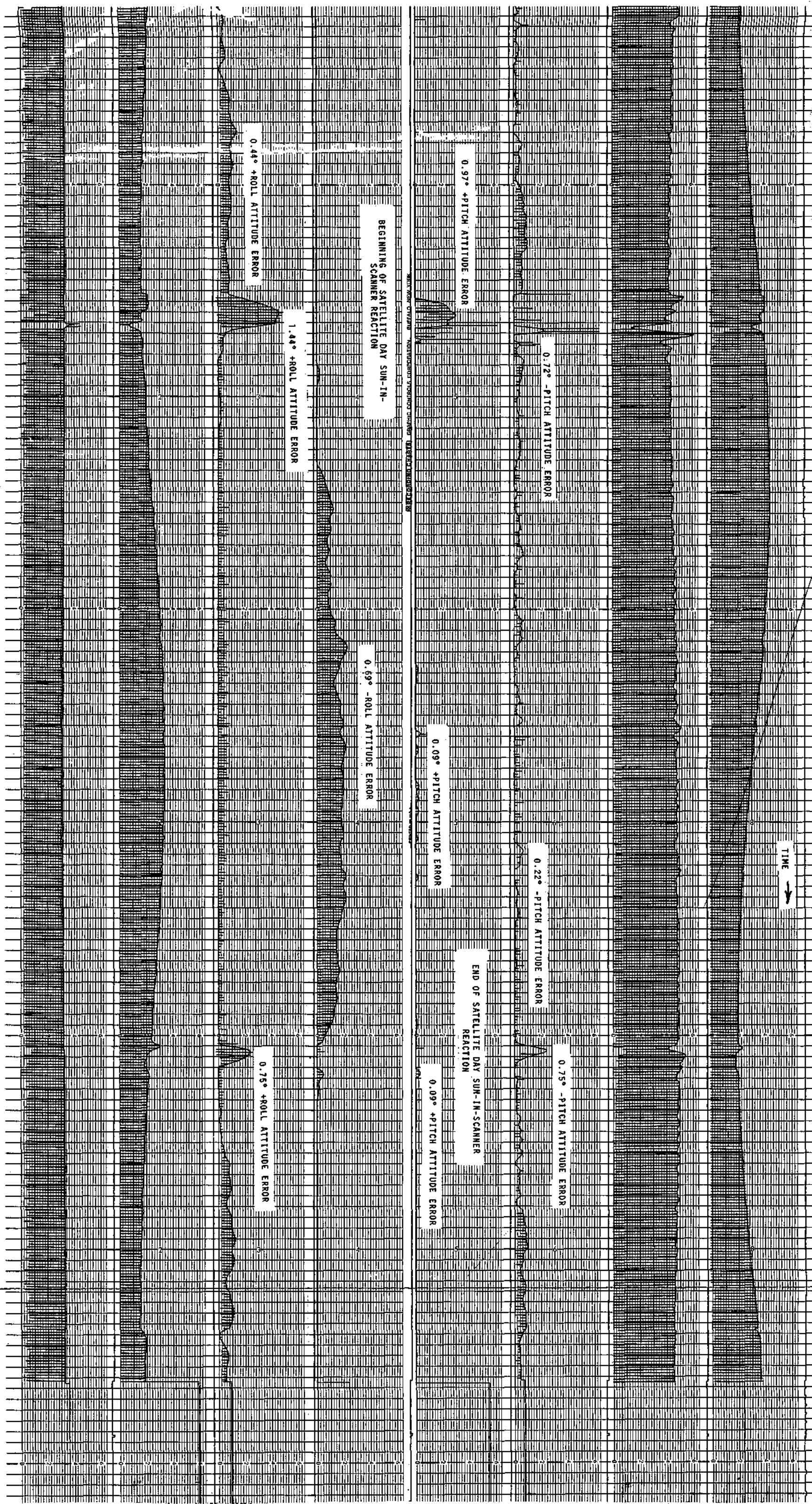
### ATTITUDE MEASUREMENT SENSOR (AMS)

The AMS has consistently produced attitude values which seem reasonable. Since no direct precise correlation can be made with the Attitude Control System the AMS values are accepted. Effort is continuing to refine techniques to evaluate AMS performance. Derived values are being used for MSS image processing in the Bulk processing subsystem. Figure 14-1 shows a strip chart presentation of a typical orbit. Table 14-1 gives typical AMS telemetry values.

Table 14-1. AMS Temperature Telemetry Summary

Function No.	Name	Units	* T/V 20°C Plateau	35	500	900	1300
3004	Case - Temp 1	°C	19.1	18.92	19.03	19.25	19.61
3005	Assembly - Temp 2	°C	18.9	19.15	19.34	19.57	19.91

\*Thermal Vacuum Test Data



CHARGE	DUMP	CHARGE	DUMP	-	+	-	+	IN	OUT	IN	OUT	IN	OUT
MMCA CAP	MMCA CAP	MMCA CAP	MMCA CAP	MMCA POL	MMCA POL	MMCA POL	MMCA POL	MMCA Y	MMCA P	MMCA P	MMCA R	MMCA P	MMCA R
K2	K3	K3	K4	K5	K6	K7	K8	COIL	COIL	COIL	COIL	COIL	COIL
1/16	1/16	1/16	1/16	1/16	1/16	1/16	1/16	1/16	1/16	1/16	1/16	1/16	1/16
4008	4009	4010	4011	4012	4013	4014	4015	4016	4017	4018	4019	4020	4021

ROLL FWD MOTOR	ROLL FWD MOTOR	ROLL REAR MOTOR	ROLL REAR MOTOR	PITCH MOTOR	PITCH MOTOR	YAW MOTOR	YAW MOTOR
DR CW	DR CCW	DR CW	DR CCW	DR CW	DR CCW	DR CW	DR CCW
ROLL LEAD AMP	ROLL DIFF TACH	AMS + ROLL	AMS - ROLL	AMS PITCH +	AMS PITCH -	PITCH FW SPEED	YAW TACH AMP
OUT	AMP OUT						
0228/0504	1218/0604	1854/0903	1009/1103	1554/1303	0846/0404	0209/1301	0819/0601
1/16 1/1	1/16 1/1	1/16 1/1	1/16 1/1	1/16 1/1	1/16 1/1	1/16 1/1	1/16 1/1
1024/1020	1023/1021	1025/3000	1022/3001	1039/3002	1038/3003	1033/1043	1034/1036

Figure 14-1. Attitude Measurement Sensor Performance Characteristics Type

## SECTION 15

### WIDE BAND VIDEO TAPE RECORDERS (WBVTR-1 AND WBVTR-2)

Initial turn-on and checkout of the WBVTR's were reported in the ERTS-1 Launch and Flight Activation Report, 72SD4255 dated 18 October, 1972.

This activity consisted of turn On and Rewind in Orbit 5; Playback in Orbit 15; and Record in Orbits 20 and 21 for the WBVTR-2; and in Orbit 26 for WBVTR-1.

After this preliminary verification stage, the two WBVTR's were put into normal operation, sequencing thru Record, Rewind, Playback, and Rewind operations. WBVTR-1 is normally configured to RBV, and WBVTR-2 to MSS. All operations were normal until orbit 148. During this orbit, while recording MSS data a probable short in WBVTR-2 from secondary power supply to ground resulted in excessive noise currents throughout the spacecraft grounding system. This apparently happened during the final minute of the video recorded session in Orbit 148, (see Figures 15-1, 15-2, 15-3) as deduced from RBV data recorded on WBVTR 1 in Orbit 148 because telemetry was inadvertently lost during Narrow-Band Recorder playback in Orbit 149 (see Appendix B). On Orbit 149, when WBVTR-2 was commanded On in preparation for recording MSS data, the USB telemetry downlink simultaneously turned Off. When it was turned back On, large transients were observed in the telemetry from the Spacecraft Power and the Attitude Control Subsystems. A simultaneous turn Off of RBV, MSS and both WBVTR's caused all telemetry noise indications to stop immediately, and the spacecraft began normal recovery from a  $30^{\circ}$  pitch up and  $8^{\circ}$  roll attitude. See Figure 15-4 for strip chart display. None of these payload systems was turned back On until Orbit 180, in order that careful analyses of telemetry records, and simulation bread-board tests could clarify the nature of the anomaly. The most probable cause was determined to be a power short to ground in WBVTR-2. Because this short cannot be removed or by-passed, this recorder has not been used since Orbit 149. On Orbit 180 the payloads above were turned back On and operated normally.

On Orbit 187 WBVTR-1 was re-configured from the RBV equipment to the MSS replacing the inoperative WBVTR-2. It has been operating in that configuration since that time. All telemetry readings have been normal as shown in the typical values of Table 15-1.

WBVTR-2 was powered since launch for a total period of 9 hours, 26 minutes and 33 seconds. From launch thru Orbit 1300, WBVTR-1 has been powered for a total period of 124 hours, 57 minutes and 54 seconds.

The WBVTR's have operated about 15% longer in Playback than they have in Record, because of the need to provide overlap, and to guard against uncertainty in the footage count.

In order to measure the fidelity of the Wide Band Video Tape Recorder Subsystem against time, the MSS Minor Frame Sync Error (MFSE) was used as a figure of merit. The average MFSE count over 10-second intervals was compared between real-time MSS data transmissions and Playback MSS data transmission during adjacent orbits to provide a uniform test basis (i. e. the same ground equipment and test personnel); only the observations at Alaska were used.

MFSE count for Real-Time transmissions were invariably zero. It was then only necessary to plot the count for Playback mode against orbits. In Figure 15-5, the error count for typical orbits distributed over the 90 day time interval is shown. During P/B of multiple segment recorded data, the error rate count increased significantly during the transition from one data interval to the next recorded interval (due to time required to get the recorder up to recording speed).

It is evident that WBVTR-1 is performing well with no major degradations. The high error rate counts noted in the tabulation are transition counts, i. e., obtained at the transition between two recorded intervals. It is significant that there are no consecutive readings of high error rate counts during a single P/B which would be indicative of recorder problems or data degradation.

No apparent decline in WBVTR fidelity can be seen in this chart throughout the 90 day operating period.

Figure 15-6 is a strip chart for a typical orbit. This strip chart displays 12 functions shown on Table 15-1 for the active parts of this orbit. Increasing time is to the right.

Each vertical line represents about 1 minute. The sequence of events are:

04:50:55	WBR-1	Playback
04:59:37		Standby
05:07:03		Rewind
05:09:12		Standby
05:09:14		Off
05:24:34	WBR-1	On
05:24:36		Standby
05:24:40		Record
05:28:08		Off

Table 15-2 shows the values for the indicated functions for each operational mode in this orbit. These values are typical for all orbits.



Table 15-1. WBVTR Telemetry Values

WBVTR-1 Functions			Telemetry Values				
Number	Name		In	In Orbits			
			T/ V*	15	500	913	1251
13022	Pressure Trans	(PSI)	16.3	16.12	16.25	16.36	16.32
13023	Temp Trans	(DgC)	22.0	19.50	20.53	22.91	22.68
13024	Temp Elec	(DgC)	28.7	22.78	25.41	24.79	23.79
13026	Capstan Speed	(%)	98.0	100.51	101.16	99.70	99.54
13027	Headwheel Speed	(%)	99.6	95.16	90.31	96.68	94.82
13028	Capstan Mot I	(Amp)	0.24	0.25	0.27	0.23	0.24
13029	Input P/ B Volt.	(VVP) ②	0.76	0.72	0.44	0.42	0.43
13030	Headwheel Mot I	(Amp)	0.55	0.55	0.57	0.50	0.53
13031	Rec Input I	(Amp)	3.55	3.15	3.32	2.68	3.02
13032	Lim Volt Out	(VPP)	1.48	1.44	1.46	1.46	1.41
13033	Servo Volt	(%)	50.0	50.03	50.03	50.25	49.99
13034	+5.6 VDC Conv	(VDC)	5.66	5.66	5.92	5.77	5.86
13200	-24.5 VDC	(VDC)	①	-24.91	-24.91	-24.90	-24.90
13201	-12 VDC	(VDC)	①	-12.08	-12.08	-12.08	-12.08
13202	Temp APU	(DgC)	①	25.79	26.30	26.74	26.86

WBVTR-2 Functions			Orbit Number				
Number	Name		In				
			T/ V *	15	64	103	147
13122	Pressure, Trans	(PSI)	③	15.99	16.25	16.25	16.11
13123	Temp Trans	(DgC)		18.46	19.19	20.72	21.09
13124	Temp Elec	(DgC)		21.50	22.00	24.00	21.92
13126	Capstan Speed	(%)		99.91	100.53	100.80	99.38
13127	Headwheel Speed	(%)		94.16	95.48	97.64	98.78
13128	Capstan Mot I	(Amp)		0.17	0.24	0.24	0.28
13129	Input P/ B Volt.	(VPP)		0.66	0.63	0.62	0.61
13130	Headwheel Mot I	(Amp)		0.55	0.59	0.52	0.53
13131	Rec Input I	(Amp)		3.70	3.53	3.07	3.43
13132	Lim Volt. Out	(VPP)		1.34	1.41	1.41	1.39
13133	Servo Volt	(%)		49.47	49.60	49.80	49.48
13134	+5.6 VDC	(VDC)		5.47	5.64	5.58	5.59
13200	-24.5 VDC	(VDC)		-24.91	-24.90	-24.90	-24.90
13201	-12 VDC	(VDC)		-12.08	-12.08	-12.08	-12.09
13202	Temp APU	(DgC)		25.79	26.31	27.64	26.19

\*Thermal Vacuum Test Data

1 Thermo Vac Values not given

2 After Orbit 196 WBVTR-1 configured to MSS: Thermo Vac Value then 0.40.

3 Thermal Vacuum Data are not available for WBVTR-2.

Table 15-2

## Function Values by Mode in Orbit 913

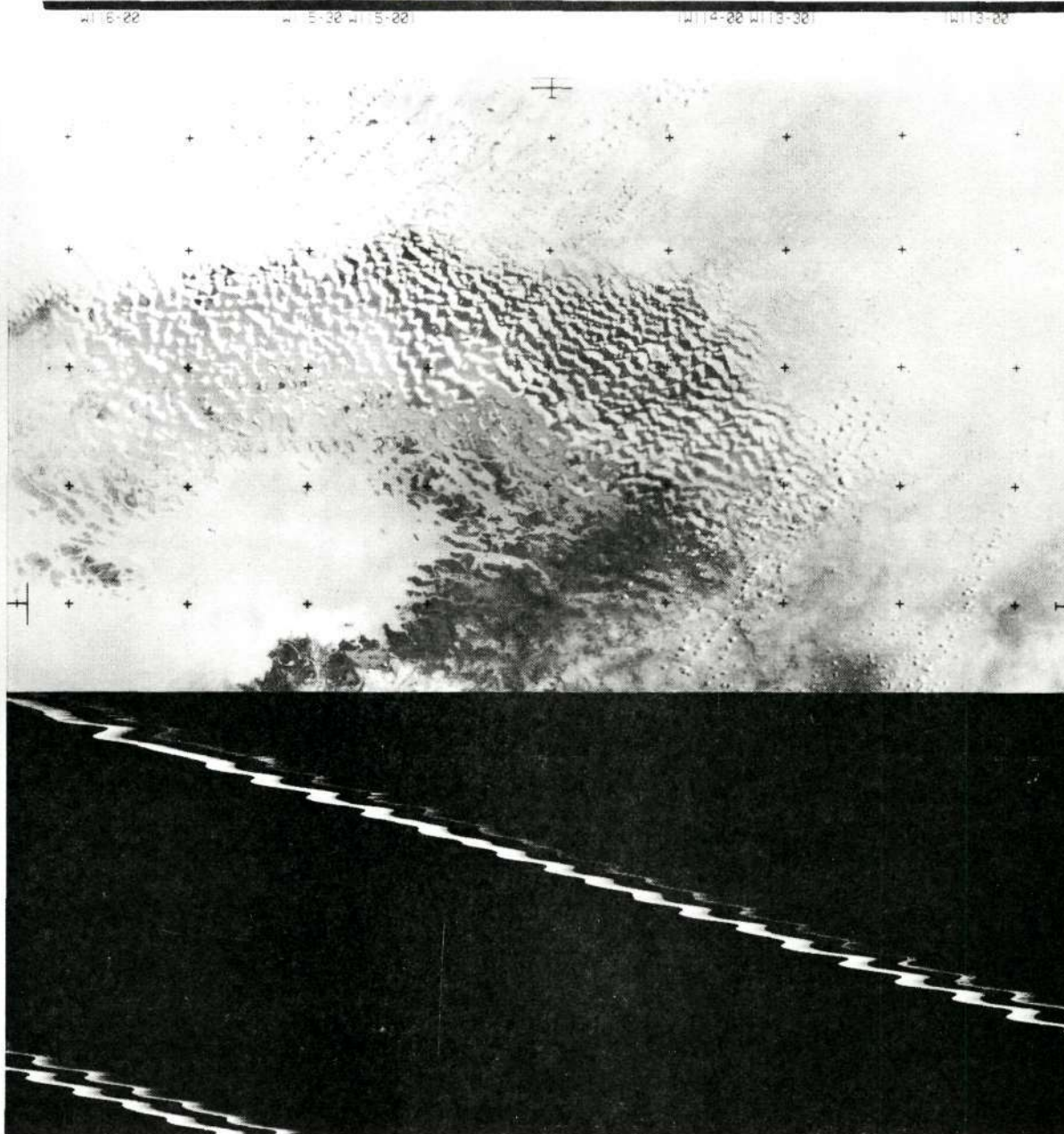
Function	Playback		Standby		Rewind		Record	
	T/V	913	T/V	913	T/V	913	T/V	913
13034	5.66	5.30	5.86	5.75	5.86	5.69	5.63	5.58
13029	0.37	0.40	0	0	0	0	0	0
13028	0.25	0.25	0	0	0.18	0.23	0.28	0.23
13030	0.56	0.56	0.45	0.47	0.50	0.47	0.55	0.58
13031	3.27	3.85	2.04	1.96	2.16	2.20	3.55	3.70
13022	16.3	16.9	16.3	16.9	16.3	16.9	16.3	16.9
13032	1.48	1.47	0	0	0	0	0	0
13033	50.0	50.30	0	0	0	0	0	0
13026	98.0	98.40	0	0	102.20	101.70	99.60	98.50
13027	99.7	97.10	103.10	100.70	101.90	100.72	99.60	97.10
13023	22.0	22.0	22.0	22.0	22.0	22.0	22.0	22.0
13024	28.7	25.0	28.7	25.0	28.7	25.0	28.7	25.0



Figure 15-1. Last Triplet Exposed in Orbit 148

(During remote recording readout from camera 3 (first camera to readout) normal.  
Exposure time 216:08:50:38.)

Reproduced from  
best available copy.



W116-001 W115-30 W115-001 W114-00 W113-301 W113-00  
17 ABCDEFGHIJKL MNOPQRS RV 2 DXB Z 1 2 3 4 5 6 7 8 9 RNC EFGHIJKL MNOP 2 01

Figure 15-2. Last RBV Triplet Exposed in Orbit 148

During remote recording readout from camera 2 normal until 08:50:43.5  
when video breaks up and loses sync.

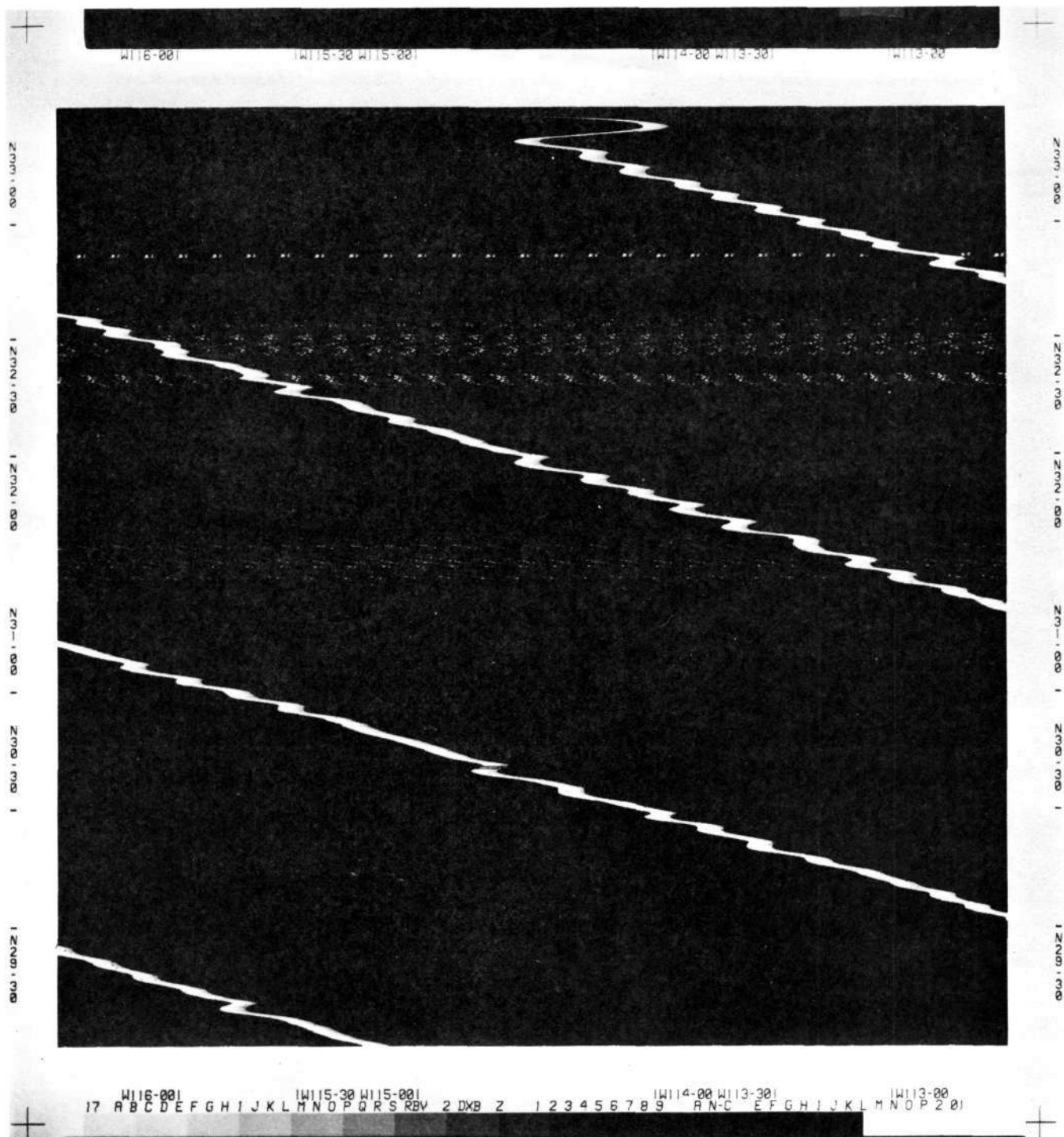
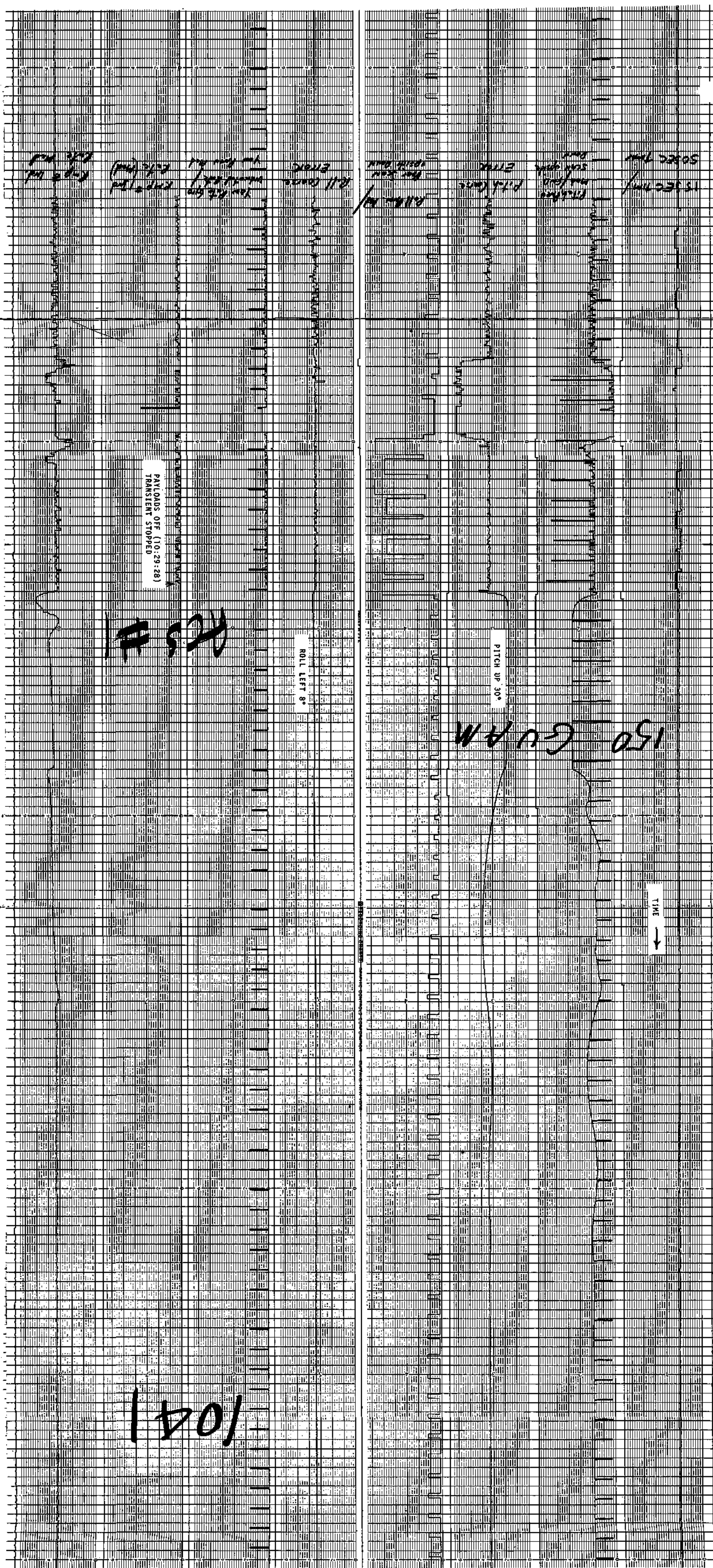


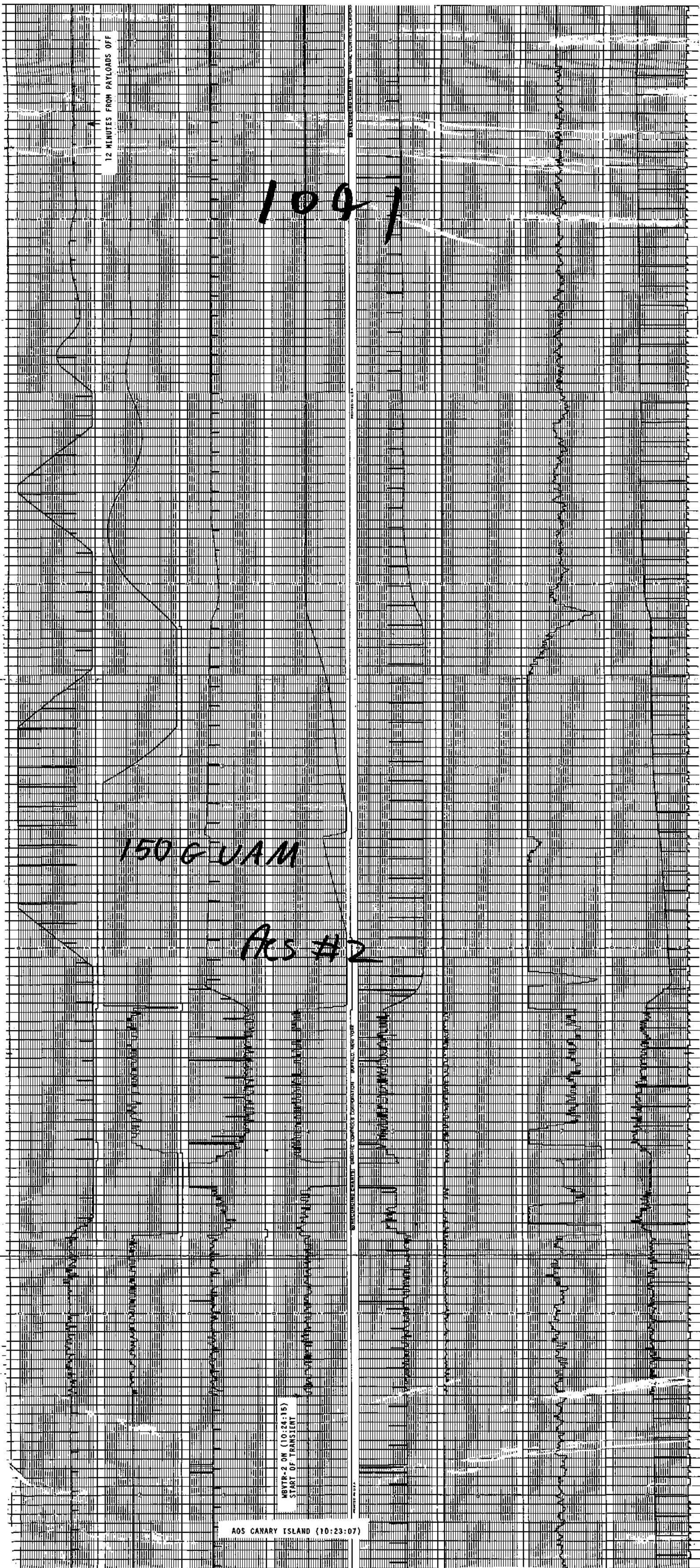
Figure 15-3. Last RBV Triplet Exposed in Orbit 148

During remote recording readout from camera 1 continues to show video breakup and loss of sync. At next turn on (during station pass-CY1) of WBVTR-2 in Orbit 149 transients were noticed immediately. (See Figure 15-4.)



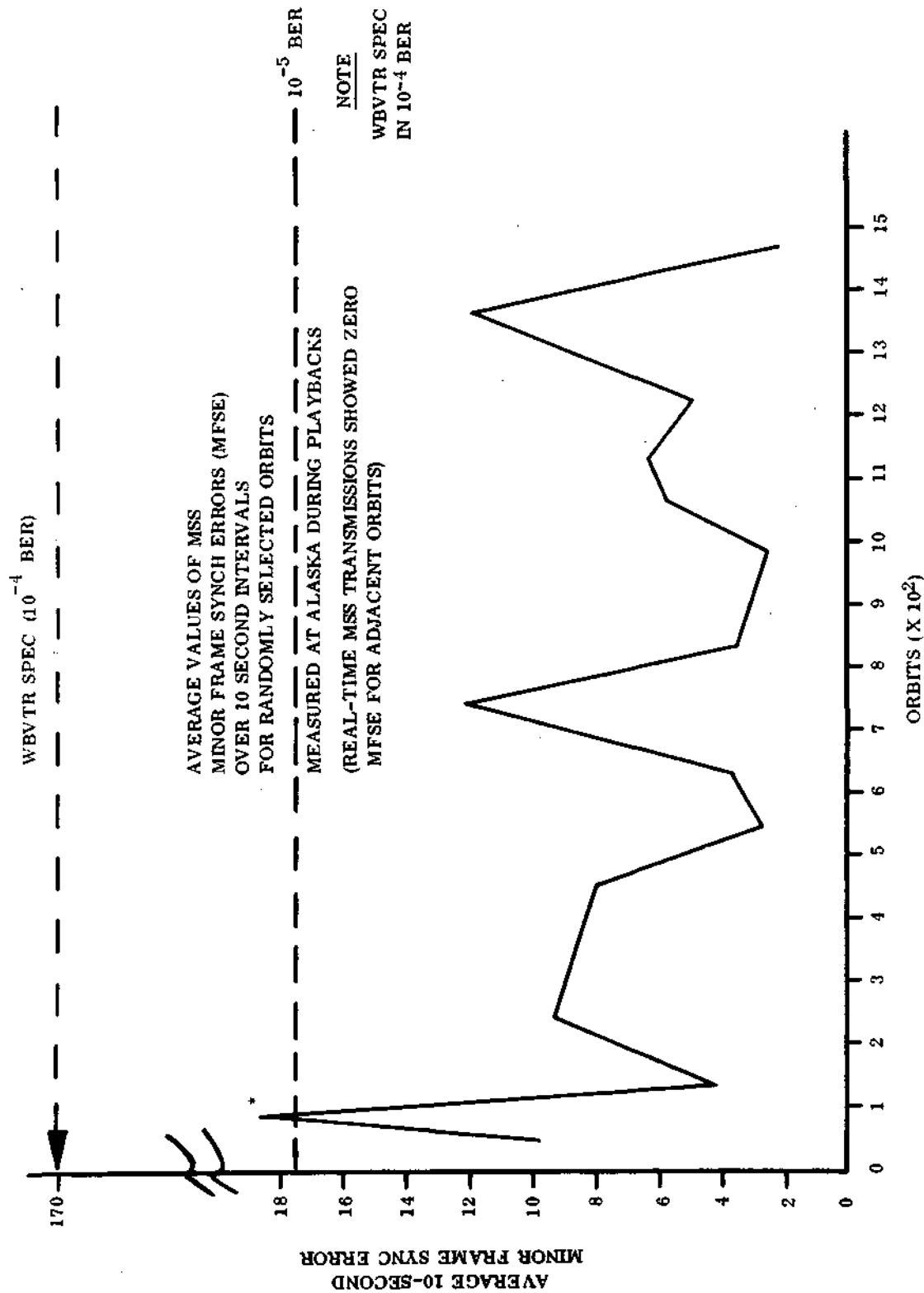


17 **FOLDOUT FRAME**



- PITCH SOL. 1065		+ PITCH SOL. 1064		- ROLL SOL. 1063		+ ROLL SOL. 1062		SCAN 1 1008		SCAN 2 1017		SCAN DS. SLT. 1291											
<div><div>0</div><div>250 RPM-250 RPM</div><div>+4.25°</div><div>0°</div><div>-5.0°</div><div>500</div><div>RPM</div><div>1500</div><div>+4.5°</div><div>0°</div><div>-6.0°</div><div>500</div><div>RPM</div><div>1500</div><div>+12°/h</div><div>0°/h</div><div>+12°/h</div><div>-10°/h</div><div>0°/h</div><div>+10°/h</div><div>+1950</div><div>0</div><div>-10</div><div>RPM</div></div>																							
PITCH F/W SPEED/ ROLL DIFF. TACH.				PITCH FINE ERROR		ROLL FWD. F/W SPEED/ ROLL FINE ERROR		ROLL REAR F/W SPEED/ ROLL FINE ERROR		RMP IND. RATE #1 (HI-RES.)		RMP IND. RATE #2 (HI-RES)		YAW TACH AMP. OUT ± PITCH POS. BIAS/ A&B STATUS									
STATUS 1301/0864				1101 1/1		CLB # A CLOCK 1106/1872		0601 1/1		CLB # B CLOCK 1300/0108		0901 1/1		1102 1/1		0601/1235 1/1 1/16							
1043/1031				1041		1026/1053		1030		1027/1054		1087		1097		1035/1049							

Figure 15-4. Strip Chart For Orbit 149 WBVTR 2 Anomaly



\* ATTRIBUTED TO START STOP ERRORS, NO HIGH MFSE NOTED DURING DATA AT RUN SPEED

Figure 15-5. Average Values of MSS Minor Frame Sync Error (MFSE) over 10 Second Intervals for Randomly Selected Orbits





## SECTION 16

### RETURN BEAM VIDICON (RBV)

Initial turn-on and checkout of the RBV subsystem were reported in the ERTS-1 Activation Report referenced in Appendix A. This activity consisted of an abortive test in orbit 19 and a complete test in orbit 26.

Subsequently the RBV was used operationally through 91 On-Off cycles. Neglecting the pre-initiation orbits (0-18) and the payloads-off interval following the WBVTR-2 failure (reported in Section 15), the RBV was operated in 65% of the remaining orbits. 1690 scenes were photographed covering 14.7 million square nautical miles of earth surface.

Beginning with orbit 187, the RBV was used in a real-time mode only, because its normally associated WBVTR-1 was reconfigured to the MSS (see Section 15). Throughout its operation, the RBV equipment operated normally as shown in the telemetry values of Table 16-1, which are typical.

During orbit 196 when the RBV was turned ON for a real-time pass over Alaska, a short to ground occurred in the Power Switching Module (PSM) between the Payload Regulated Bus and ground. A high current transient peak of about 200 amperes occurred for approximately half a second, after which the RBV operated normally throughout its scheduled picture-taking operations. When the scheduled time for turn OFF arrived, the cameras failed to turn off by all normal means. Auxiliary means - disabling of the Payload Regulator Module - were used to disconnect the RBV. Subsequently, each RBV component was commanded off and the Payload Regulator Module was turned back on.

Investigations, analyses, and breadboard tests led to the conclusion that the failure is integral to the PSM between the relay and the RBV fuses, and that the RBV itself was not the cause of the failure, nor affected by it.

Table 16-1. RBV Telemetry Values

FUNCTION		ORBITS				
NO.	NAME	T/V VALUE	26	85	149	196
14001	CCC Board Temp. (DgC)	(1)	18.61	20.04	19.30	19.53
14002	CCC Pwr. Sup. Temp (DgC)	(1)	19.93	21.58	20.70	21.21
14003	+15 VDC Sup. (TMV)	3.95	3.69	3.95	3.78	3.95
14004	+6V-5.25 VDC Sup. (TMV)	3.05	2.84	2.93	2.98	3.05
14100	VID OUT CAM 1 (TMV)	1.06	1.04	1.15	1.13	1.12
14200	VID OUT CAM 2 (TMV)	1.09	1.05	1.26	1.23	1.24
14300	VID OUT CAM 3 (TMV)	1.05	1.03	1.21	1.19	1.20
14102	Comb. Align I Com 1 (TMV)	3.95	3.67	3.94	3.87	3.94
14202	Comb. Align I Com 2 (TMV)	3.92	3.90	3.91	3.89	3.91
14302	Comb. Align I Com 3 (TMV)	4.04	3.75	4.03	3.80	4.03
14103	Cam 1 Elec Temp. (DgC)	(1)	20.84	23.37	22.64	25.38
14203	Cam 2 Elec Temp. (DgC)	(1)	18.64	21.06	20.62	22.87
14303	Cam 3 Elec Temp. (DgC)	(1)	21.05	23.61	23.23	25.57
14104	Cam 1 LV Pwr Sup T. (DgC)	(1)	21.71	23.94	23.49	25.92
14204	Cam 2 LV Pwr Sup T. (DgC)	(1)	18.38	20.63	19.40	23.30
14304	Cam 3 LV Pwr Sup T. (DgC)	(1)	20.75	23.02	22.73	25.67
14105	Cam 1 Def. + 10 VDC (TMV)	4.01	3.73	4.00	3.77	4.00
14205	Cam 2 Def. + 10 VDC (TMV)	4.00	3.71	3.98	3.77	3.98
14305	Cam 3 Def. + 10 VDC (TMV)	3.97	3.95	3.95	4.02	3.95
14106	Cam 1 + 6V -6.3 VDC (TMV)	3.71	3.45	3.70	3.61	3.70
14206	Cam 2 + 6V -6.3 VDC (TMV)	3.69	3.42	3.67	3.49	3.67
14306	Cam 3 +6V -6.3 VDC (TMV)	3.73	3.47	3.72	3.47	3.72
14107	Cam 1 Telec I (TMV)	2.62	2.50	2.54	2.55	2.64
14207	Cam 2 Telec I (TMV)	2.65	2.53	2.56	2.41	2.64
14307	Cam 3 Telec I (TMV)	2.64	2.54	2.51	2.45	2.61
14108	Cam 1 Vid Fil I (TMV)	2.47	2.30	2.36	2.38	2.46
14208	Cam 2 Vid Fil I (TMV)	2.54	2.37	2.52	2.39	2.52
14308	Cam 3 Vid Fil I (TMV)	2.61	2.44	2.60	2.53	2.60
14110	Cam 1 TARVOLT (TMV)	3.43	3.42	3.42	3.45	3.42
14210	Cam 2 TARVOLT (TMV)	3.36	3.13	3.22	3.26	3.32
14310	Cam 3 TARVOLT (TMV)	3.47	3.23	3.46	3.45	3.47
14113	Cam 1 Vert Def V (TMV)	2.96	2.75	2.90	2.85	2.97
14213	Cam 2 Vert Def V (TMV)	3.00	2.86	2.98	2.86	3.01
14313	Cam 3 Vert Def V (TMV)	3.45	3.45	3.47	3.37	3.45
14114	Cam 1 Vid FPT (DgC)	(1)	18.15	20.77	17.91	20.99
14214	Cam 2 Vid FPT (DgC)	(1)	20.62	20.11	20.52	20.62
14314	Cam 3 Vid FPT (DgC)	(1)	18.54	20.88	19.08	20.20
14115	Cam 1 Foc Coil T (DgC)	(1)	17.71	21.67	18.74	19.70
14215	Cam 2 Foc Coil T (DgC)	(1)	17.70	21.60	19.25	19.97
14315	Cam 3 Foc Coil T (DgC)	(1)	18.03	22.09	19.88	20.56

(1) Thermo-Vacuum temperatures for these functions were not reported.

Alternate modes of RBV power switching are available, but have not yet been used. The RBV has remained in the OFF condition since orbit 196. See Figure 16-1 for Strip Chart Display of Anomaly. A more extensive discussion of this anomaly is contained in Appendix B.

In Appendix C a scene in the vicinity of Phoenix, Arizona is analyzed for the three RBV bands and the four MSS bands.

Annotation was judged well within measurement uncertainty. Resolution was judged to be in agreement with analytic expectations. Location Accuracy was less than desired. Radiometric Transfer Functions were obtained and showed some double values near the highest radiance end of the gray scale, but were judged to have negligible effect because only a small fraction (like 3%) of the scenes had density readings low enough to be double-valued. Radiometric Measurements are plotted for sand, rock and crop areas, as well as the equivalent reflectance in cloud-shadowed areas.

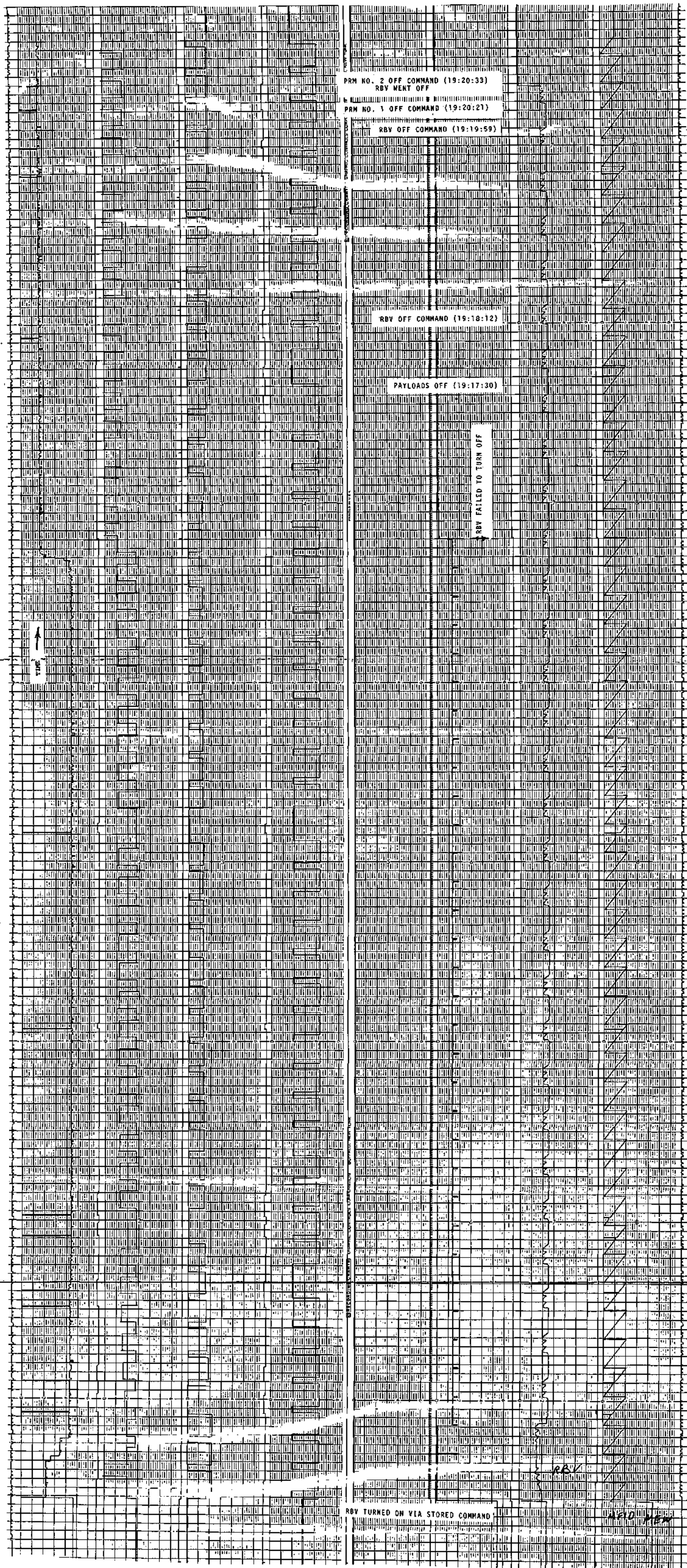
In Appendix C, 18 ground points common to both RBV and MSS images were compared to check NDPF relative registration accuracy. The report concludes that the NDPF is approaching the pre-launch goals.

In Appendix C, an assessment is made of the RBV and MSS resolution. It concludes that the resolution is in close agreement with expected performance, the resolution being about 80 meters.

FOLDOUT FRAME 1

FOLDOUT FRAME 2

FOLDOUT FRAME 3



OFF ON MSS PWR/HI VOLT 1000-0201 15001-15006	OFF ON RBV SHTR/PWR 0102-1201 14014-14017	OFF ON DE ENA RBV CC PWR/MAG COMP 0202-0100 14015-14409	NO YES WBR 1-REWIND 1109 13005	NÓ YES WBR 2 RCO/PB 1703-1604 13008-13004	NO YES WBR 2 STBY/RWO 1604-0202 13101-13105	NO YES WBR 2 RCO/PB 1703-1604 13102-13104	
5.5A 13.5	ON 65°C 17° 2°C	ON 67°C 17° 0°C	0 8 15 22 30 1 11 18 24 32 1.75	AMP 1.5 3.95	25 33 40 28 34 41	5 10 15	
S/C REG BUS-CURRENT 0600-1302 1/1 6055-6056	WFM +15V INV. A/ WPA CLTR TEMP 1 1510/1243 1/16 12232/12001	WFM +15V INV. B/ WPA CLTR TEMP 2 0125/1043 1/16 12233/12101	WBR 1&2 TAPE MIN. 1031/1849 1/16 13025/13125	WBR 1 INPUT 1 0704 1/1 13031	WPA 1/2 REF 1 PWR DBM 1876/1879 1/16 12005/12105	P/L REG. BUS 0702/1704 1/1 6072/6100	MFID 1/1

GENERAL STATUS 2

Figure 16-1. Orbit 196, RBV Anomaly Strip Chart

## SECTION 17

### MULTISPECTRAL SCANNER SUBSYSTEM (MSS)

Initial turn-on and checkout of the MSS subsystem were reported in the ERTS Activation Report 72SD4255 dated 18 October 1972. This activity consisted of initial turn-on and checkout of modes in Orbit 20, with a sun calibration in Orbit 21.

The subsystem has subsequently been put in operational use in the Prime-Low-Linear mode, with sun calibrations in the Prime-Low Compressed mode. During the period of this report, the MSS had 947 cycles of ON-OFF operations and took images of 18,194 scenes, covering  $158.55 \times 10^6$  square nautical miles of the earth's surface, amounting to 3 times the total earth land mass. The operating on-time was 173 hours, 4 minutes and 49 seconds. Except for lower-than-expected sun calibration outputs, and a gradual decrease with time of the calibration wedge amplitude which are currently under investigation, the performance of the MSS has been completely satisfactory. A more detailed discussion and analysis follows.

There have been no command anomalies associated with the MSS over this period.

There has been no telemetry anomalies traceable to the MSS. All telemetry (SCEST analog telemetry printout) has been examined and typical orbits tabulated as in attached Table 17-1. The FOPT is cycling in the  $18^{\circ}\text{C}$  to  $20^{\circ}\text{C}$  range and the max mux temperature over a 20 + minute on period reaches  $30^{\circ}\text{C}$ .

Measured line length varied from 3215 to 3225 words during S/C testing over nominal temperature ranges. Table 17-2 is a sampled tabulation of line lengths obtained in orbits. No problems are evident.

Mid scan symmetry is evaluated by commanding mid scan code on and processing the resultant data to 70 mm film, and dimensionally measuring the mid scan assuming 3220 elements per line. This method was adapted as it yields a measure of EBR variations during film processing. Data is as tabulated below.

Table 17-1. MSS Telemetry Values

FUNC.#	NAME	T/V Val %	20	409	921	1256
15044	FOPT 2 T	(DGC) 20.5	17.46	18.55	19.84	20.10
15046	ELEC CVR T	(DGC) 21.5	19.37	20.86	21.76	21.98
15048	SCAN MIR REG T	(DGC) 22.8	16.35	19.27	20.26	20.37
15050	SCAN MIR DR. COIL T	(DGC) 22.4	15.94	18.44	19.75	19.85
15052	ROT SHUT HSG T	(DGC) 20.8	16.91	18.09	19.35	19.61
15043	FOPT 1 T	(DGC) 20.6	17.67	18.75	20.04	20.26
15045	MUX PWR CASE T	(DGC) 22.4	21.19	23.76	22.53	22.86
15047	PWR SUP T	(DGC) 21.6	17.41	19.22	20.28	20.44
15049	SCAN MIR DR. ELC T	(DGC) 22.8	16.12	19.09	20.00	20.09
15051	SCAN MIR HSG T	(DGC) 21.1	15.60	17.97	19.37	19.64
15040	MUX -6 VDC	(TMV) 3.95	4.03	3.99	3.94	4.03
15042	AVG DENS DATA	(TMV) 1.76	1.67	2.20	2.08	2.00
15054	CAL LAMP CUR A	(TMV) 1.06	1.08	1.11	1.10	1.09
15056	BAND 2 $\pm$ 15 VDC	(TMV) 5.05	5.10	5.06	4.99	5.10
15058	BAND 4 $\pm$ 15 VDC	(TMV) 5.00	5.10	5.06	4.99	5.10
15060	+12 - 6VDC REG	(TMV) 4.90	4.82	4.98	4.92	5.02
15062	+19 VDC REC OUT	(TMV) 4.81	4.80	4.96	4.89	4.84
15064	BAND 1 HV A	(TMV) 5.21	5.10	5.10	5.12	5.12
15066	BAND 2 HV A	(TMV) 4.46	4.50	4.50	4.52	4.52
15068	BAND 3 HV A	(TMV) 4.58	4.60	4.63	4.62	4.62
15070	SHUT MOT CON OUT	(TMV) 2.46	2.43	2.50	2.46	2.43
15041	A/D CONV REF V	(TMV) 5.82	5.93	5.89	5.80	5.93
15053	SCAN MIR REG V.	(TMV) 4.44	4.42	4.58	4.52	4.46
15055	BAND 1 $\pm$ 15V	(TMV) 4.94	4.97	4.97	4.97	4.97
15057	BAND 3 $\pm$ 15V	(TMV) 4.94	5.00	4.96	4.89	5.00
15059	-15 VDC TEL.	(TMV) 5.02	5.02	5.02	5.02	5.02
15061	+5VDC LOGIC REG	(TMV) 4.80	4.82	4.77	4.79	4.81
15063	-19 VDC REG OUT	(TMV) 3.42	3.43	3.51	3.48	3.44
15071	SCAN MIR DR. CLK	(TMV) 1.94	1.93	1.98	1.96	1.97

\* THERMAL VACUUM TEST DATA

(HV SUPPLY B NOT USED YET IN ORBIT)

Table 17-2. Sampled Tabulation of Line Length Code (LLC)

LLC (WORDS)					
ORBIT	DATA	MIN	MAX	MEAN	CONFIG.
20	VD	3221	3221	3221	P-L-C
111	VD	3219	3219	3219	P-L-C
131	SC	3223	3223	3223	P-L-L
209	VD	3223	3223	3223	P-L-C
220	VD	3222	3233	3222.0	P-L-C
326	SC	3221	3222	3221.4	P-L-L
403	VD	3218	3219	3219.0	P-L-C
500	VD	3220	3221	3220.1	P-L-L
521	SC	3221	3221	3221	P-L-L
619	SC	3221	3221	3221	P-L-L
640	VD	3220	3220	3220	P-L-C
696	VD	3220	3220	3220	P-L-C

NOTE - VARIES AS 3219 to 3220 THRU ORBIT 1300

NOTES - VD=VIDEO DATA, SC=SUNCAL, P-L-C=PRIMARY-LOW- COMPRESSED,  
P-L-L = PRIMARY - LOW - LINEAR



<u>Source</u>	<u>Mid Scan Symmetry</u>	<u># Elements (LS to MS)</u>
V/T	0.4995	1608.4
Orbit 103	0.5009/0.5006	1612.9/1611.9
Orbit 326	0.5000	1610

It has been noted in thermal vacuum testing at Valley Forge that all sensors in Bands 1, 2 and 3 exhibited calibration wedge saturation except for sensor #5 which was slightly out of saturation. The general form of the saturated calibration wedge is shown in Figure 17-1.

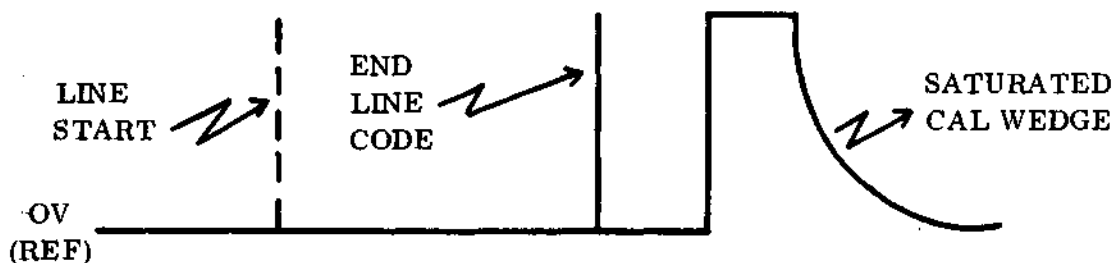
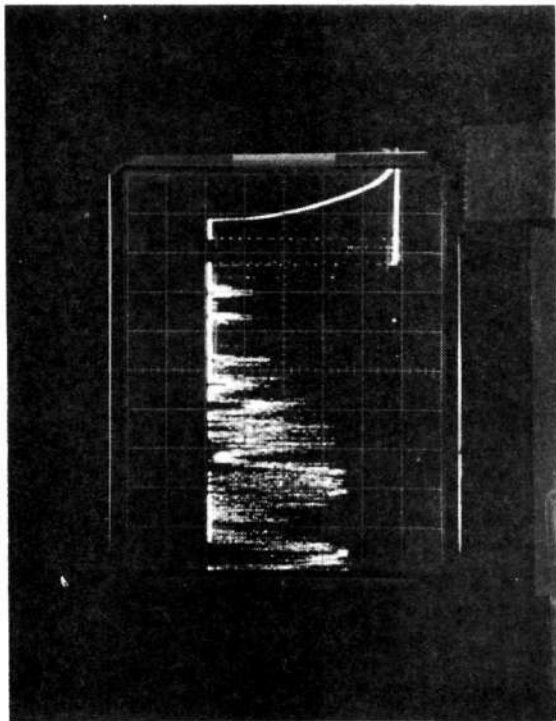


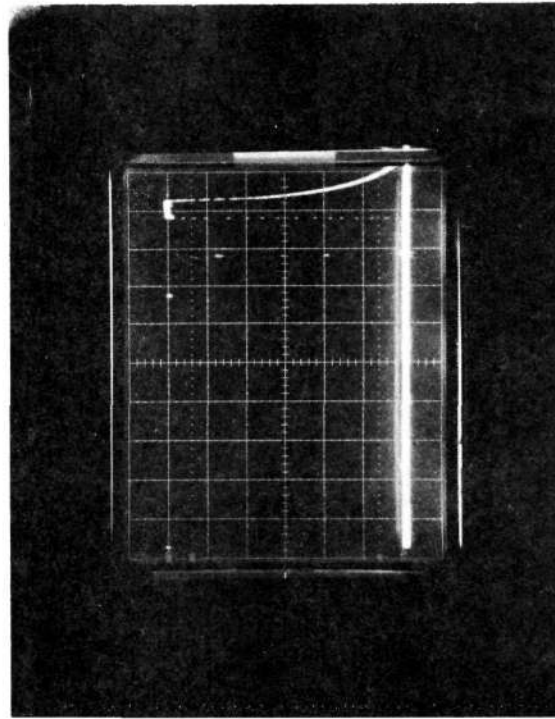
Figure 17-1. MSS Calibration Wedge

Note that when the calibration wedge shows saturation, both end of line code and the saturated portion of the calibration wedge are at the same level above ground (level 63) irrespective of scope scale values.

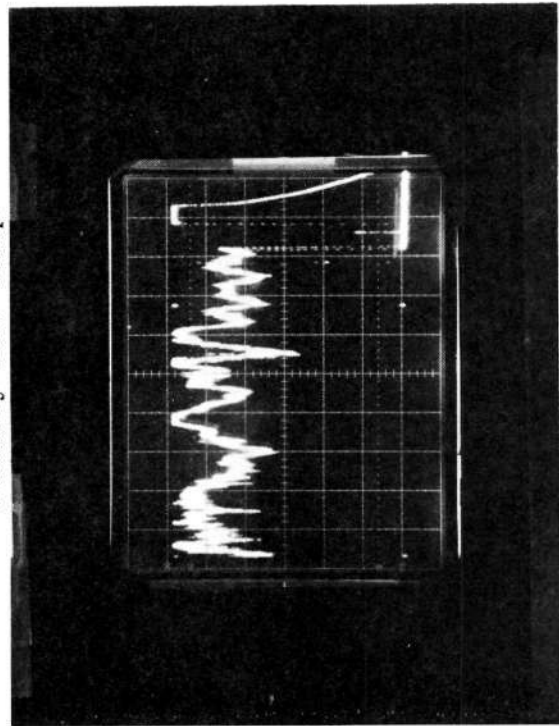
It was noted on day 225 that some of the sensors in Band 1 had come out of saturation by slight amounts. The scope photos of Figure 17-2 show the degradation clearly. Day 208 photos (3 days after launch) show previously noted thermal vacuum observations. Day 225 scope pix shows degradation in channel 3. Later observations during tape screening show all Band 1 channels have come out of saturation.



Orbit 208 - Channel 1  
Primary-Low-Comp

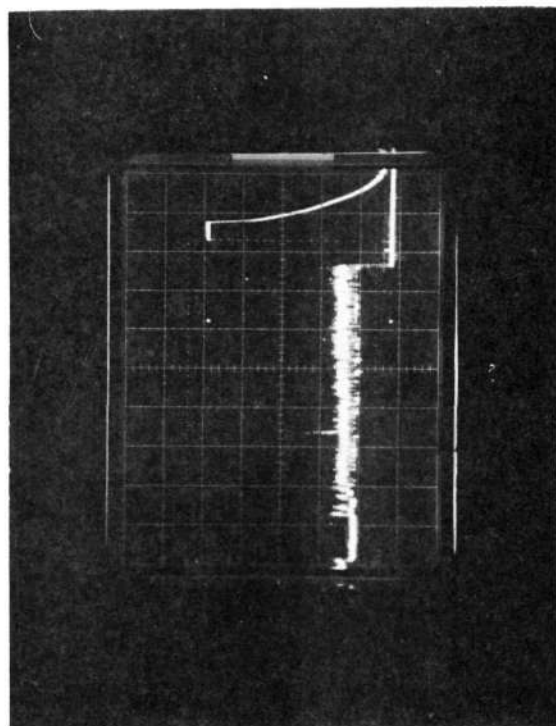


Orbit 243 - Channel 1  
Primary-Low-Linear

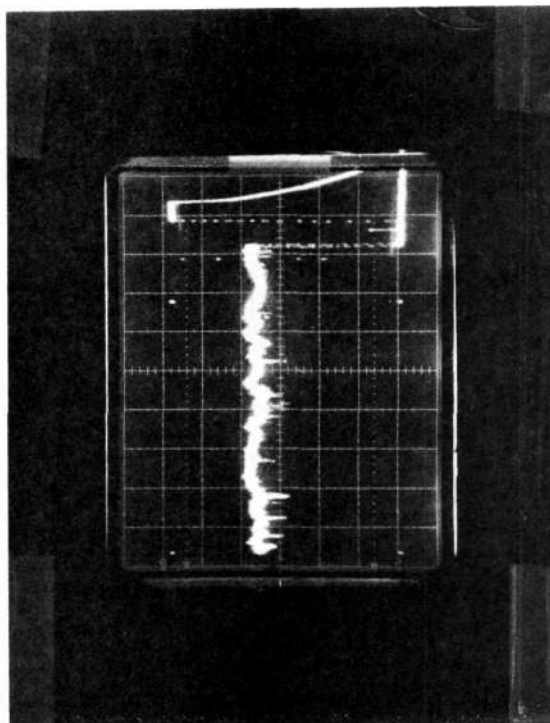


Orbit 225 - Channel 1  
Primary-Low-Comp

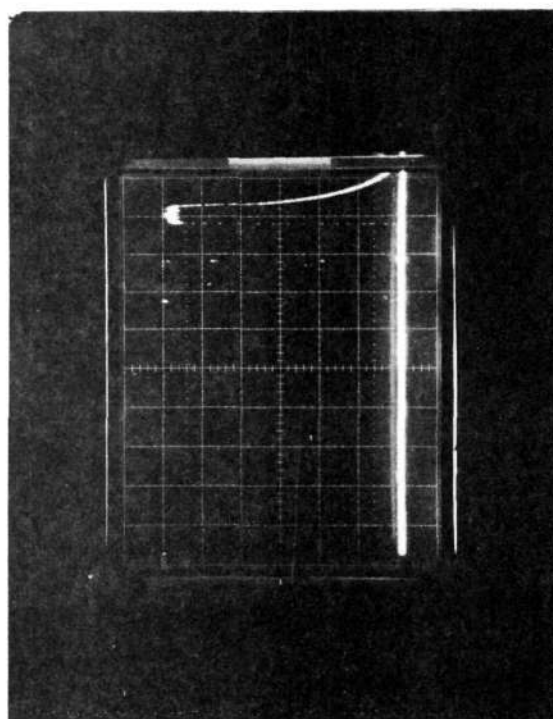
Figure 17-2. MSS Orbital Sensors Response



Orbit 208 - Channel 2  
Primary-Low-Comp

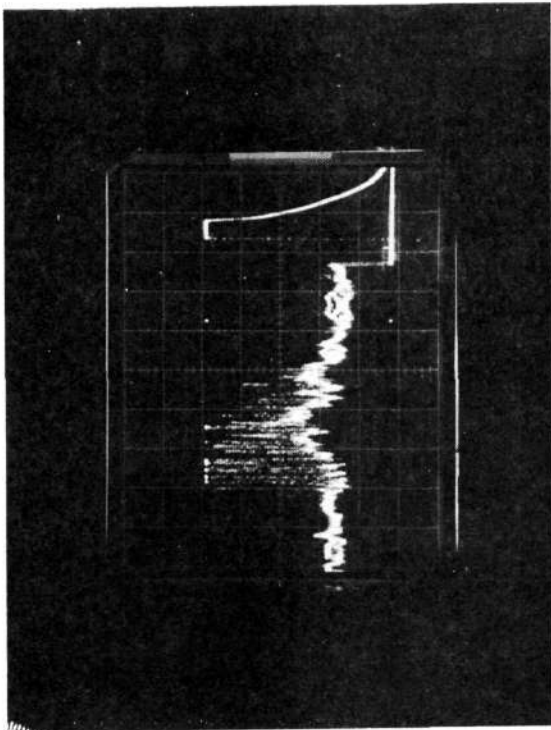


Orbit 225 - Channel 2  
Primary-Low-Comp

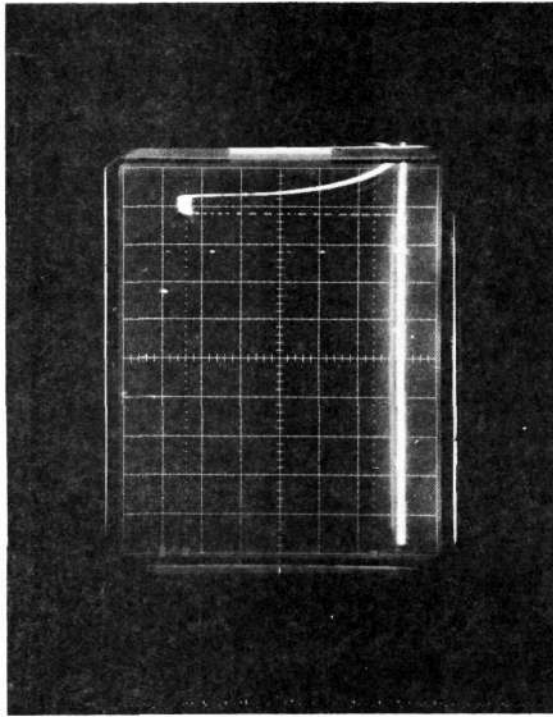


Orbit 243 - Channel 2  
Primary-Low-Linear

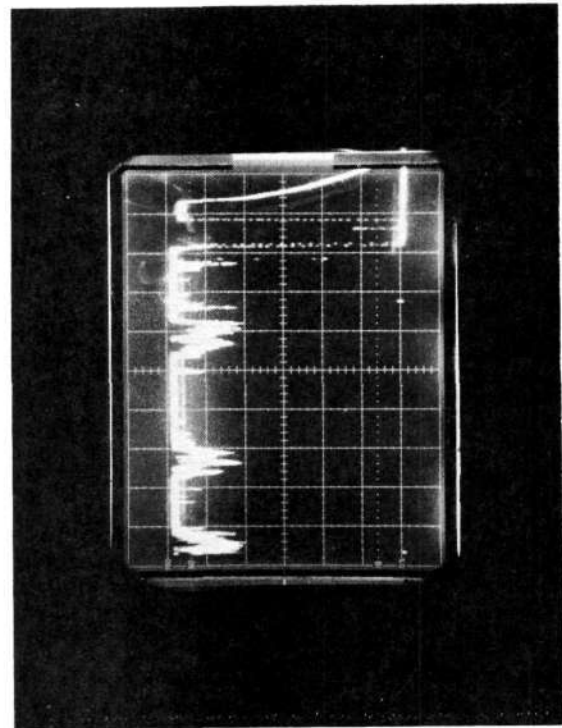
Figure 17-2. MSS Orbital Sensors Response (Cont)



Orbit 208 - Channel 3  
Primary-Low-Comp

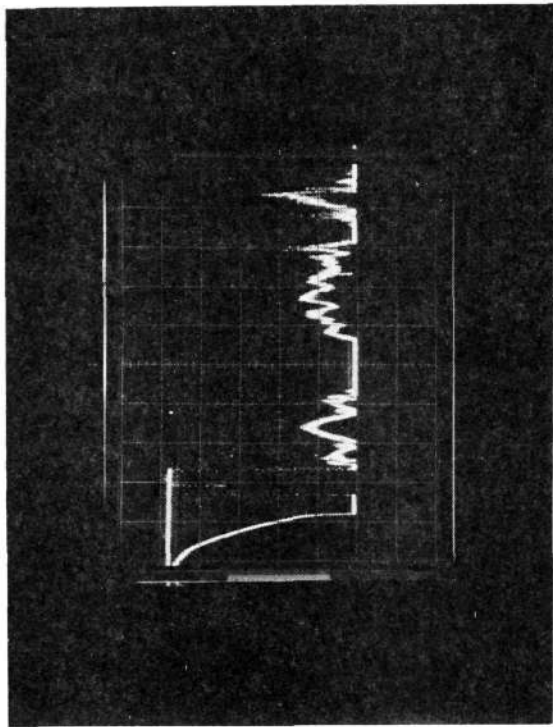


Orbit 243 - Channel 3  
Primary-Low-Linear

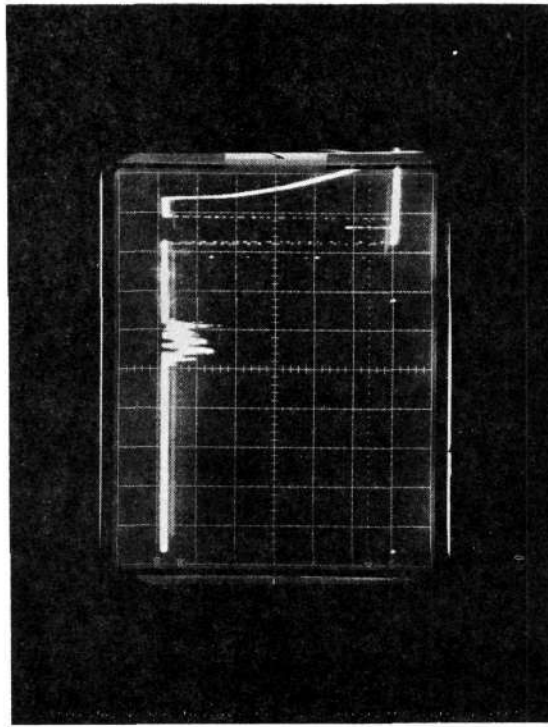


Orbit 225 - Channel 3  
Primary-Low-Comp

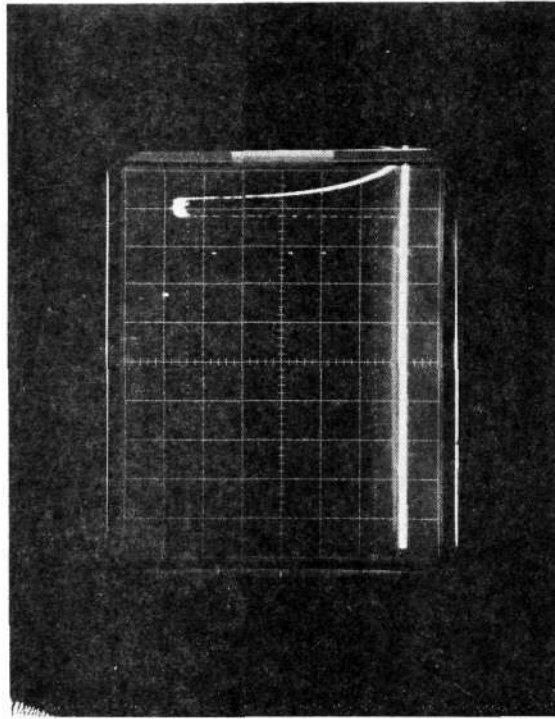
Figure 17-2. MSS Orbital Sensors Response (Cont)



Orbit 208 - Channel 4  
Primary-Low-Comp

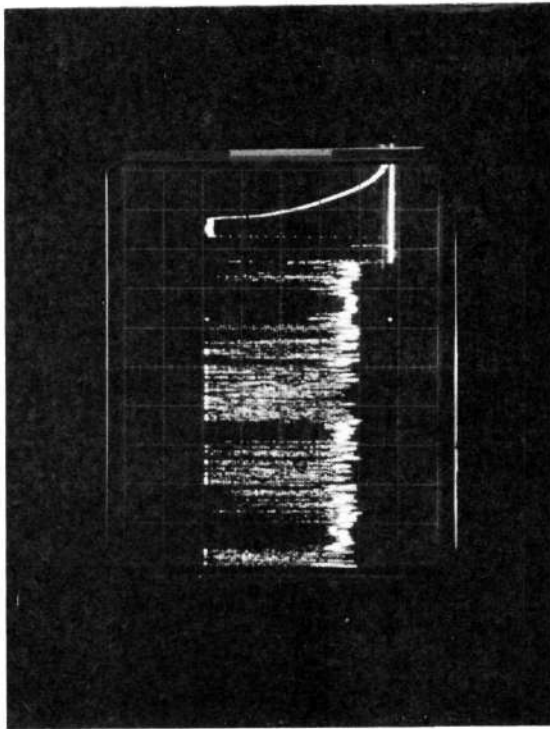


Orbit 225 - Channel 4  
Primary-Low-Comp

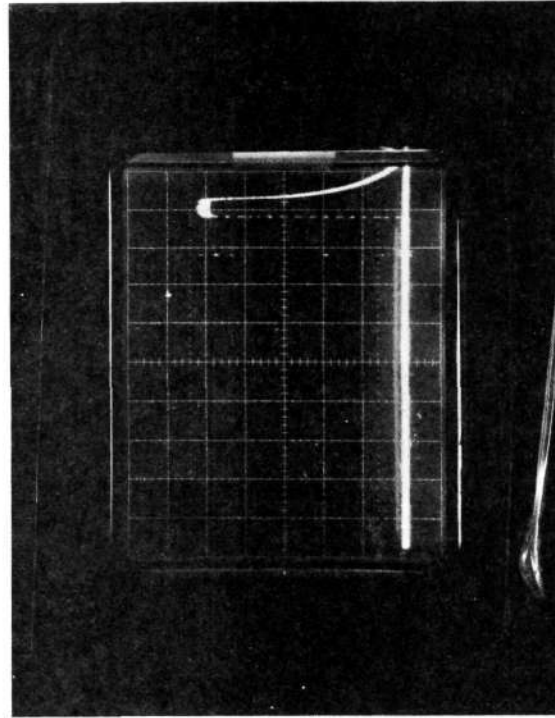


Orbit 243 - Channel 4  
Primary-Low-Linear

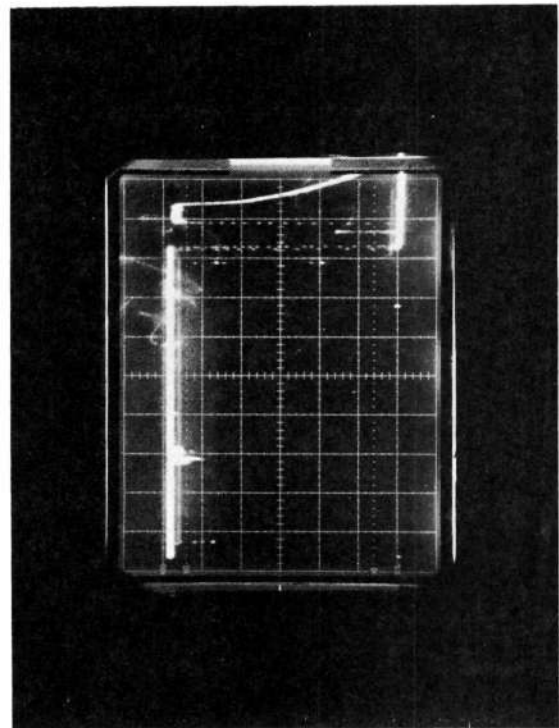
Figure 17-2. MSS Orbital Sensors Response (Cont)



Orbit 208 - Channel 5  
Primary-Low-Comp



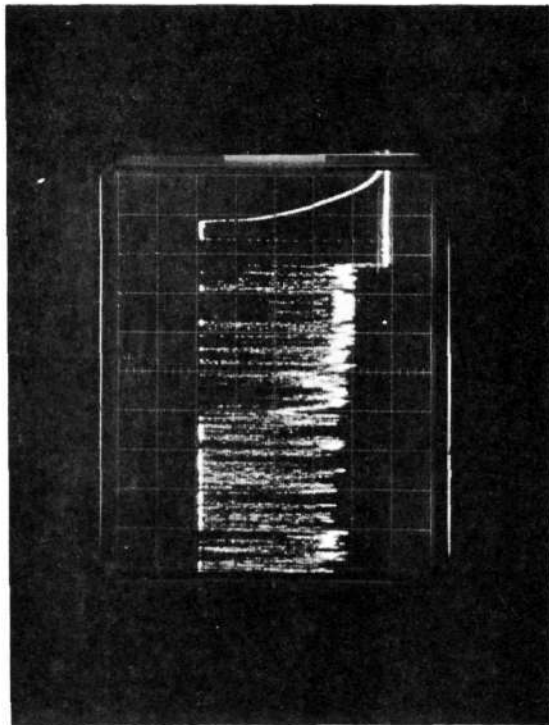
Orbit 243 - Channel 5  
Primary-Low-Linear



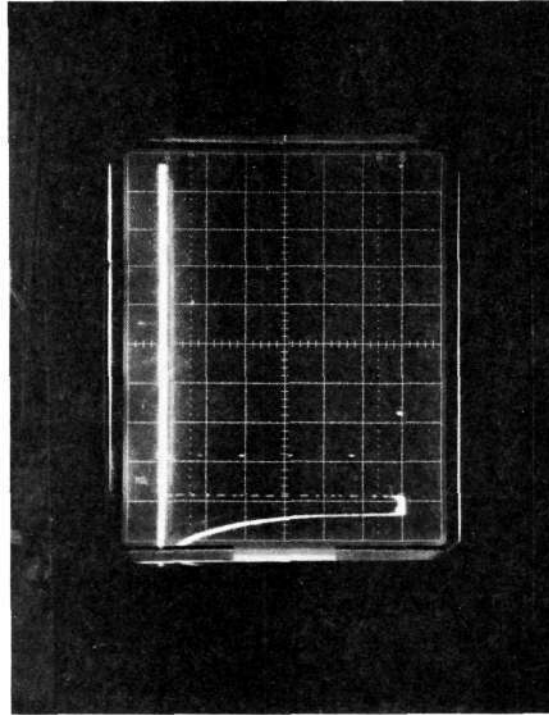
Orbit 225 - Channel 5  
Primary-Low-Comp

Figure 17-2. MSS Orbital Sensors Response (Cont)

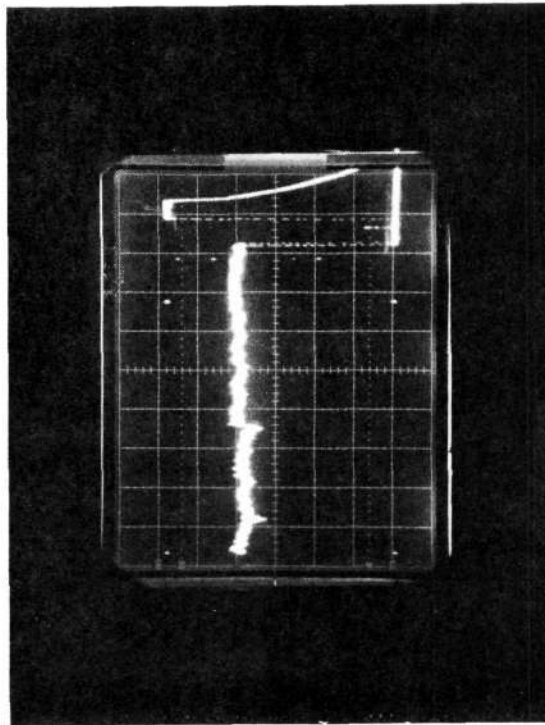




Orbit 208 - Channel 6  
Primary-Low-Comp



Orbit 243 - Channel 6  
Primary-Low-Linear



Orbit 225 - Channel 6  
Primary-Low-Comp

Figure 17-2. MSS Orbital Sensors Response (Cont)

Table 17-3. MSS, T/V vs Orbit 548 Calibration Wedge Comparison

NOTE-4S = 4 segment tape  
D35 = V/T orbit reference 19°C  
NOTE-Δ = (D35-4S)

DATA RUN 9/11/72 at Valley Forge

SENSOR	LEVEL 55*		LEVEL 45		LEVEL 35		LEVEL 25		LEVEL 15		LEVEL 5							
	4S	D35	4S	D35	4S	D35	4S	D35	4S	D35	4S	D35						
1	263	285	-22	314	343	-29	384	410	-26	474	504	-30	590	607	-17	753	776	-23
2	265	280	-25	318	338	-20	386	406	-20	482	503	-21	599	611	-12	805	816	-11
3	260	276	-16	310	334	-24	373	400	-27	476	495	-19	592	608	-16	785	805	-20
4	262	283	-21	311	340	-29	380	407	-27	467	500	-33	578	603	-25	745	774	-29
5	253	258	-5	300	307	-7	363	371	-8	460	472	-12	574	584	-10	756	763	-7
6	264	280	-16	320	338	-18	388	407	-19	485	503	-18	589	607	-18	778	789	-11
7	410	426	-16	480	490	-10	545	555	-10	640	648	-8	766	775	-9	1008	1003	+5
8	395	397	-2	464	462	+2	529	529	0	621	620	+1	740	736	+4	991	983	+8
9	408	421	-13	475	487	-12	539	551	-12	625	635	-10	735	750	-10	985	985	0
10	399	380	+19	465	445	+20	531	513	+18	623	605	+18	743	720	+23	986	985	+1
11	407	416	-9	471	483	-12	536	545	-9	624	634	-10	737	747	-10	980	982	-2
12	398	400	-2	465	466	-1	533	530	+3	618	623	-5	729	732	-3	993	980	+13
13	388	375	+13	451	437	+14	524	504	+20	610	594	+16	738	715	+23	960	978	-18
14	373	368	+5	438	430	+8	502	492	+10	595	586	+9	710	701	+9	942	940	+2
15	385	375	+10	445	437	+8	519	503	+16	603	592	+11	714	699	+15	890	914	-24
16	344	330	+14	400	391	+9	474	455	+19	566	547	+19	673	650	+23	905	864	+41
17	353	345	+8	416	407	+9	483	472	+11	574	564	+10	684	670	+14	893	886	+7
18	362	356	+6	425	419	+6	490	486	+4	579	572	+7	685	679	+6	898	896	+2
19	234	232	+2	243	242	+1	256	255	+1	298	290	+8	372	359	+13	560	550	+10
20	---	---	---	---	---	---	---	---	---	---	---	---	---	---	---	---	---	---
21	234	231	+3	243	241	+2	261	254	+7	---	286	---	360	361	+9	524	512	+12
22	---	---	---	---	---	---	---	---	---	---	---	---	---	---	---	---	---	---
23	---	---	---	---	---	---	---	---	---	---	---	---	---	---	---	---	---	---
24	---	---	---	---	---	---	---	---	---	---	---	---	---	---	---	---	---	---

1 reading in doubt  
\* Quantum levels



Table 17-4. MSS, T/V vs Orbital Sensor Response Comparison

Comparison of V/T and orbits  
111 and 20, at referenced  
temperature of 19°C\*

SENSOR #	V/T	* 111	$\Delta L$	V/T	* 111	$\Delta L$	V/T	* 111	$\Delta L$	V/T	* 20	$\Delta L$
1	38.2	36.1	-2.1	33.9	31.8	-2.1	10.8	10.1	-0.7	38.2	40.4	+2.2
2	38.0	36.2	-1.8	33.4	31.8	-1.6	10.6	10.3	-0.3	38.0	38.1	+0.1
3	35.9	33.9	-2.0	31.6	29.8	-1.8	10.1	9.8	-0.3	35.9	37.4	+1.5
4	38.2	35.8	-2.4	33.7	31.4	-2.3	10.7	10.0	-0.7	38.2	39.5	+1.3
5	32.2	33.0	+0.8	28.4	28.1	-0.3	9.1	9.2	+0.1	32.2	32.7	+0.5
6	37.5	34.5	-3.0	33.0	30.5	-2.5	10.6	10.0	-0.6	37.5	40.1	+2.6
7	46.6	45.3	-1.3	39.8	38.3	-1.5	13.9	13.4	-0.5	46.6	47.6	+1.0
8	41.7	41.8	+0.1	36.3	35.9	-0.4	12.5	12.2	-0.3	41.7	41.4	-0.3
9	45.8	43.5	-2.3	39.1	37.0	-2.1	13.7	12.4	-1.3	45.8	46.0	+0.2
10	39.7	42.3	+2.6	34.0	36.3	+2.3	11.9	12.4	+0.5	39.7	35.7	-4.0
11	44.8	43.5	-1.3	38.3	37.0	-1.3	13.4	12.3	-1.1	44.8	46.0	+1.2
12	41.3	41.3		35.2	35.1	-0.1	12.3	12.0	-0.3	41.3	42.0	+0.7
13	42.9	42.1	-0.8	35.3	35.4	+0.1	26.0	25.7	-0.3	42.9	43.0	+0.1
14	39.0	39.7	+0.7	32.7	33.0	+0.3	23.6	23.1	-0.5	39.0	39.8	+0.8
15	41.1	42.9	+1.8	34.2	36.1	+1.9	24.9	25.8	+0.9	41.1	41.1	
16	33.0	33.6	+0.6	27.5	28.4	+0.9	20.0	20.6	+0.6	33.0	31.5	-1.5
17	35.3	35.5	+0.2	29.5	29.7	+0.2	21.4	21.7	+0.3	35.3	35.1	-0.2
18	37.8	37.9	+0.1	31.6	31.8	+0.2	22.8	23.2	+0.4	37.8	37.5	-0.3
19	34.5	41.2	+6.7	25.0	28.5	+3.5	19.2	21.7	+2.5	34.5	40.1	+5.6
20	31.6	37.4	+5.8	22.9	25.7	+2.5	17.7	19.4	+1.7	31.6	35.8	+4.2
21	34.5	39.7	+5.2	24.8	27.0	+2.2	19.2	20.2	+1.0	34.5	38.5	+4.0
22	29.9	33.9	+4.0	21.5	23.2	+1.7	16.6	17.5	+0.9	29.9	33.2	+3.3
23	28.7	33.3	+4.6	20.8	22.8	+2.0	15.1	17.1	+2.0	28.7	32.6	+3.9
24	31.0	35.4	+4.4	22.5	24.1	+1.6	17.2	18.2	+1.0	31.0	34.8	+3.8

\* All tabulations are in quantum levels(Q.L.)

$\Delta L$  = difference in Quantum levels

\* Word count selection varies for each band. (Same word used in comparison)

V/T VS Orbit 111 and 20 mean signal level at  
selected cal wedge word counts.\*

Table 17-3 is a tabular comparison of vacuum thermal orbit D35 (p-c-1 at 18.7°C and orbit 548 calibration wedges as evaluated on the GPE calibration wedge extractor. It is evident that Band 1 calibration wedges have in general decreased by significant amounts.

Computer performance evaluations to date also indicate that all sensors in Bands 1 and 2 have decreased in sensitivity. All sensors in Band 4 are relatively constant throughout the orbits examined.

A comparison of vacuum thermal data and orbital data (referenced a nominal 19°C fiber optics plate temperature) is tabulated in Table 17-4. It is evident that there have been significant changes in Bands 1 (decreased sensitivity) and 4 (increased sensitivity) after launch.

Consider the MSS system and some of the effects that have been observed to date with respect to the following Figure 17-3.

The cal wedge outputs have been noted to be decreasing in Bands 1, 2, 3, especially in Bands 1 and 2. The cal wedge output in Band 4 is noted to be quite repeatable over all orbits to date. A number of direct causes are evaluated in the sections below.

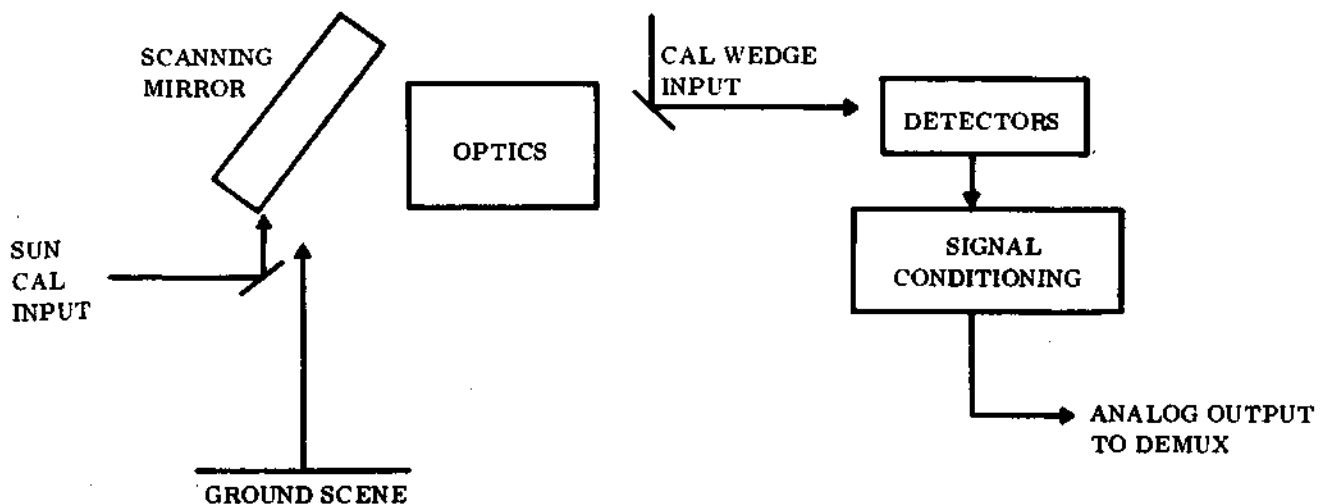


Figure 17-3. MSS Signal Path

1. If the cal wedge lamp energy at the fiber optics input changes distribution (i. e., it has been previously determined that the photon distribution at the F. O. input is nonuniform over the sensors), then the cal wedge output would shift. Since no changes have been noted in Band 4, it is expected that this has not occurred.
2. The cal lamp current (excitation is constant current) has been a constant 1.12 TMV from launch to date (telemetry resolution step is 0.025 volts). If the lamp was aging, i. e., depositing metal on the bulb envelope and increasing resistance, then the output at the fiber optics would be expected to rise due to filament evaporation ( $P = i^2 R$ , increases as R increases) and decrease due to metallic deposition on the bulb envelope. Darkening of the envelope is expected to yield a neutral type filter and all bands would decrease. The increased resistance would result in a higher color temperature and all bands would increase in cal wedge output. Note that Band 4 changes have not been observed.
3. The input voltage (each band has a high voltage power supply) to the PMT could be changing. It would not be expected to change in two bands at the same time (could be verified by switching to the redundant configuration). It is noted that some of the sensors in Bands 3 and 4 showed thermal hysteresis. In any event, none was observed in Bands 1 and 2 and the temperature of the fiber optics plate from launch varied only over a small range.

Further, all sensors in Bands 1 and 2 would not be expected to age in so uniform a manner especially over such a short period of time (effect was not observed in the 2 V/T cycles at Valley Forge). The most likely candidate for a valid explanation is contamination, i. e., of the fiber optics inputs.

The sun calibrate inputs are of lower magnitude than predicted by modeling and measurements made on the earth's surface. The output in Band 1 is especially low while that in Band 4 is closest to predicted value. It has been demonstrated that some of the products of thermal vacuum contamination (or outgassing) when exposed to UV, turn a redish brown in color. Pre UV exposure, they exhibit no spectrally dependent reflectance or transmittance. This would explain why degradations in both sun cal and cal wedges are spectrally or band dependent.

Assume that the system was contaminated before launch with a material which under normal conditions was transparent in the  $0.5 \rightarrow 1.1\mu$  spectral range. In orbit the unfiltered UV radiation has transformed this contamination into a substance exhibiting selective spectral reflectance, and the sun cal outputs are degraded in the sense noted (see figure 17-5). There is no reason to believe with such a substance, the scanning mirror, optics, and fiber optics were not also contaminated. The sun cal mirror sits to the side of the MSS and receives radiation with no shielding. The scanning mirror and other internal MSS optical components are shielded by the sun shield from direct UV radiation but scattered UV can impinge on these components through the input aperture. The transformation of the contamination to the selective spectral material would then necessarily proceed at a much slower pace

than possibly occurred with the sun cal mirror. It is significant that Band 1 for the cal wedge appears to be decreasing most rapidly. If this is the case, then continued degradation for all bands (slowly for Band 4 and more rapidly for Band 1) could be expected until the chemical change has been completed. Other causes may be considered and it is considered necessary to monitor behavior so that conclusions can be reached, experiments planned and measures and checks taken to insure this does not occur in the next ERTS MSS System. Preliminary recommendations have been made in other documentation.

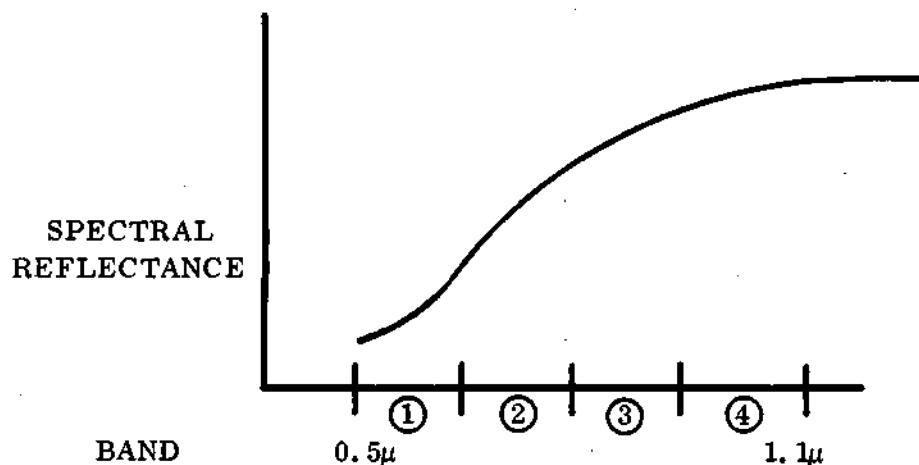


Table 17-5 lists expected and measured outputs for sun calibration.

Table 17-5. Sun Calibration Measurements

Band	Expected 4V ref output	Nominal Orbit output	% Degradation
1	2.76	0.4	85
2	2.96	1.3	56
3	2.60	1.7	35
4	1.96	1.5	23

All bands are of lower amplitudes than expected (especially Bands 1 and 2) and the degradation exhibits a spectral dependence. Note that the amplitudes are not all decreased by a % F. S. amount as might be expected if the sun cal mirror had been physically moved.

Table 17-6 tabulates the sun cal inputs, corrected and uncorrected. Table 17-7 is a list of the orbits on which sun calibrations were made. Effort has been started on the derivation of input corrections for debanding the photos. This is especially evident in low quantum level areas and in color pictures in all regions. It is recommended that this effort be continued and degradation effects factored into results.

Video noise at black level in orbit has been compared to that obtained in T/V. The characteristics are noted to be similar by a visual assessment. Effort should be initiated to obtain more definitive results and do some S/N comparisons.

Table 17-6. MSS Sun Calibration Data

SUN CAL INPUT, CORRECTED AND UNCORRECTED SIGNAL LEVEL,

SENSOR #	UNCORRECTED				CORRECTED					
	619	730	814	915	1012	619	730	814	915	1012
1	5.393	5.428	5.303	5.239	5.040	8.545	7.551 *	5.565	8.580	8.414
2	5.544	5.590	5.522	5.423	5.191	8.505	8.556	8.678	8.667	8.424
3	5.456	5.578	5.554	5.376	5.226	8.489	8.826	8.958	8.939	8.762
4	4.895	4.891	4.880	4.785	4.596	8.244	8.509	8.530	8.467	8.217
5	4.837	4.843	4.902	4.717	4.560	8.241	8.332	8.455	8.296	8.800
6	5.916	5.917	6.004	5.833	5.815	7.832	7.979	8.260	8.161	8.070
8A	1.079	1.074	1.124	1.116	1.255	0.714	1.275	----	0.778	0.730
7	22.039	22.080	21.858	21.808	21.246	23.660	24.186	24.264	24.562	24.152
8	18.986	19.098	19.005	18.820	18.445	23.460	23.898	24.186	24.277	24.106
9	20.658	20.814	20.819	20.437	20.105	23.123	23.762	24.215	23.860	23.740
10	18.948	19.169	19.299	18.914	18.591	22.829	23.102	23.735	23.497	23.371
11	20.614	20.646	20.811	20.314	19.825	22.326	22.807	23.266	23.093	22.654
12	19.815	19.965	20.164	19.671	19.405	22.082	22.318	22.923	22.493	22.300
8A	3.091	2.982	2.853	2.988	2.801	1.578	1.868	1.341	2.069	1.852
13	27.954	28.415	27.984	28.226	28.029	26.316	26.590	26.670	26.750	26.675
14	24.943	25.193	24.920	24.861	24.559	25.525	25.922	26.011	26.009	25.722
15	27.663	27.854	27.854	47.457	27.089	26.041	26.353	26.527	26.269	26.238
16	23.687	23.959	23.957	23.587	23.492	25.199	25.813	26.156	25.968	25.921
17	25.108	25.365	25.162	25.020	24.621	25.690	25.927	26.353	25.728	25.990
18	24.337	24.541	24.548	24.263	24.014	26.530	26.763	27.248	26.808	27.137
8A	4.267	4.456	4.027	4.639	4.537	1.331	0.950	1.237	1.080	1.415
19	23.337	23.502	23.643	23.616	23.678					
20	-----	23.389	23.601	23.524	23.460					
21	23.440	23.603	23.856	23.710	23.543					
22	23.307	23.488	23.794	23.560	23.386					
23	23.620	23.856	24.273	24.000	23.866					
24	22.506	21.856	23.301	21.966	23.009					
8A	1.114	2.000	0.972	2.034	0.857					
						NO CORRECTION				

NO CORRECTION

\*Circled readings are bad histograms.

**Table 17-7. MSS Sun Calibration Orbits**

21	326	915
47	423	1012
89	521	1207
103	619	
131	730	
214	814	

SECTION 18  
DATA COLLECTION SUBSYSTEM

Initial turn-on and checkout of DCS subsystem were reported in the ERTS-1 Launch and Flight Activation Report, 72SD4255, dated 18 October 1972.

This activity consisted of turn-on of Receiver No. 1 in Orbit 5, in which mode it has been operating satisfactorily ever since. Receiver No. 2 has not yet been turned on.

All telemetry functions have been normal as shown in the typical values of Table 18-1.

Table 18-1. DCS Telemetry Values

Number	Name	Units	T/ V* 20°C Plateau	Value in Orbits			
				16	496	910	1256
16001	Rcvr 1 Sig Str	(DBM)	-119	-124.09	-123.83	-124.89	-123.82
16002	Rcvr 1 Temp	(DGC)	23.0	22.72	23.10	23.23	23.62
16003	Rcvr 1 Inp Volt	(VDC)	12.02	12.02	12.02	12.02	12.02

\*Thermal Vacuum Test Data  
Receiver 2 has not yet been used in orbit.

For this reporting period, 45,261 messages were received of which 43,083 were good (95.5%). One hundred fifty-three platforms have been activated, with a maximum of 43 active during one orbit.

Messages are received from seven orbits per day at two ground stations, Greenbelt and Goldstone.



For this reporting period there were 27 users divided as follows, all located in the U. S. (including Alaska) and Canada:

Federal	13 (including Alaska)
Foreign	6 (all Canadian)
Universities	4
States	1
Private	<u>3</u>
*Total	27

\*See Table 18-2

Investigators, with their addresses, are shown in Table 18-2, identification of platforms with users is shown in Table 18-3. Platform locations are shown in Table 18-4.

Evaluation of the performance of the Data Collection System (DCS) required consideration of platform "on" times, platforms radiated power and frequency, platform antenna pattern, platforms geographic location, platform repetition cycle, relative geographic locations of spacecraft and of ground stations, factors affecting electromagnetic propagation (such as ducting, masking, daylight terminator line), and the mass of data on good and bad messages received and processed. Manipulation of this data in a computer would provide a more complete evaluation. The attached evaluation uses average performance figures, and tests the results with a detailed examination of a few typical platforms.

When the spacecraft is in mutual view of a Data Collection Platform (DCP) and one of the two (Goldstone and Greenbelt) ground receiving sites, it can relay the 38 millisecond data burst from the DCP to the ground station. Up to nine minutes of mutual visibility is possible. One of two duty cycles can be selected for the DCP's: one data burst per 90 seconds, or one data burst per 200 seconds, nominal. This visibility period occurs twice per 24-hour day centered about 0930 and 2130 local time. Up to eight messages per orbit may be received on a 90-second duty cycle, and up to four messages for a 190-second duty cycle.

Table 18-2. DCS Data Mailing Addresses

<u>User ID</u>	<u>Investigator</u>	<u>Data Mailing Address</u>
UN103	Hoffer	Dr. Roger G. Barry Institute for Arctic Research University of Colorado Boulder, Colorado 80302
UN661	Kanemasu	Edward T. Kanemasu Evapotranspiration Lab. Department of Agronomy Kansas State University Manhattan, Kansas 66502
ST351	Sweet	Mr. Robert C. Behn Battelle Columbus Laboratories 505 Kings Avenue Columbus, Ohio 43215
DE002	Cooper	Saul Cooper N. E. Div. U. S. A. Corps of Engineers 424 Trapelo Road Waltham, Massachusetts 02154
UN603	Hendrickson	Miss Christine Flannagan Department of Biological Science University of Arizona Tucson, Arizona
IN386	Eaton	Mr. Peter Ward Office of Earthquake Research and Crustal Studies National Center for Earthquakes Research 345 Middlefield Road Menlo Park, California 94025
IN066	Schuman	Herbert H. Schumann U. S. Geological Survey Room 5017 Federal Building 230 N. First Avenue Phoenix, Arizona 85025
IN340	Paulson	Richard W. Paulson U. S. Geological Survey P. O. Box 1107 Harrisburg, Pa., 17108

Table 18-2. DCS Data Mailing Addresses (Cont'd)

<u>User ID</u>	<u>Investigator</u>	<u>Data Mailing Address</u>
NA024	Krieger	Mr. James F. Bettle Chesapeake Bay Ecological Program Office NASA-Wallops Station Wallops Island, Virginia 23337
PR568	Greeley	Mr. Robert Pikul MITRE Corporation Westgate Research Park McLean, Virginia 22101
IN016	James F. Daniel	U. S. Geological Survey 2222 Schuetz St. Louis, Missouri 63141
AG014	Heller	Mr. Fredrick P. Webber Pacific Southwest Forest and Range Experiment Station P. O. Box 245 Berkeley, California 94701
DE011	Kee	Mr. Robert Kee Development Engineering Division U. S. Naval Oceanographic Office Washington, D.C. 20390
IN023	Friedman	Dr. Jules Friedman U. S. G. S Geophysics Washington, D.C. 20242
UN604	Henry	Dr. Edward T. Miller Civil and Mineral Engineering Dept. University of Alabama University, Alabama 35486
IN414	Higer	Aaron L. Higer Water Resources Division USGS Room 730, Federal Building 51 SW 1st Avenue Miami, Florida 33130

Table 18-2. DCS Data Mailing Addresses (Cont'd)

<u>User ID</u>	<u>Investigator</u>	<u>Data Mailing Address</u>
FO501	Zubrycky	Dr. L. W. Morley Dept. of Energy, Mines & Resources Ottawa, Canada
FO461	Kruus	Dr. L. W. Morley Dept. of Energy, Mines & Resources Ottawa, Canada
FO041	Lane	Dr. L. W. Morley Dept. of Energy, Mines & Resources Ottawa, Canada
FO502	MacPhail	Dr. L. W. Morley Dept. of Energy, Mines & Resources Ottawa, Canada
FO503	Vockeroth	Dr. L. W. Morley Dept. of Energy, Mines & Resources Ottawa, Canada
FO368	Perrier	Dr. L. W. Morley Dept. of Energy, Mines & Resources Ottawa, Canada
FO360	Campbell	Dr. L. W. Morley Dept. of Energy, Mines & Resources Ottawa, Canada
NA347	Erb	Bryan R. Erb Code TF 2 Earth Observation Division NASA MSC Houston, Texas 77058

Table 18-2. DCS Data Mailing Addresses (Cont'd)

<u>User ID</u>	<u>Investigator</u>	<u>Data Mailing Address</u>
IO15	Preble	Duane M. Preble USGS/ WRD Inst. Development Unit Gulf Coast Hydro Science Center NASA, Mississippi Test Facility, Building 2101 Bay St. Louis, Mississippi 39520
IN381	Barnes	H. H. Barnes Office of District Chief MCR/WRD USGS 144 Federal Office Building Nashville, Tenn., 37203
IN390	Beamer	N. H. Beamer Office of District Chief ACR/WRD USGS P. O. Box 1107 4th Federal Building 228 Walnut Street Harrisburg, Pa., 17108

Table 18-2. DCS Data Mailing Addresses (Cont'd)

Federal

Cooper	DE002
Eaton	IN384
Erb	NA347
Heller	AG014
Higer	IN414
Kee	DE011
Krieger	NA024
Paulson	IN340
Preble	IN015
Schuman	IN066
Barnes	IN381
Beamer	IN390
Koputska	IN382

Private

Greeley	PR568
Wood	PR550
Smith	

Foreign

Campbell	F0360
Perrier	F0368
Kruus	F0461
MacPhail	F0502
Vockeroth	F0503
Zubrycky	F051

Universities

Henry	UN604
Hoffer	UN103
Kanemasu	UN661
Hendrickson	UN603

State

Sweet	ST351
-------	-------

Table 18-3. 153 Platforms, 27 Users 10/24/72

<u>Eaton</u>	<u>Paulson</u>	<u>Preble</u>	<u>Cooper</u>	<u>Campbell</u>	<u>Henry</u>
6066	6124	6327	6147	6232	6060
6162	6030	6004	6101	6353	6105
6176	6223	6136	6220	6150	6346
6315	6332	6017	6207	6260	6061
6370	6344	6245	6246	6102	6120
6320	6331	6020	6355	6354	6156
6365	6343	6104	6127	6126	6224
6342	6115	6056	6271	6137	6323
6005	6306	6251	6356	6366	6357
6043	6116	6166	6021		6164
6103	6341	6107	6071		6264
6057	6067		6010		
6213	6367				
6163	6047				
6247	6114				
6262	6371				
6034	6277				
6154	6215				
6334	6275				
6011	6322				
6276	6312				
6036	6227				
6240					
6132					
6372					
6311					
6117					
6274					

Table 18-3. 153 Platforms, 27 Users 10/24/72 (Cont'd)

<u>Higer</u>	<u>Schuman</u>	<u>ERB</u>	<u>Kreeger</u>	<u>Heller</u>
6031	6016	6125	6401	6317
6070	6151	6077	6221	6140
6256	6006	6112	6072	6175
6033	6261	6044	6305	
6321	6177	6235	6032	
6250	6165	6244	6022	
6141	6225	6152		
6236		6234		
		6211		
		6045		
<u>MacPhail</u>	<u>Vockeroth</u>	<u>Zubrycky</u>	<u>Kruus</u>	<u>Beamer</u>
6135	6330	6222	6210	6402
<u>Hendrickson</u>	<u>Sweet</u>	<u>Hoffer</u>	<u>Kaputska</u>	
6167	6155	6054	6264	
6261		6007		
6047				
<u>Greeley</u>	<u>Kanumasu</u>	<u>Perrier</u>	<u>Wood</u>	<u>Smith</u>
6073	6131	6270	7000	7707
6373	6310		7001	7701
<u>Barnes</u>	<u>Kee</u>			
6037	6074			
6203	6336			
	6153			



Table 18-4. DCP Locations



Maine	Florida
Massachusetts	Ohio
Connecticut	South Dakota
Rhode Island	Kansas
New York	Mississippi
Pennsylvania	Arizona
Delaware	California
Maryland	Alaska
Virginia	Canada

The number of messages received from each platform is dependent on that platform's location, the number and location of all other platforms in the system, and communication system interference. With less than 5% of the total system capability now being utilized, active platforms most distant from the two receiving sites during the first five cycles were selected to determine if they met the specifications of receiving at least one quality message every 12 hours with a probability of 0.95. Figure 18-1 summarizes the number of orbits that messages were received from the selected platform/day. Multiple messages within one orbit (1 1/2 or 3 minutes apart) are considered redundant and only the average number of messages per orbit are shown in the figures.

The graphs of Figure 18-1 indicate that, for the platforms selected, at least one quality message has been received every 12 hours when the platform has been activated.

A random examination of about 5% of the orbits indicate the performance of these samples is equalled or exceeded by the other platforms.

The transmitting antenna of the DCP subtends an angle of  $\pm 70^\circ$  from the vertical which at the S/C altitude of 500 nm, results in a slant range of 2000 kilometers at this lower limit of  $20^\circ$  elevation. The DCS system performance has exceeded these expectations.

LEGEND:  ASCENDING NODE PASSES (NIGHT)  
 DESCENDING NODE PASSES (DAY)

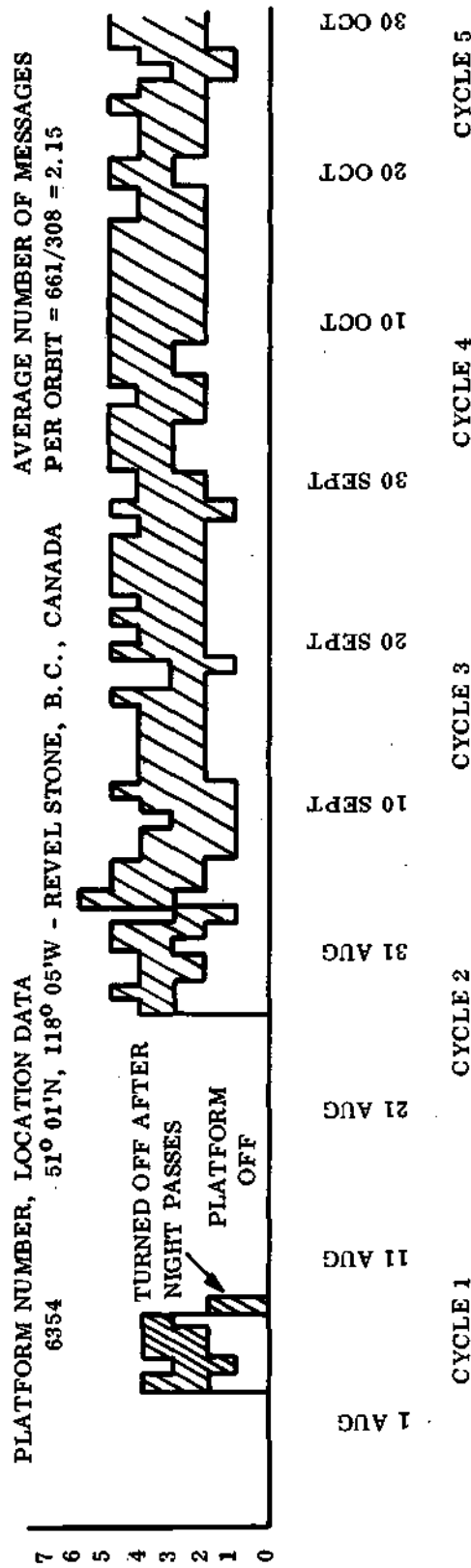
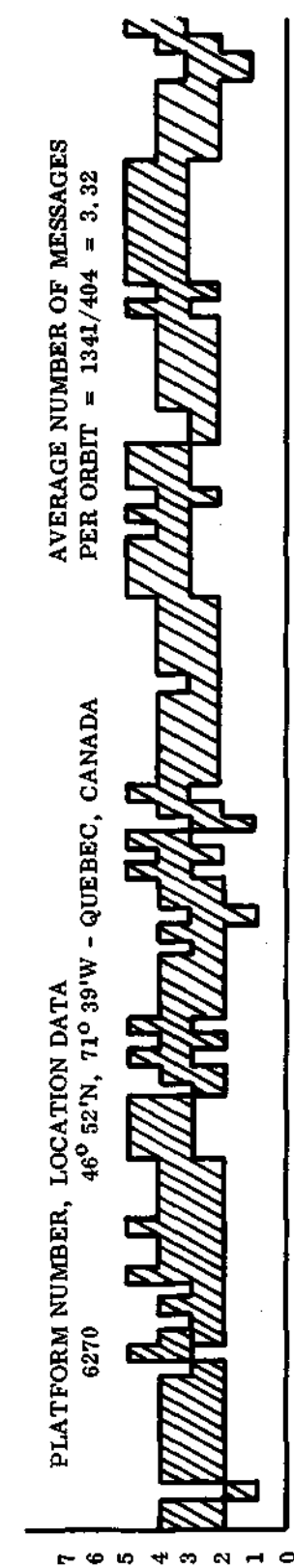
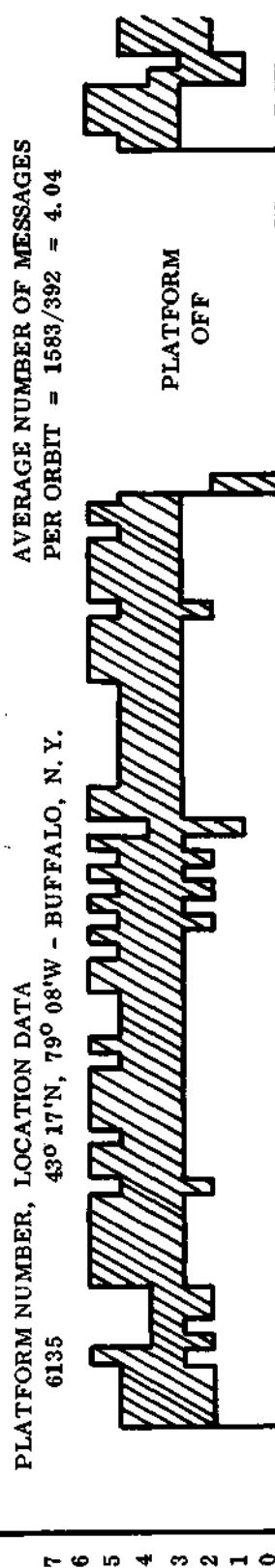


Figure 18-1. DCS Non-Redundant Message Frequency

Messages are regularly received at ranges up to 3400 kilometers and elevation angles down to near zero.

Although the maximum range is specific-platform dependent, several examples are shown to indicate typical operation. The great circle distance from the Platform to the subsatellite point was calculated for the orbit having the greatest range from the platform which provided a quality message. These values are shown in Table 18-5. This distance represents only the platform to spacecraft subsatellite point range since the orbit intercept is well within the visibility cone of the receiving antenna. Consistent and uniform performance out to 3400 kilometers slant range is being experienced.

Table 18-5. DCS Range

Platform ID	Approximate Location	Max. range of quality message from platform to sub-satellite point
6135	43° 17 N 79° 08 W	3400KM
6270	46° 52 N 71° 39 W	2950KM
6354	51° 01 N 118° 05 W	2630KM

To establish the probability of reception of each message transmitted when the spacecraft was visible to both DCP and ground station, data from 126 orbits (12%) were examined. As shown in Table 18-6, of 128 opportunities for message reception from DCP-6115 (Decimal ID-77), only one miss could not be excused by virtue of extreme range (greater than 3500 kilometers). This shows a reception probability of 99.216%.

From launch through October 29, 1972, a total of 45,261 DCS messages were received at the two ground stations. Of these, 2178 were non-perfect. (See Table 18-7). This results

Table 18-6. Reception Probability

Orbit	Number of Messages	Misses
695	3	None
696	4	None
697	1	None
702	3	None
703	3	None
711	1	None
725	1	None
730	4	None
731	3	None
737	3	None
738	4	None
710	3	None
717	2	None
723	2	None
724	3	None
744	3	None
836	3	None
841	3	None
842	1	None
849	3	1*
850	2	None
855	4	None
856	2	None
862	2	None
863	3	None
864	2	None
869	3	None
870	2	None
876	2	None
877	3	None
1002	3	None
1003	2	None
1009	4	None
1010	2	None
1016	2	None
1017	3	None
1022	3	None
1023	4	None
1143	2	None
1148	3	None
1149	3	None

\*DCP Decimal ID 1023 received at this time.

Table 18-6. Reception Probability (Cont'd)

Orbit	Number of Messages	Misses
1156	4	None
1157	2	None
1163	3	None
1169	3	None
1170	4	None
1171	1	None
1176	4	None

Table 18-7. DCS Data-Quality and Quantity

Through 29 October:

Platforms Shipped	168
Platforms Which Have Transmitted	62
Currently Active	37
Active for Majority of First 90 Days	10
Maximum Number Active During 1 Orbit	43

	Dates	24 Jul	1 Aug	19 Aug	6 Sep	24 Sep	12 Oct	Totals
	Cycle No.	31 Jul	18 Aug	5 Sep	23 Sep	11 Oct	29 Oct	0 to 5
Average Number of Active Platforms		7.0	11.4	14.9	21.1	29.6	37.9	24.1
Total Number of								
Messages at Receiving Stations		4117	4320	6116	7898	10344	12466	45261
Messages at OCC		3882	3708	5841	7674	10187	12146	43438
Test Messages		2569	633	792	481	0	0	4475
Non-Perfect Messages		72	247	319	457	444	639	2178
Messages Eligible for Delivery		556	1716	1103	6017	8655	11013	29060
Total Messages Delivered by Product								
Card		693	1717	1102	5323	8083	10335	27389
Listing		116	273	272	731	820	1079	3290
Tape		0	0	0	89	63	89	241

in an error rate of 4.5%. During this time interval several periods of interference were experienced. A study showed these to be the result of electronic emissions from equipment as listed in Table 18-8. Statistically, the interference inhibits DCS operation only 0.055% of the available time.

Table 18-8. DCS Interference

Orbit No.	Duration (minutes)	Source	Location
252	2	IRLS	N. Canada
279	2	IRLS	N. Canada
292	8	Broadband	Colorado
306	6	Broadband	Colorado
711	2	IRLS	N. Canada
739	2	IRLS	N. Canada

Messages to the spacecraft at earth-grazing angles have been received regularly, and no discernible degradation in error rate has been observed for these signals. No misses due to multi-path have been detected. There is no recognizable problem from this aspect.

Two DCP's located adjacent to each other were compared in performance. Table 18-9 shows there was no detectable interference, even when the duty cycles were of a different duration as occurred in orbit 787. Table 18-9 also shows the minor variations in duty cycle that typically occur.

Ground components consist of two ground receiving sites, data transmission facilities, data processing system, information distribution system and eventually of up to 1000 DCP's. All of these systems have been active, except for the reduced number (less than 10%) of possible active platform. The output is shown in Table 18-7. A proper figure-of-merit may be the ratio of "Messages Eligible for Delivery" to "Messages at Receiving Station". In Table 18-7 this ratio is 0.643. This figure is low, partly because of the abnormally large number of test messages associated with inauguration of the system.

Table 18-9. Performance of Geog-Adjacent DCP's.

Orbit	Duty Cycle (min:sec)		Spacing	Station <sup>ⓑ</sup>
	DCP-84	DCP-77		
780	3:15	3:08	0:44	N&G
	3:04	3:09		
	3:05			
785	3:06	3:02	0:54	N
		3:02		
786	3:06	3:03	1:04	N
	3:06	3:03		
	3:07	3:02		
787	3:07	3:04	0:02	N&G
793	3:06	3:08	0:56	N
	3:06	3:08		
		3:08		
799	3:07	3:08	1:18	N
800	3:07	3:07	1:28	N
	3:08	3:08		
		3:08		
904	3:06	3:10	0:30	N
905	3:07	3:09	0:48	N
	3:06	3:10		
	3:06	3:09		
906	3:05	Ⓐ	0:46	G
	3:06			
918	3:06	3:08	1:36	N
		3:08		
919	3:07	3:08	0:46	N
	3:07	3:08		
	3:07	3:08		
920	3:06	Ⓐ	0:13	G
	3:06			

## NOTES:

- Ⓐ Only one msg received; missed 2 opportunities; range exceeds 3500 km.  
 Ⓑ Station ID Key: N = Greenbelt; G = Goldstone



Table 18-9. Performance of Geog-Adjacent DCP's (Cont'd)

Orbit	Duty Cycle (min:sec)		Spacing	Station <sup>ⓑ</sup>
	DCP-84	DCP-77		
925	3:07	3:06	0:54	N
	3:07	3:07		
	3:07	3:06		
926	3:07	3:07	0:55	N
	3:07	3:07		
	3:07	3:07		
1087	3:14	3:16	0:24	N&G
	3:13	3:16		
	3:14			
1120	3:13	3:13	1:01	N
	3:14	3:13		
	3:13			

Table 18-10 summarizes the results and demonstrates satisfactory performance.

Table 18-10. Summary Performance

Reception probability	99.216%
Error rate	4.5%
System Threshold (max reliable range)	3400 Km
Grazing angle effects	none
Adjacent DCP performance	no adverse effect
Ground transmission system	satisfactory
Data processing system performance (msg received - msg delivered)	0.643

# ERTS-1 ISSUED DOCUMENTS

<u>DOCUMENT NO.</u>	<u>TITLE</u>
OCC #221	Task 20-ERTS Anomaly Review (Revised, combined with Task 26), Revision A, August 23, 1972.
OCC #227	ERTS Anomaly Review Task 40, Response to Action Items relating to Anomalies occurring in Orbits 149 and 196 of ERTS-1, August 21, 1972.
OCC #228	Anomaly Review Task 38 - Chronological Commands, August 23, 1972.
OCC #235	Review of Turn-On Transients for Wideband Video Tape Recorder (Task 42), September 19, 1972.
OCC #239	DCS Data Flow, September 22, 1972.
O/L #31	Initial ERTS-1 (Orbit 149) Anomaly Report, August 11, 1972.
O/L #33	Initial ERTS-1 (Orbit 196) Anomaly Report, August 11, 1972.
O/L #44	NBTR 2 Anomaly on Orbit 913, October 3, 1972.
O/L #47	Recent Comstor Loading Difficulties, October 4, 1972.
O/L #48	Decrease in USB Power Output, October 10, 1972.
*DOSR#1	ERTS-1 Daily Operation Summary Reports
DOSR#2	ERTS-1 Daily Operation Summary Reports
DOSR#3	ERTS-1 Daily Operation Summary Reports
1R54-ERTS-641	Thermal Anomaly of Right Forward Sun Sensor (RFSS) on ERTS-A, August 21, 1972.
1H05-ERTS-133	Requirements for Modified Sun Cal Run Every 7 Days.
72SD4249	ERTS-1 Telemetry Brush Charts Orbits 148/9 and 196 Anomalies and Reference Orbits 147 and 195.
1H05-ERTS-134	Alternate Method Proposed for MSS calibration Wedge Evaluation in a Timely Manner.
1H05-ERTS-141	WBVTR #1 Performand and Status as Determined by Demux MNFS Errors
1H05-ERTS-139	MSS Analog Telemetry
1H05-ERTS-135	Changes in MSS Cal Wedge, Band 1 Scope Evaluation.

<u>DOCUMENT NO.</u>	<u>TITLE</u>
1H05-ERTS-136	Changes in MSS Cal Wedge, GPE Cal Wedge Extractor Evaluation.
	MSS PEG Performance Program, Cal Wedge Evaluation
1H05-ERTS-400	Comparison of Vacuum Thermal and Orbital Cal Wedge Outputs.
1H05-ERTS-401	Initial Sun Calibration Results
1H05-ERTS-403	MSS Banding Considerations and Deviation of Input Corrections.
1H05-ERTS-131	ERTS-A MSS Video Noise at Black Level for all Sensors in all Operating Modes.
1H05-ERTS-402	Requirements for MSS Ground Station Time Code/Sun Cal/Cal Wedge Extractor.
1H05-ERTS-137	Orbital Mid Scan Code Scan Symmetry Evaluation.
1H05-ERTS-138	Orbital Mid Scan Code Scan Symmetry, 2nd Evaluation (orbit 326).
72SD4255	ERTS-1 Launch and Flight Activation Report, dated 18 October 1972.
1H05-ERTS-490	ERTS-1 DCS Interference, dated October 13, 1972.

APPENDIX B  
ERTS-1 ANOMALY LIST/REPORTS

ERTS-1 ANOMALY LIST

Since launch, July 23, 1972, the ERTS-1 Spacecraft has exhibited the following problems which are being investigated to establish impact on the ERTS-1 Mission.

<u>Item</u>	<u>Refer to:</u>
1. Thermal Anomaly of right forward sun sensor (orbit 4)	Appendix E ERTS-1 Launch and Activation Report dated 18 October 1972 (72SD4255)
2. Power Transient associated WBVTR No. 2 (orbit 148, 149)	Section 15 Appendix B, Page B-2 thru B-5
3. Failure of RBV power circuit to respond to off Command (Orbit 196)	Section 10 Section 16 Appendix B, Page B-6 thru B-14
4. Intermittant addition of 256 sec. to execute time of Cell 12 in Comstor B. (orbit 583)	Section 5
5. Three power step-downs in USB transmitter power output. (orbit 808, 988, 1258)	Section 9

UNITED STATES GOVERNMENT

# Memorandum

TO : For the Record

DATE: 6 October 1972

FROM : ERTS Anomaly Review Committee

SUBJECT: Summary Report of the Findings of the ERTS Anomaly Review Investigations  
for Orbits 148 and 149

## Summary Statement

During orbits 148 and 149 while remote recording of Return Beam Vidicon (RBV) and Multispectral Scanner (MSS) data was in process, a short from Wideband Video Tape Recorder #2 (VTR #2) secondary voltage supply to ground resulted in excessive noise currents throughout the spacecraft grounding system. This noise condition upset many of the spacecraft support systems. When ground control became aware of the problem, VTR #2 was shut down and has not been reactivated.

## Orbital History

In preparation for recorded data operation of the ERTS payload during orbit 149, the RBV, MSS and Unified S-Band (USB) Transmitter were commanded on from command storage. Next, spacecraft communication was acquired by the Canary Island MSFN station. Following command link verification, VTR #2 was commanded on into standby. Coincident with this command the USB transmitter shut down. Real time commands continued to be uplinked in an attempt to turn on the USB transmitter to regain telemetry downlink and to turn VTR #2 and VTR #1 on in the record mode. When the USB downlink was re-established, large transients were observed on spacecraft power and Attitude Control System (ACS) telemetry. At that time all payloads (RBV, MSS, and both VTR's) were turned off simultaneously. Telemetry noise indications stopped immediately, and the spacecraft began recovering from a 30° pitch up and 20° rolled attitude.

Analysis of playback telemetry data indicated that VTR #2 was the most probable cause of the noise condition, so the RBV, MSS and VTR #1 were reactivated in a manner similar to that followed during initial payload activation. All systems indicated proper operation at reactivation as did all spacecraft support systems following VTR #2 shut down.

Analysis of playback RBV data recorded on VTR #1 during orbits 148 and 149 showed that the anomaly had caused recorded RBV data to be extremely noisy and that the problem first occurred during the final one minute of recorded data operation in orbit 148. Unfortunately, telemetry data from orbit 148 was lost due to premature shut off of the telemetry downlink during the telemetry retrieval pass over the Guam MSFN station immediately following the anomaly.



Buy U.S. Savings Bonds Regularly on the Payroll Savings Plan

Reconstruction of the events of orbit 149 through telemetry and RBV data analysis show that the high noise currents caused 1.) the USB shut down through premature time out of a backup timer circuit in the Auxiliary Processing Unit (APU), and 2.) ACS logic was upset two minutes after VTR turn on when the noise frequency changed from 40 Khz to 20 Khz.

### Conclusions

Conclusions that have been drawn as a result of the investigations and analysis performed are listed below. The bases for these conclusions are discussed in the next section.

1. The anomaly was caused by excessive noise currents through the spacecraft grounding system.
2. The ground noise currents were generated by a short in VTR #2.
3. The short in VTR #2 was between the power converter transformer secondary winding and the primary power return.
4. Wiring dress and construction of the VTR power supply allowed occurrence of the short.
5. The problem still exists in the VTR.
6. No other spacecraft systems were permanently affected.

### Bases for Conclusions

1. Spacecraft Anomaly Caused by Excessive Noise on Spacecraft Grounds.

Tests run on the bench spacecraft have shown that all orbital anomaly symptoms can be caused by the injection of DC levels and noise between spacecraft grounds. These symptoms can be broken down into four major categories: ACS upset; APU upset; Telemetry noise; and noisy RBV data playback from VTR 1.

Depending on frequency, the ACS has shown similar symptoms to Orbit 148/149 with from 350 mv to 700 mv between power return and spacecraft Unipoint ground. Noise between payload return and spacecraft Unipoint ground on the bench spacecraft caused the APU to stop processing VTR Search Track data and to stop timing the payload on time. This same noise was also present in the RBV data recorded on VTR 1 during the noise injection. Noise generated during testing was 1/2 video amplitude while orbital data shows noise varying from 1/4 to full video amplitude.

Tests run on the VIP showed that any noise between its analog voltage reference (S/C Unipoint ground) and the reference of any particular telemetry point would show up as noise on that point. A review of the spacecraft telemetry during the anomaly shows a correlation between the magnitude of the noise present on any telemetry point and the reference for that telemetry point.

2. Spacecraft Ground Noise Generated by Short in VTR #2.

Orbit 148 data shows that the anomaly started during a normal RBV record period and that the anomaly disappeared when all payloads were turned off (a single command).

Orbit 149 data shows that the anomaly started at VTR #2 turn-on and that the anomaly disappeared when all payloads were turned off. All spacecraft components on at the time of the anomaly have been powered since the failure with the exception of VTR #2.

3. The Short in VTR #2 was Between the Secondary Power and Primary Return.

Testing of the video tape recorder has shown the short mentioned above provides the following correlation to observed orbital data.

- a. The highest amount of generated noise (1 volt between power return and S/C Unipoint ground).
- b. Noise in the proper frequency range (40 Khz to 20 Khz).
- c. Frequency changes similar to that which occurred in orbit.
- d. Sufficient DC offsets and noise to simulate VTR #1 and VTR #2 telemetry data seen in orbit.
- e. Sufficient noise currents generated in VTR #1 ground lines to result in RBV recorded data having a noise signature similar to orbital data.
- f. Noise currents sufficient to provide correlation between other spacecraft subsystem telemetries seen in test and in orbit.
- g. The VTR will continue to operate and move tape in presence of the short.

4. Wiring Dress and Power Supply Construction Allowed Short.

Board construction and wiring are such that the wires which connect the full wave rectifiers to the transformer secondary lay on the heat sink on or near two rivets and also route past two captive nuts through which cover mounting screws protrude. A short internal to the transformer is also possible as well as a short from the transformer secondary terminal on the power supply board to the primary ground plane through which it protrudes.

5. The Problem Still Exists in the VTR.

VTR testing has shown DC/DC converter is capable of operating for an indefinite period of time with the secondary voltage supply shorted to ground.



Since it operated as a noise generator during two consecutive orbits, it is felt that it will continue to operate in this manner.

6. No Other Spacecraft Systems Were Permanently Affected.

All spacecraft subsystems which were operating at the time of the anomaly continued to function properly or were subsequently exercised and operated properly. Both telemetry data and RBV data have been used to verify this, and circuit analyses have been made to assure that no power, telemetry, ACS, or RBV damage is likely to have resulted from the transients seen.

UNITED STATES GOVERNMENT

# Memorandum

TO : For the Record

DATE: 6 October 1972

FROM : ERTS Anomaly Review Committee

SUBJECT: Summary Report of the Findings of the ERTS Anomaly Review Investigations  
for Orbit 196

During orbit 196 when the Return Beam Vidicon (RBV) was being turned on prior to a real time payload pass over Alaska, a payload regulated bus short to ground in the Power Switching Module (PSM) resulted in a high current transient of short duration. Following this transient the RBV operated normally, but attempts to turn the cameras off by normal means failed. Auxiliary means were then used to deactivate the system, which has remained off since that time.

## Orbital History

In preparation for a real time payload pass over Alaska/Goldstone during orbit 196 the Multispectral Scanner (NSS), Wide Band Power Amplifier (WBPA), Unified S-Band Transmitter (USB), Return Beam Vidicon (RBV), and Wide Band Modulator (WBM) were commanded on from command storage. At RBV turn on both Video Tape Recorder (VTR) under voltage protect relays actuated and telemetry indicated an unusually high current spike on the payload regulated bus. Payload operations proceeded normally until all payloads and the wide band system were turned off. All systems responded except the RBV which remained partially on. That is the unregulated shutter supply to the RBV shut off, but regulated power remained on. Several additional attempts were made to turn the RBV off, but all failed. Finally the Payload Regulator Module (PRM) was commanded off to deactivate the RBV.

Analysis of telemetry and RBV data gathered during the pass indicated no apparent spacecraft problems other than the RBV primary ON/OFF relay being set in the ON state.

Subsequent orbits were spent commanding the RBV off through individual module ON/OFF relays and reactivating the PRM to allow Video Tape Recorder and Orbit Adjust Subsystem operation.

## Conclusions

Conclusions that have been drawn as a result of investigations and analysis performed are listed below. The bases for these conclusions are discussed in the next section.



B-6

Buy U.S. Savings Bonds Regularly on the Payroll Savings Plan

1. Turn on of the RBV was accompanied by a current transient of approximately 100 amps for from 430 to 520 milliseconds and subsequent failure of the normal RBV turn off function.
2. A simple relay contact weld is not probable.
3. The failure was a short circuit from the payload power bus to the chassis.
4. The short circuit has cleared.
5. The failure was a short circuit internal to the PSM between the relay and the RBV fuses.
6. The RBV was not the cause of or affected by the failure.
7. Alternate modes of RBV power switching are available.

#### Basis for Conclusion

1. Turn On of RBV Accompanied by Large Current Transient and Subsequent Failure of the Normal Turn Off Function.

From orbital telemetry data correlated with test data gathered at spacecraft bench level testing, it has been determined that at the instant of RBV turn on a current transient occurred which persisted for 0.43 to 0.52 seconds. The highest observed current was 100 amps, decaying to 8 amps 0.42 seconds later. The payload regulated bus voltage dropped to an observed low of  $14.75 \pm 0.2$  volts.

At transmission of the "RBV Off" command, the relay which connects the RBV shutter drivers to the Pulse Load Bus functioned properly and removed power from the drivers but the RBV electronics remained powered indicating that the "RBV On" relay in the PSM had not opened although the command had been properly received and decoded.

Repeated transmission of the "Payloads Off" command and "PRM Off" command, which energize the same relays through different paths, also caused no effect.

2. Simple Relay Contact Weld Not Probable.

An extensive series of tests involving 14 Babcock BR-20 relays was conducted. Twelve of the relays were tested under ambient pressure conditions, while the remaining two were tested through the critical pressure region from 100 mm Hg down to 1 mm Hg. Orbital data indicates that the current drawn through the relay contact was approximately 100 amps for less than a half second as noted above. During this test sequence the relays were subjected to several different tests, some being closed under very high current (120 amps for 1 sec) into resistive loads and some being opened under nominal currents (1 amp) into an unsuppressed inductive load to induce arcing. At the completion of the tests the relays were microscopically examined for evidence of welding and none was observed. All relays operated properly throughout the tests and no appreciable contact

resistance change was noted from beginning to end.

Evaluation of the data from this series of tests has produced no likely method of relay contact welding of the BR-20 relay which correlates with the in-flight conditions surrounding the orbital anomaly.

3. Failure Was Short Circuit From Payload Power Bus to Chassis.

Simulations, using the bench spacecraft were performed to duplicate the telemetry shift observed in orbit. The PRM output was shorted to chassis, PRM return, and PSM relay return. ACS telemetry voltages were monitored for changes in level.

Telemetry showed no effect from shorts to PRM return. Shorts to PSM relay return caused a negative shift in telemetry. Shorts to chassis caused a positive shift in the telemetry voltages similar to that observed in orbit.

4. Short Circuit has Cleared.

The short cleared itself within about 1/2 second of RBV turn on as determined from the following indicators:

- a. Payload Bus regained regulation.
- b. Payload Bus current resumed normal levels.
- c. RBV operation was normal up to the time of turn off.
- d. The Payload Regulator was again turned on applying power to the area of failure. Bus currents were normal and operation of loads on the Payload Bus have been proper.

5. Failure Was Short Circuit Internal to PSM Between Relay Contacts and Fuses.

Orbital data indicates that a transient current of approximately 100 amps was drawn from the payload bus at the instant the RBV Power On/Off Relay in the PSM was set. Orbital data also indicates that the RBV was powered normally subsequent to the transient and also the reset function of the On/Off Relay is permanently inoperative. Test data has proven that the RBV fusing in the PSM would have blown in less than 5 milliseconds if the 100 amp transient had passed through the fuse. It is concluded, therefore, that the short circuit which caused the 100 amp transient occurred between the relay contacts and the RBV fuses.

In the PSM the harness appears susceptible to shorts at several points where the harnesses are routed over rivets or screws with no protection and through a wall cut-out which has no grommet protection. Relay lead wiring is suspect due to heavy packing density in that area. Relay failure at actuation cannot be ruled out although construction analysis and discussions with the vendor show no apparent cause for concern.

6. RBV Not Cause of or Affected by Failures.

Flight data taken from orbit 196 indicates that the RBV operated satisfactorily in all respects for approximately 9 minutes after the anomalous turn-on. Evaluation of this data (video and telemetry) indicates that the RBV was not affected by the Orbit 196 anomaly.

Tests on the bench spacecraft, simulating the failure, demonstrated that the RBV would not be adversely affected by a momentary short to chassis between the On/Off relay and the fuses.

7. Alternate Modes of RBV Power Switching Available.

As a result of the Orbit 196 anomaly, the primary RBV Power On/Off function has been permanently disabled.

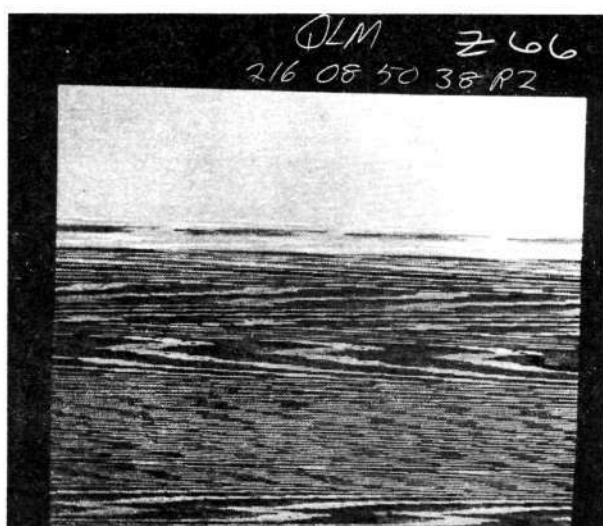
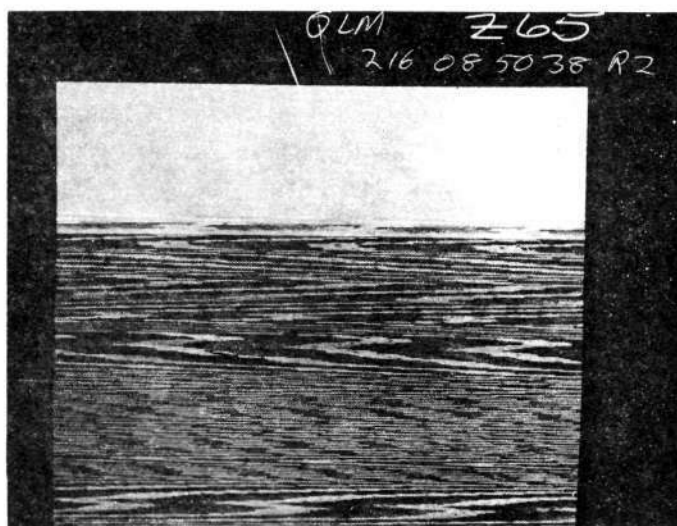
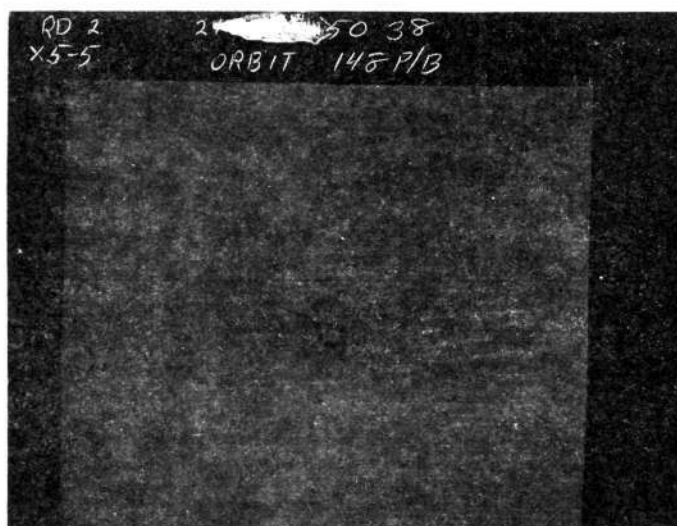
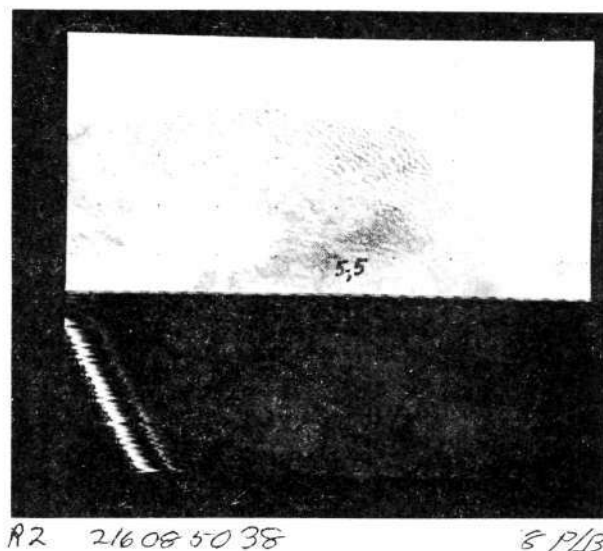
Each RBV component, however, contains an individual Power On/Off relay (4 total) which can be commanded from the ground.

All four of these individual On/Off functions were exercised extensively during the spacecraft test program.

Orbital data subsequent to the Orbit 196 anomaly indicates that these functions are still operational and can be utilized if required.

Spacecraft bench tests turning RBV type relays on into a short circuit with the PRM fuse blow tap open have shown no danger of relay welding under this condition.

# QUICK LOOK MONITOR PICTURES OF ANOMALY IN 148 P/B

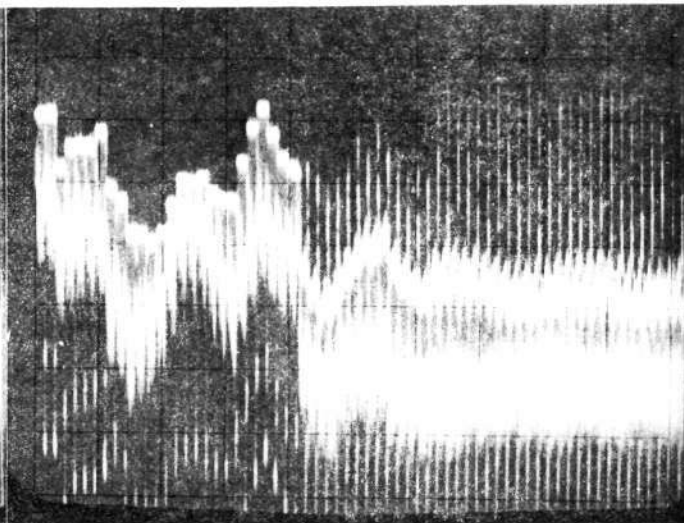
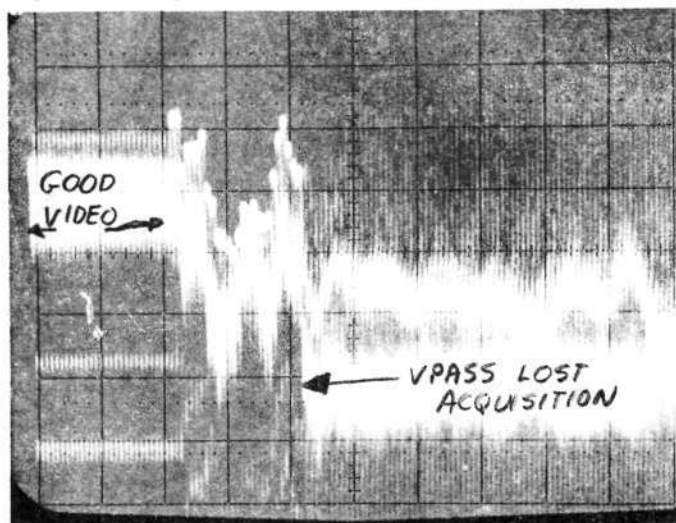


ORBIT 148 P/B

ANOMALY OCCURS IN READ 2 OF  
TRIPLER AT 216:08:50:38

1 25 lines = .02 seconds

2

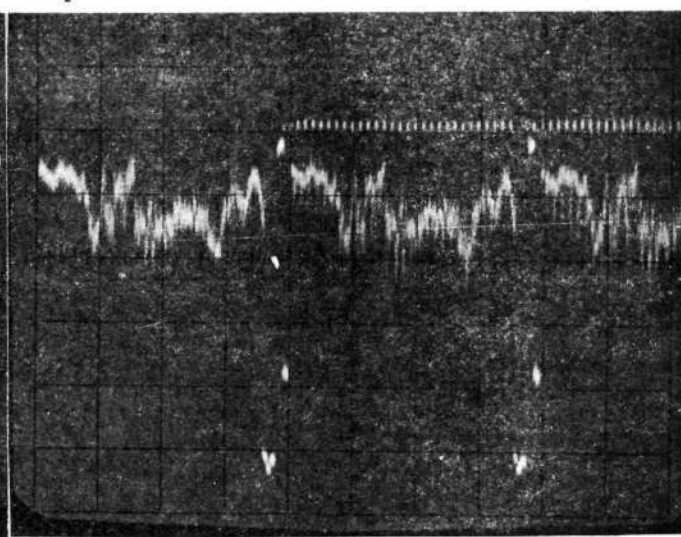
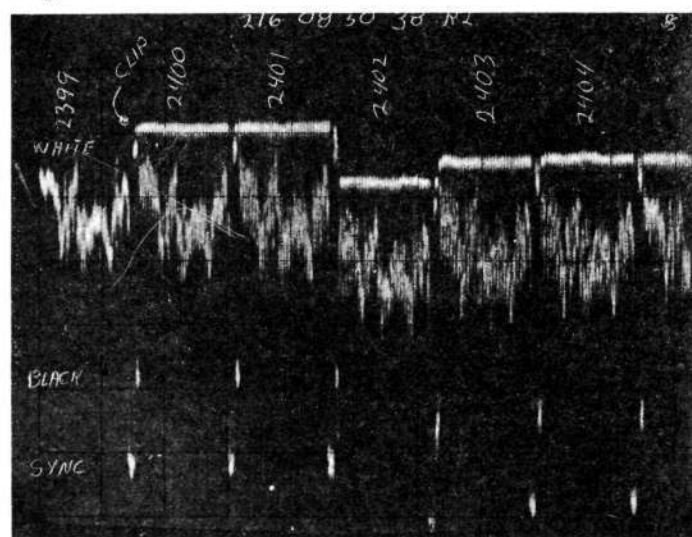


L2400 10 MS/CM

L2400 5 MS

3

4

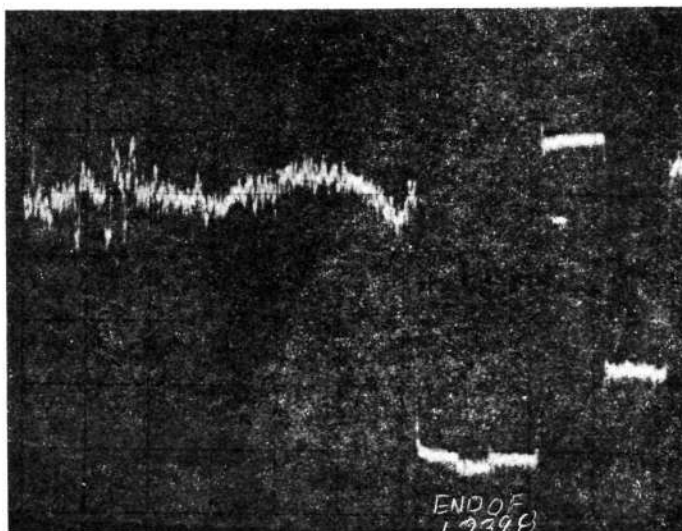


2399 .5 MS

2399 .2 MS

5

GOOD VIDEO



20  $\mu$ sec/cm

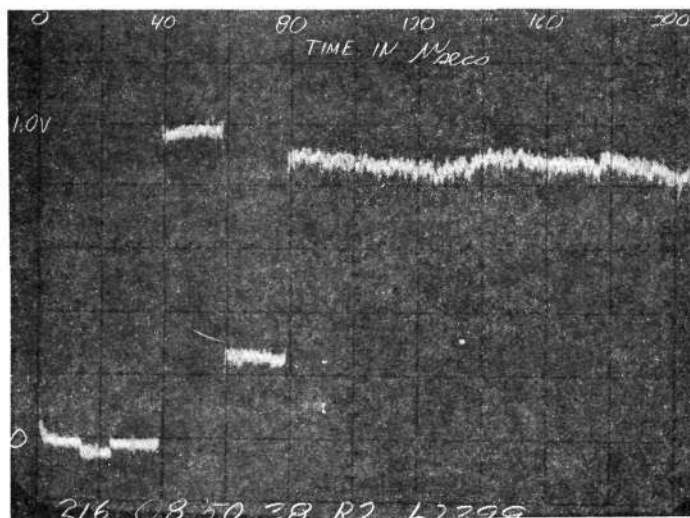


BLOW-UPS OF INDIVIDUAL LINES SHOW THAT NOISE STARTED @ 50  $\mu$ secs.  
 INTO LINE 2400 (see PIX 8) and HAD THE FOLLOWING SIGNATURE ON TOP  
 OF NORMAL VIDEO

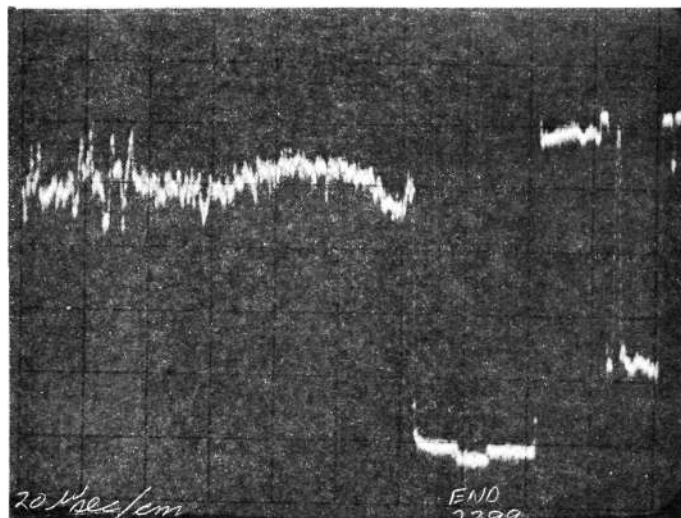


- LARGE SPIKES AT 40 KC REP. RATE
- 200 ~~to~~ 250 KHZ NOISE

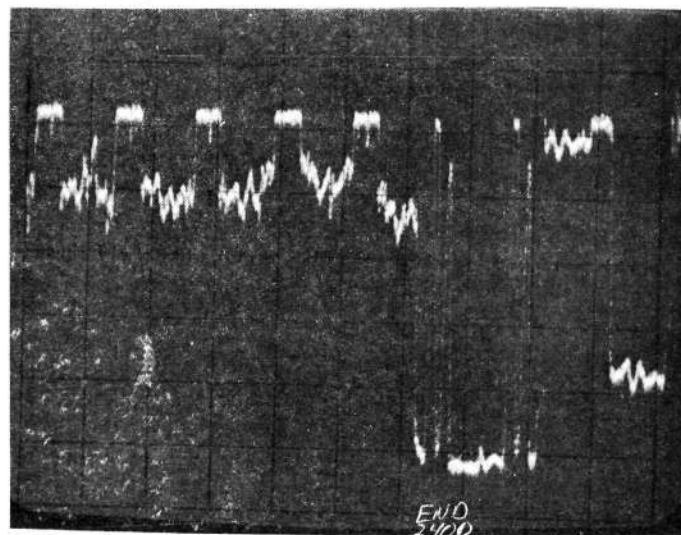
6



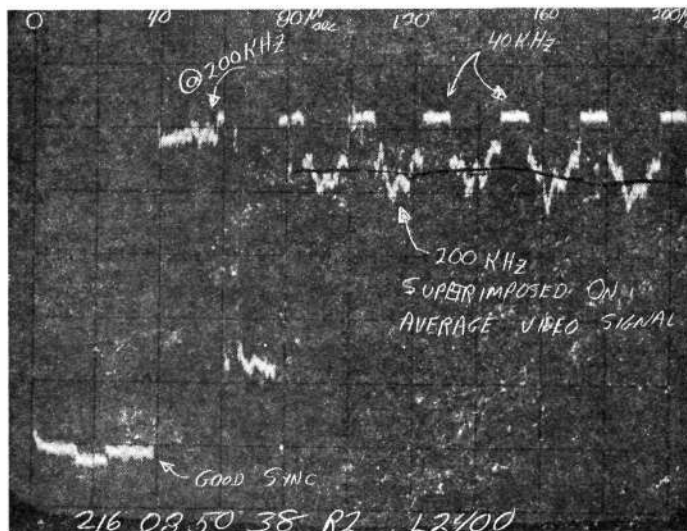
7



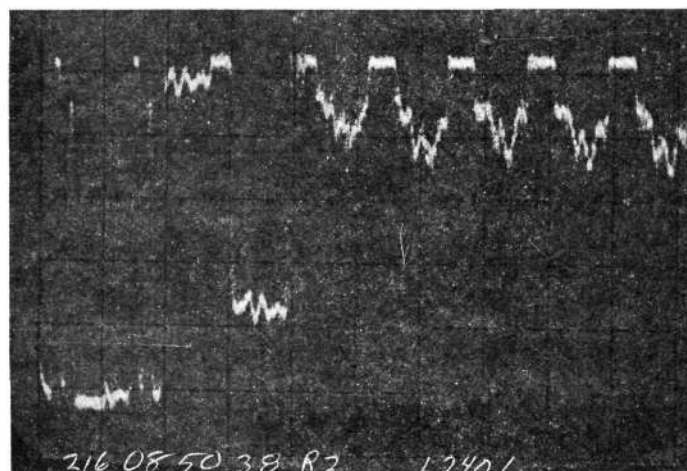
9



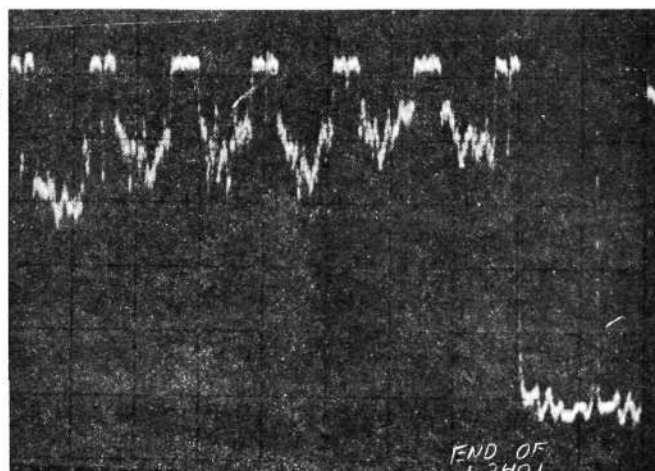
8



10

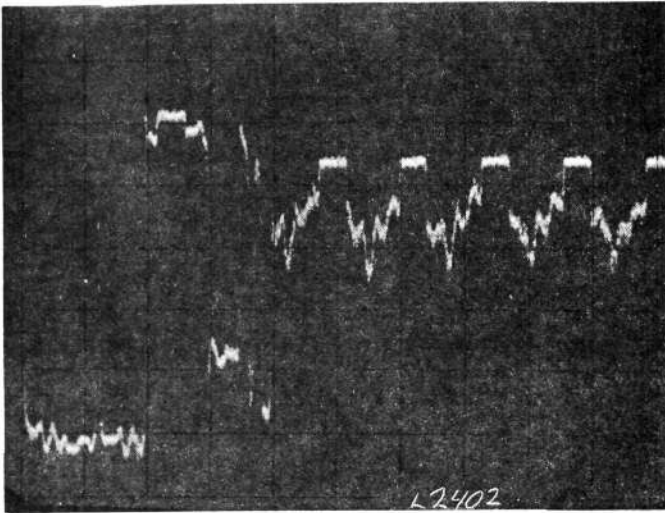


11

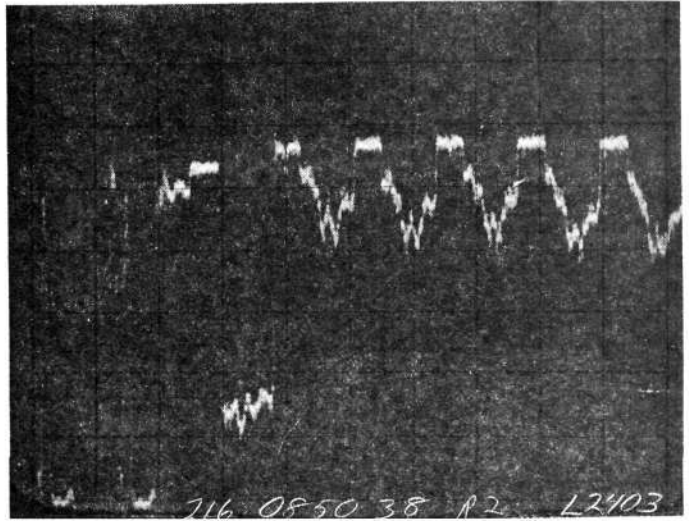




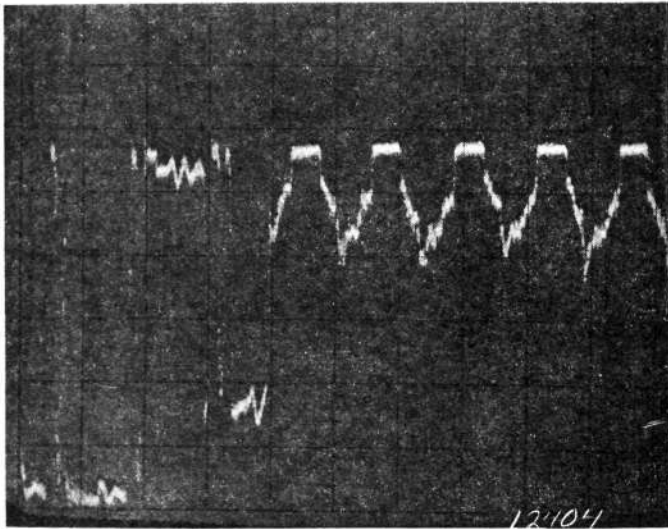
12



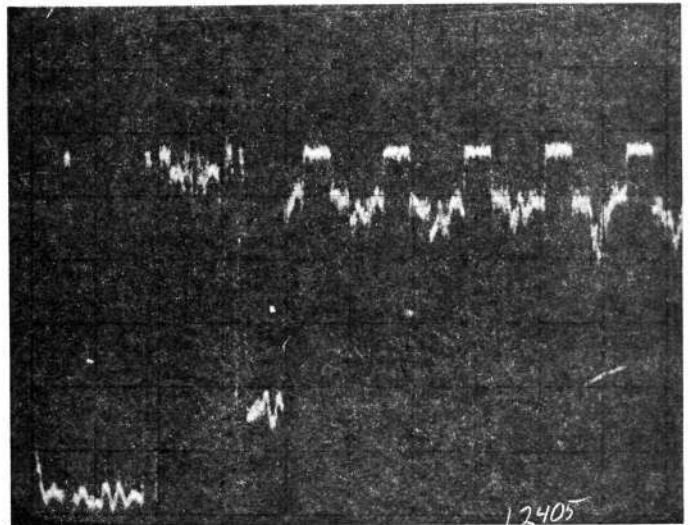
13



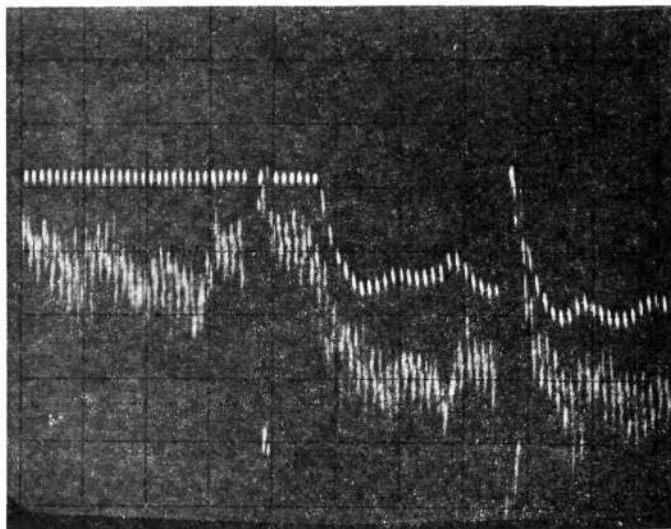
14



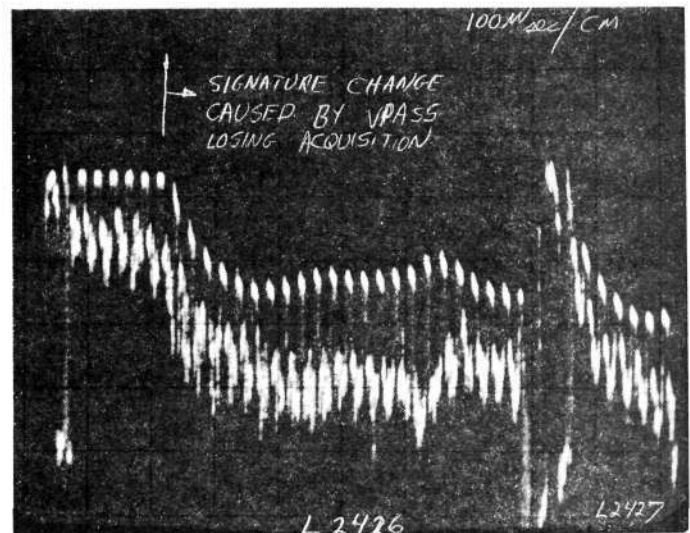
15



16



17

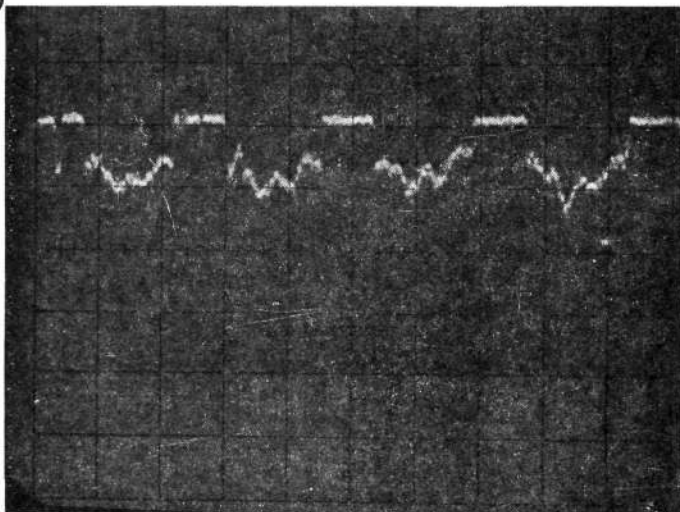


2425

2426

2427

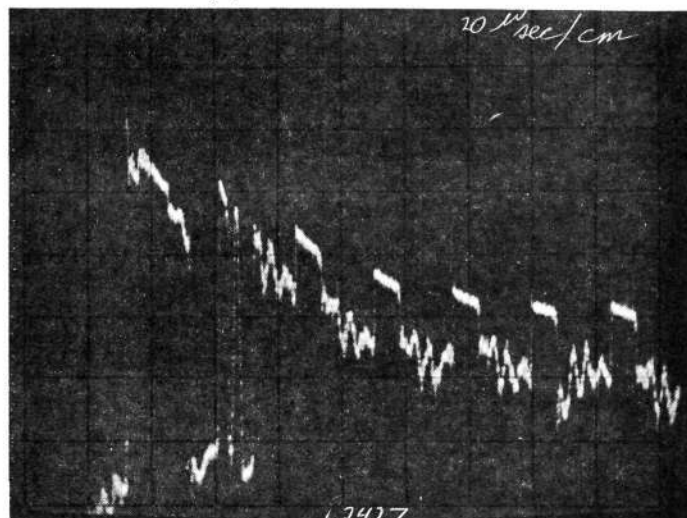
18



2400

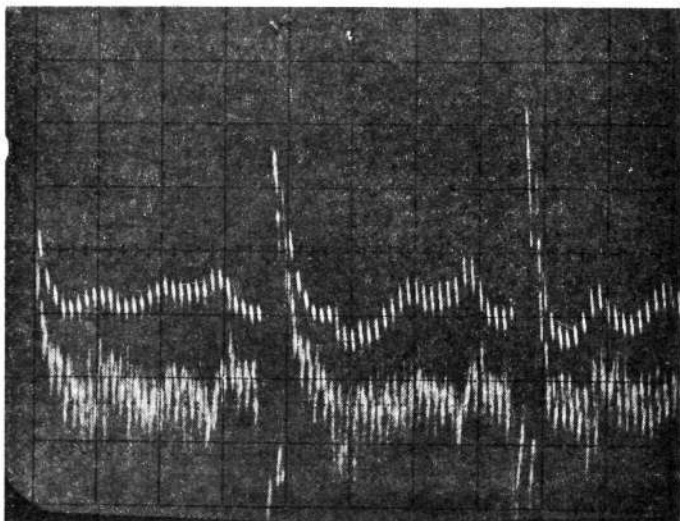
10  $\mu$ S

19



2427

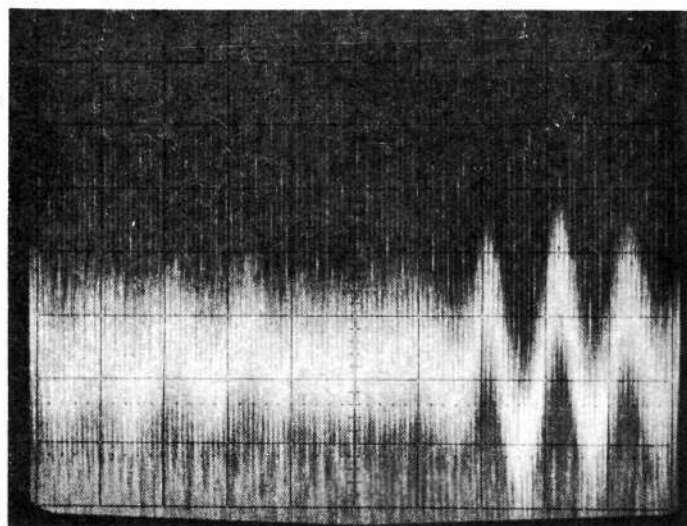
20



2429

.2 MS

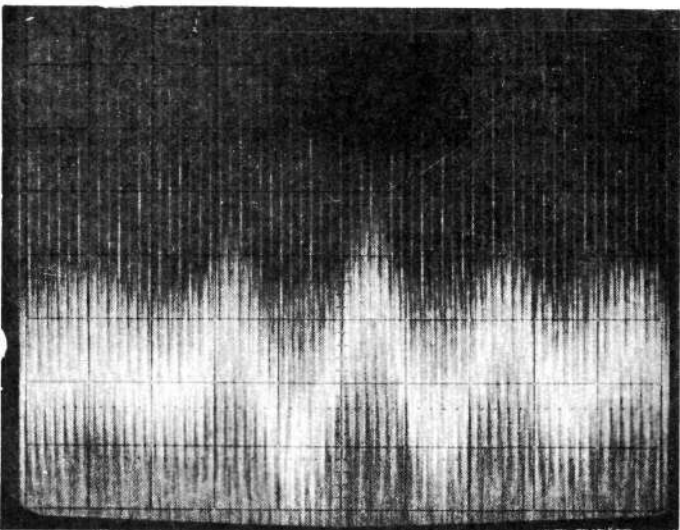
21



L 2700

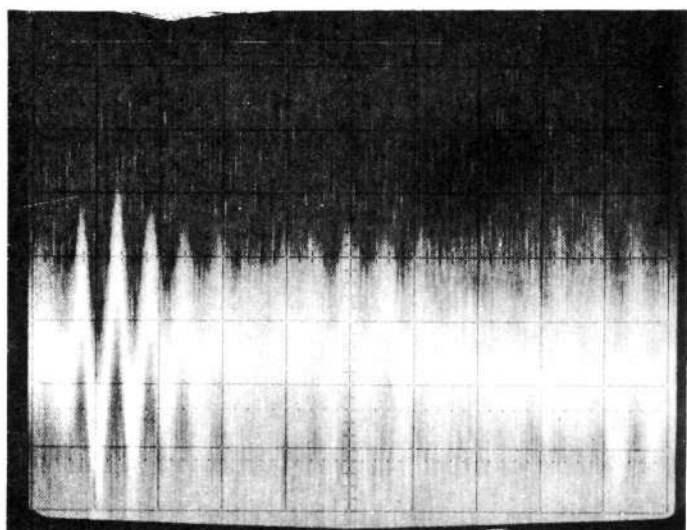
10 MS/CM

22



L 2770

5 Msec/cm



L 2776

20 MS/CM

**APPENDIX C**  
**IMAGE ASSESSMENT REPORTS**

C-1

QUICK LOOK ASSESSMENT  
OF  
MSS AND RBV PHOENIX SCENE  
FROM  
FIRST COVERAGE CYCLE IMAGED 8/6/72

Memo #040

S.J. Schramm/T. Rooney

12 October 1972

### GENERAL COMMENTS

Both 9.5 inch and 70 mm images of Phoenix, Arizona were ordered for all bands with no cloud cover restrictions. The order was completely received at VF on 9/28/72 (53 days after scene was taken). All images were of good quality except MSS Band 5. This image contains two .5 mm wide black lines across the scene at 50 mm and 45 mm from the bottom.

Cloud cover estimate is below 10%, but this cannot be verified until data past 8/5/72 is included in the U.S. Standard Catalog.

The original request specified  $N34^{\circ}$  and  $W112^{\circ}$  as the required scene coordinates. Unfortunately, the city of Phoenix was missed because the image center received was 35 minutes north and 37 minutes west of the requested location (see Figure 1). The Death Valley scene was also northwest of the requested location. Philadelphia imagery appears to be right on, although first images were completely cloud covered.

### ANNOTATION

The annotation on all images is consistent and complete and appears to be accurate. The annotated image center is  $N34^{\circ} 35'$  and  $W112^{\circ} 37'$ . By a crude measurement, the format center was located via reg marks and lat-long tic marks to be  $N34^{\circ} 34.77'$  and  $W112^{\circ} 37.30'$ . This small difference is well within the measurement uncertainties.

### RESOLUTION

Visual assessment of the 9.5 inch images with the aid of a 12X comparator and 1:250000 topological maps was made to measure small detail. Table 1 summarizes the results for the few distinguishable targets in the scenes. A subjective

estimate of contrast (C), the smallest dimension (W) and the largest dimension (L) are tabulated for bands in which the target was detectable.

Target dimensions are in agreement with analytical expectations. In the few cases where the resolution limit of the sensors is pushed, the target is a long linear feature such as a road. Very narrow (50 M) objects are easily visible since the eye tends to integrate the many small samples along the length.

#### LOCATION ACCURACY

The latitude-longitude of a road intersection was measured in the image via tic-mark interpolation and compared to the map location. Table 2 shows the results. As in the Death Valley scene, the longitude error is too large, whereas the latitude error is tolerable, but worse than predicted.

#### RADIOMETRIC TRANSFER FUNCTIONS

Densitometer measurements were made on the annotation grey scales of the 70 mm and 9.5 inch frames of the RBV and MSS third generation film. All of the grey scales on the seven enlarged frames and five of the 70 mm grey scales had regions in which the density readings were double valued near the lightest (highest radiance) end of the grey scale. This can be seen in Figures 2 and 3 where step 6 and step 7, respectively, have the same transmission as step 15 on the 9.5 inch film. Table 3 lists the percent of the voltage scale (RBV) and percent of the radiance (MSS) scale which is in the double-valued region. Also given in the table is the percent of the density readings within the image which were within the double-valued grey scale region. There are cases in which a large part of the RBV voltage or MSS radiance scale is double valued but no objects in the scene happen to be recorded in this region.

The double-valued region typically spans 6 to 8 grey steps and shows as a hook in a plot of transmission or density versus grey step number. Two of the RBV

70 mm grey scales were not double-valued but had a plateau in the transfer function plot. Adjacent grey steps had the same density. The RBV band 2 grey scale has two plateaus.

The double-valued density percentages were obtained from the 24 to 38 density readings per frame which were taken to obtain the average ground reflectivity.

Except for the two RBV and one MSS frame, all density readings were above the double-valued region. The 3.7% MSS band 5 double-valued densities was one reading out of 27. Therefore, the double-valued grey scale has negligible effect upon MSS radiometry for this particular scene using the low-gain mode. This conclusion may not be valid for a different scene composition, higher haze, or the high-gain mode.

The fact that five out of seven 70 mm frames were double valued indicates that the EN-70 enlarger is not the sole cause of the problem.

The density versus grey scale step curve has a low slope in the region under discussion and is probably partly the cause of the problem. Using a densitometer measurement random error of 0.01 and a film non-uniformity per generation of 0.01, the RSS error sum is 0.02. The lightest step in band 6 had a measured density of 0.38 (41.7% transmission). Starting with this density and using 2.94% transmission increase between steps and applying the 0.02 density tolerance, Table 4 has been constructed. The possible density range about the ideal permits adjacent steps to have the same density but does not explain step 9 or 10 having the same density as step 15.

In order to isolate the cause(s) of the double-valued problem, it is recommended that an image and an annotation grey scale be recorded and that density readings be made in each 70 mm and 9.5 inch generation.

The film transmission versus grey steps curve, Figures 2 and 3, for 9.5 inch film and MSS 70 mm film exceeds the linearity specification in the upward direction. One consequence of this is that the transparencies are light even though the maximum grey scale density is within specification. Table 5 gives the density decrease from nominal for the average scene reflectivity and the corresponding transmission increase. Band 4 MSS 70 mm has almost twice the nominal transmission.

#### RADIOMETRIC MEASUREMENTS

Measurements were made on the photographs and the density readings were converted to radiance through use of the grey scale and RBV light transfer characteristics. Ground reflectance was computed from the radiance by using an atmospheric model. The accuracy of the computed reflectance is dependent upon the accuracy of the model for the prevailing conditions, and the meaningfulness of the evaluation in assessing absolute performance is dependent upon the ability to identify the type of reflector from the photograph and maps and correlate the reflector type with a published spectral reflectance curve.

A relative assessment between RBV and MSS is also helpful, particularly in these cases where computed and expected reflectance values differ, since the same atmospheric conditions apply for both instruments.

Table 6 gives the average reflectance of the scene and the reflectance of specific objects in the scene. The averages are obtained from 24 to 38 measurements on each frame using a 1 mm densitometer aperture. The average reflectances given for the RBV bands 2 and 3 should be disregarded because of the large number of readings either in a defective part of the grey scale or below the grey scale. The average reflectance measured in the 70 mm frames is 1.5 to 2 times higher than that measured in the 9.5 inch frames. There is no explanation for this at present. It would be expected that the 70 mm measurements would be more accurate



because of the relationship of the aperture size to the photographic scale.

Table 6 gives the reflectances derived from density readings for sand, rock and crop areas and, also, the equivalent reflectance in cloud-shadowed areas. Also listed is the typical range of reflectance expected for each of the areas. When the derived reflectance is above or below the typical range by greater than 10% it is indicated by a square or circle around the number.

Rock areas 2 and 3 appear to be misidentified because of the correlation between RBV and MSS results. The derived reflectance for the crop area in RBV band 2 and MSS band 5 is unusual for growing vegetation. In the following areas the results from the RBV and MSS are not correlated and there is an apparent radiometric error:

- Sand area 2; MSS 4
- Crop area; MSS 4
- Cloud area 1; RBV 3
- Cloud area 2; RBV 2 and 3

There is no indication that any band is consistently high or low in its radiometric measurements.

TABLE 1

TARGET	RBV BAND						PHOENIX (9.5+3)						MSS BAND					
	1		2		3		4		5		6		7		8		9	
	C	W	L	C	W	L	C	W	L	C	W	L	C	W	L	C	W	L
Luke AF Aux Runway #2	-	-	-	-	-	-	Lo	100	1100	Med	100	1100	Med	100	1100	Med	100	1100
Atchison Topeka and Sante Fe Rail Road Line	Lo	50	15000	Lo	50	24000	Lo	50	18000	Lo	50	24000	Lo	50	24000	Lo	50	26000
Agro Field	Lo	250	700	Med	300	800	-	-	-	Med	300	700	H1	200	700	-	Lo	500
Agro Field	H1	300	700	H1	300	800	Lo	300	800	Med	300	700	H1	300	800	-	-	-
Spring	-	-	-	Lo	250	750	Med	200	700	Lo	200	700	Med	200	750	H1	200	800
Spring	-	-	-	Lo	150	900	Med	150	800	Lo	150	1000	Med	150	900	H1	100	1000
Spring	-	-	-	-	-	-	-	-	-	-	-	-	-	-	-	H1	100	200

Note: All target dimensions in meters.

C = Estimate contract

W = Width

L = Length

TABLE 2

PHOENIX  
ROAD INTERSECTION  
(MSS 7)

	<u>LATITUDE</u>	<u>LONGITUDE</u>
MEASURED FROM IMAGE	34° 8.089'	112°52.703'
MAP LOCATION	34°7.466'	112°57.000'
	.623'	4.297'
LOCATION ERROR IN METERS	1134	6368

..

TABLE 3 ANNOTATION GREY SCALE DEFECTS

Sensor	Band	Format	Defect	% of Grey Scale	In Defect	Density Readings (percent) In or $\pm$ 0.01 about defect
RBV	1	70 mm	Double-valued	14	3.8	3.8
	2	70 mm	Plateaus (2)	16	15	23
	3	70 mm	Plateau	8	19	31
	1	9.5"	Double-valued	46	0	0
MSS	2	9.5"	Double-valued	44	(16.5 + 16.5 BGS)	33
	3	9.5"	Double-valued	48	(8 + 29 BGS)	42
	4	70mm	Double-valued	14	0	0
	5	"	"	10	3.7	3.7
	6	"	"	28	0	0
	7	"	"	16	0	0
	4	9.5"	"	37	0	0
	5	"	"	36	0	0
	6	"	"	28	0	0
	7	"	"	36	0	0

BGS: Below Grey Scale

TABLE 4 EFFECT OF ERROR AND NON-UNIFORMITY ON DENSITY

STEP	POSSIBLE RANGE DENSITY	MEASURED BAND 6 DENSITY
15	.36 - .4	.38
14	.392 - .432	.40
13	.425 - .465	.38
12	.462 - .502	.38
11	.505 - .545	.40

• TABLE 5 EFFECT OF NON-LINEARITY  
ON AVERAGE DENSITY OF SCENE

Sensor	Format	Bands	Density Decrease Density	Transmission Increase Times
RBV	70 mm	1,2,3	0.05	1.12
RBV	9.5 inch	1,2,3	0.24	1.7
MSS	70 mm	4	0.28	1.9
MSS	70 mm	5,6	0.23	1.7
MSS	70 mm	7	0.26	1.8
MSS	9.5 inch	4	0.2	1.6
MSS	9.5 inch	5,6,7	0.16	1.45

TABLE 6 REFLECTANCE DERIVED FROM PHOTOGRAPHS

	RBV 1	MSS 4	TYP	RBV 2	MSS 5	TYP	RBV 3	MSS 6	TYP	MSS 7	TYP
Average Reflectance											
70 mm	30	29		58	31		58	34		41	
9.5 inch	16	21		23	22		27	24		32	
Sand											
Area 1	B	30	25-30	B	38	30-40	B	38	40	40	40
Area 2	24	<u>36</u>		X	36		X	38		42	
Rock											
Area 1	26	32	22-55	XX	40	35-60	XX	39	37-65	46	40-65
Area 2	<u>17</u>	<u>20</u>		<u>22</u>	<u>24</u>		XX	<u>27</u>		38	
Area 3	<u>16</u>	<u>20</u>		<u>30</u>	<u>26</u>		XX	<u>27</u>		38	
Area 4	24	32		XX	32		52	38		46	
Area 5	34	32		X	36		X	34		45	
Crop	14	<u>20</u>	10-15	<u>25</u>	<u>19</u>	5-10	30	38	20-40	54	30-50
Cloud Shadow											
Area 1	0	4	0-4	2	0	0-4	<u>14</u>	0	0-4	3	0-4
Area 2	0	3		<u>7</u>	0		<u>18</u>	0		2.5	

□ Higher than typical range

○ Lower than typical range

B Area is beyond edge of RBV frame

All reflectances of specific objects measured on 9.5" film.

Figure 1

Death Valley and Phoenix

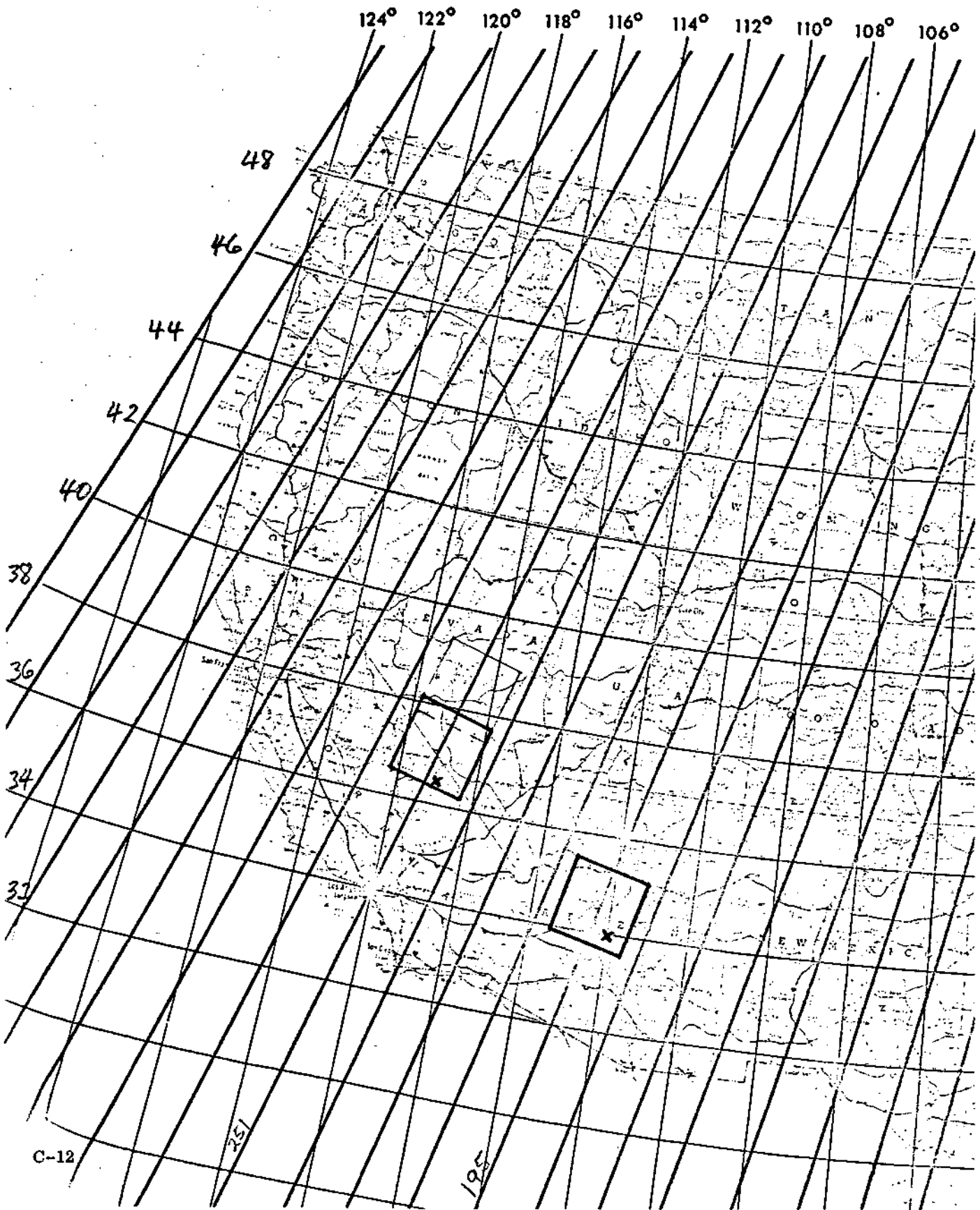


FIGURE 2

PHOENIX MSS 4

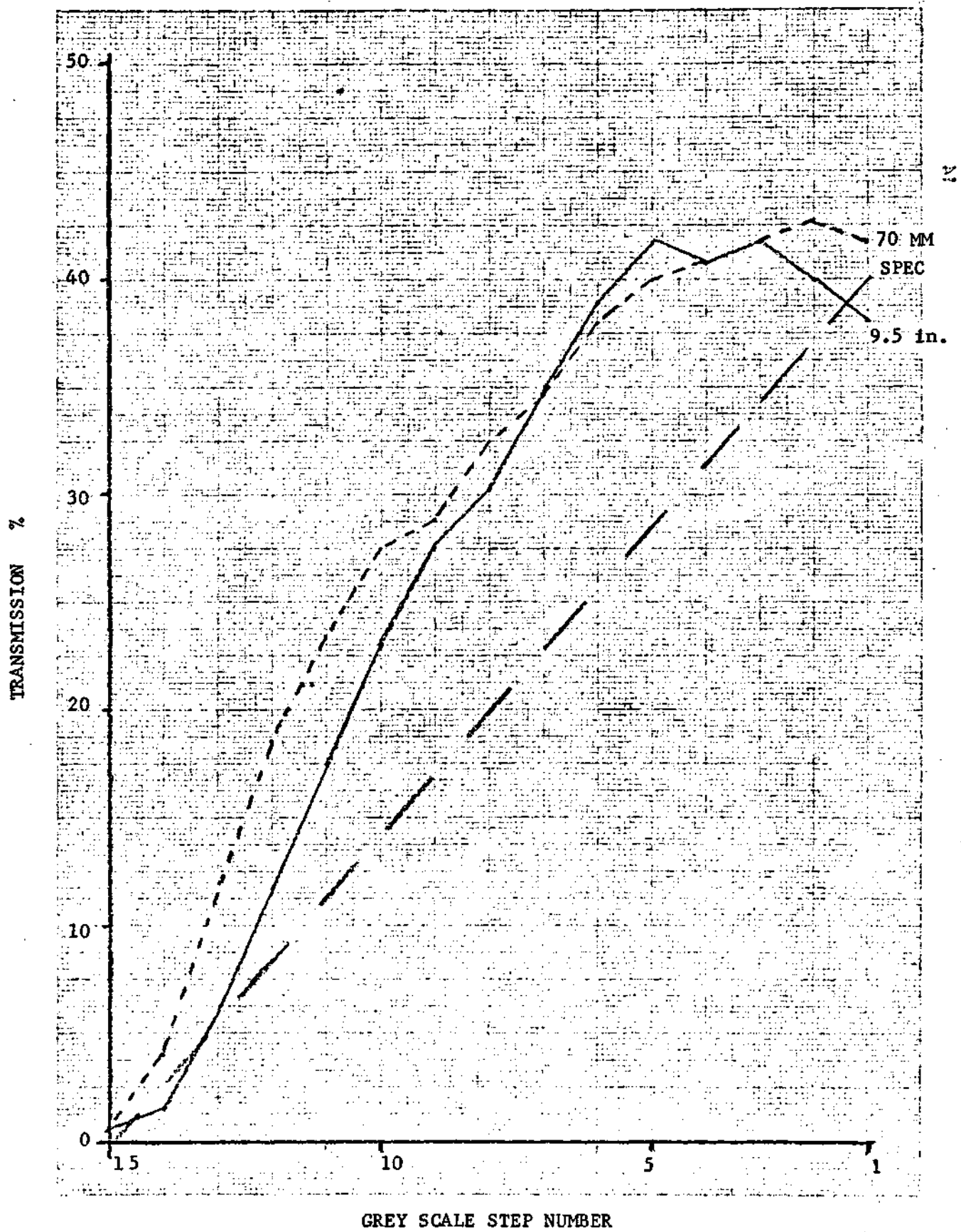
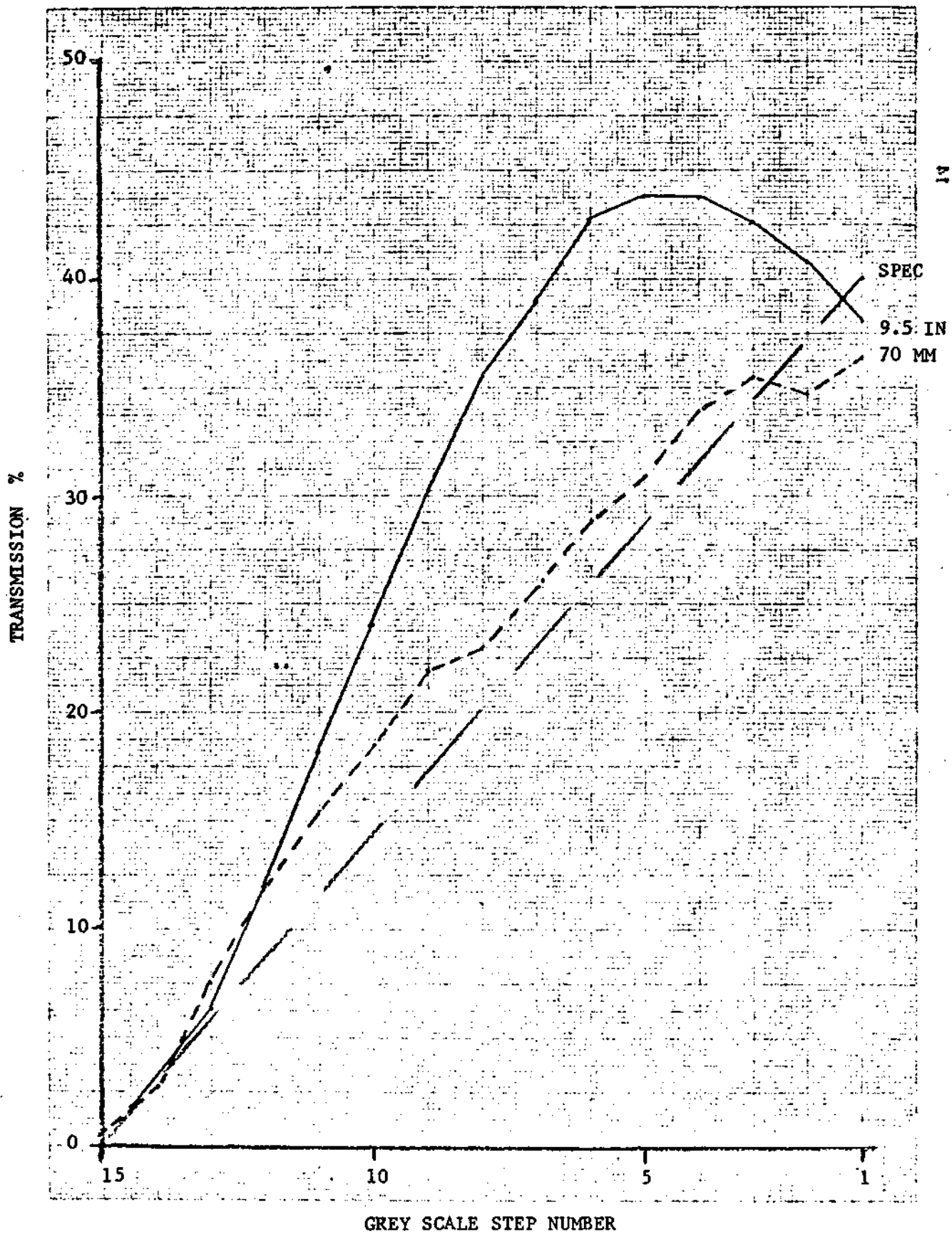




FIGURE 3  
PHOENIX RBV 1



# GENERAL ELECTRIC

ANALYSIS AND IMAGE DIVISION  
SPRINGFIELD

## PROGRAM INFORMATION REGIMENT/RELEASE

CLASS. LVL.	OPERATION	PROJECT	SEQ. NO.	REV. LVL.
U	1H05	ERTS	239	
*USE "C" FOR CLASSIFIED AND "U" FOR UNCLASSIFIED				

FROM D. Smith		TO Bruce T. Bachofer	
DATE SENT 9/29/72	DATE INFO. RECEIVED	PROJECT AND REG. NO.	REFERENCE DIR. NO.

### RBV MSS RELATIVE GEOMETRIC REGISTRATION MEASUREMENTS

#### SUMMARY

Scene corrected processing reduces relative geometric registration accuracy by approximately 57%. Eighteen arbitrarily selected ground points in both system and scene corrected RBV and MSS images of the same area were measured and compared as a check of present NDPF relative registration accuracy. The selected points in the system corrected images were located within 378 meters RMS of each other in the RBV and MSS images. A similar measurement using scene corrected images resulted in a 164 meter RMS difference. The pre-launch estimates for the measurement are 263 and 137 meters RMS respectively. The NDPF appears to be approaching this goal as additional refinements are introduced into the system.

#### PROCEDURE

Bulk (+) 70 mm film of Channel 3 RBV and Channel 3 MSS of the Spokane Washington area (E-1003-18150) taken on 26 July 1972 were observed on a MANN Comparator to measure relative registration at selected ground control points with an updated BIATS and with AMS data smoothing. The lower left registration marks were used as zero references and checked before and after the measurement set to within several microns. Eighteen features within the image were selected that met the criteria of being easy to locate precisely and also covered the entire image format.

The differences between the measured location in the RBV band 3 image and the MSS band 3 image were measured to a measurement accuracy of  $\pm 16$  meters. The readings were converted to ground distances (1 micron on 70 mm film equals 3.367 meters on the ground). Average static differences between the RBV and MSS measurements were removed (the MSS data points had mean translations of 74 meters west and 3670 meters south). The resultant vector registration error was 378 meters RMS. Figure 1 indicates the location and magnitude of the registration errors.

A similar set of measurements were made on MSS images produced using a slightly modified mirror velocity profile, but the resultant ground point location shifts were quite small with an average of only 6.5 microns in E-W and 4.7 microns N-S.

C-15

Distribution: VFSC: B. Bachofer  
GSFC: L. Gonzales W. Guard  
J. Sos S. Schramm  
J. Grebowsky T. Rooney  
P. Fishman  
GE-Bldg. 23: Phucas  
S. Portner C. Cahill B. Hookes

Scene corrected images of the same frames processed on 24 September were measured also. To make the measurements on the MANN Comparator, it was necessary to set up four sets of reference axis (one for each quadrant) using the inside edge of the black outline border and a reference tic mark. Measurement accuracy was about the same as with the 70 mm film,  $\pm 16$  meters. The readings were converted to ground distances (1 micron on 9.5 inch film equals 1.000 meter on the ground). Average static differences between the RBV and MSS measurements were removed (the MSS data points had mean translations of 17 meters east and 52 meters north). The resultant vector registration error was 164 meters RMS. Figure 2 indicates the location and magnitude of the registration errors.

VECTOR = (MSS BAND 3 - RBV BAND 3) - OFFSET

OFFSET = 3670 METERS MSS  
22 METERS RBV

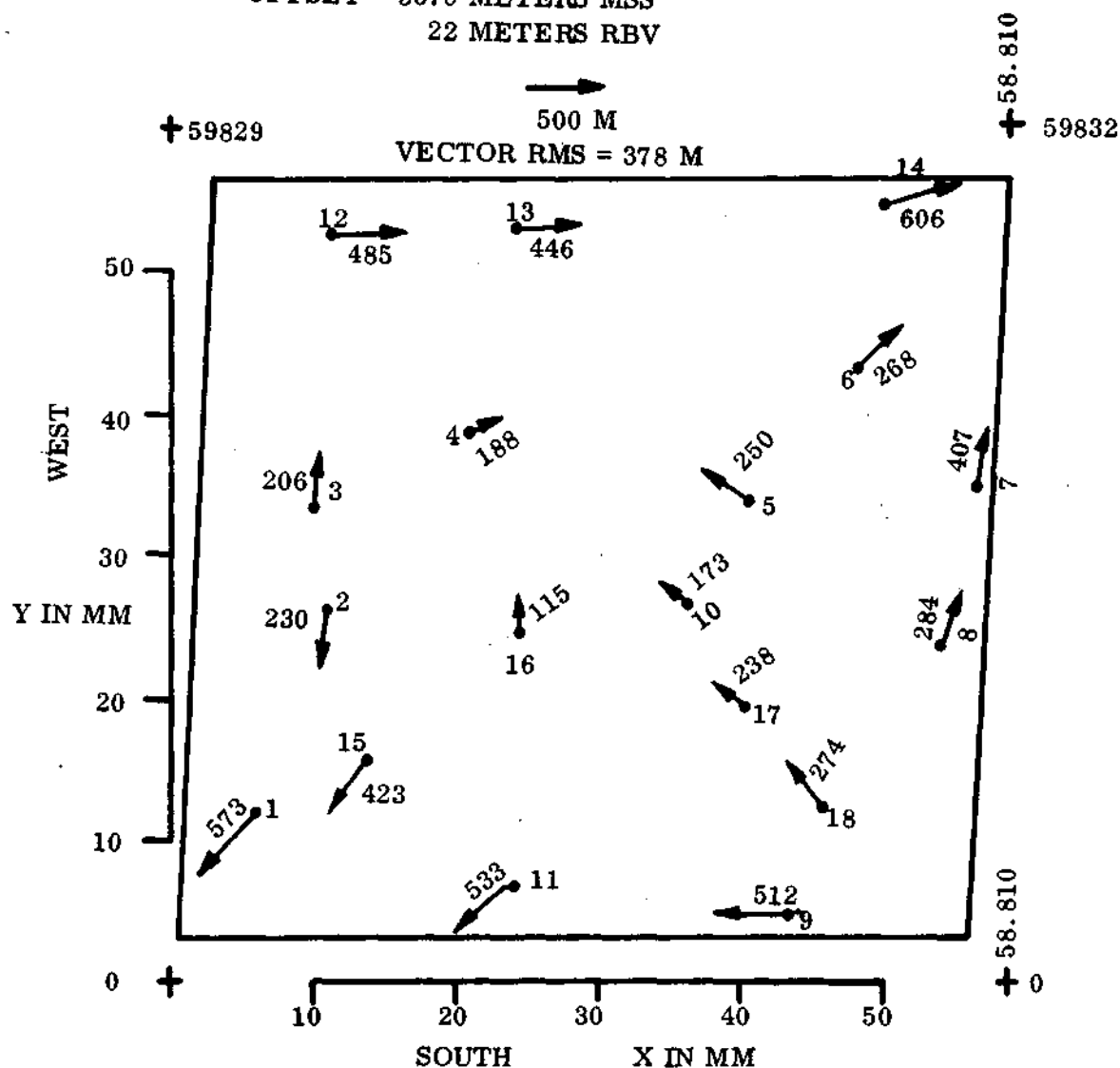


Figure 1. Measured on +70 MM Sys. Corr. of Spokane, Wash.  
E-1003-12150 Taken on 26 July '72

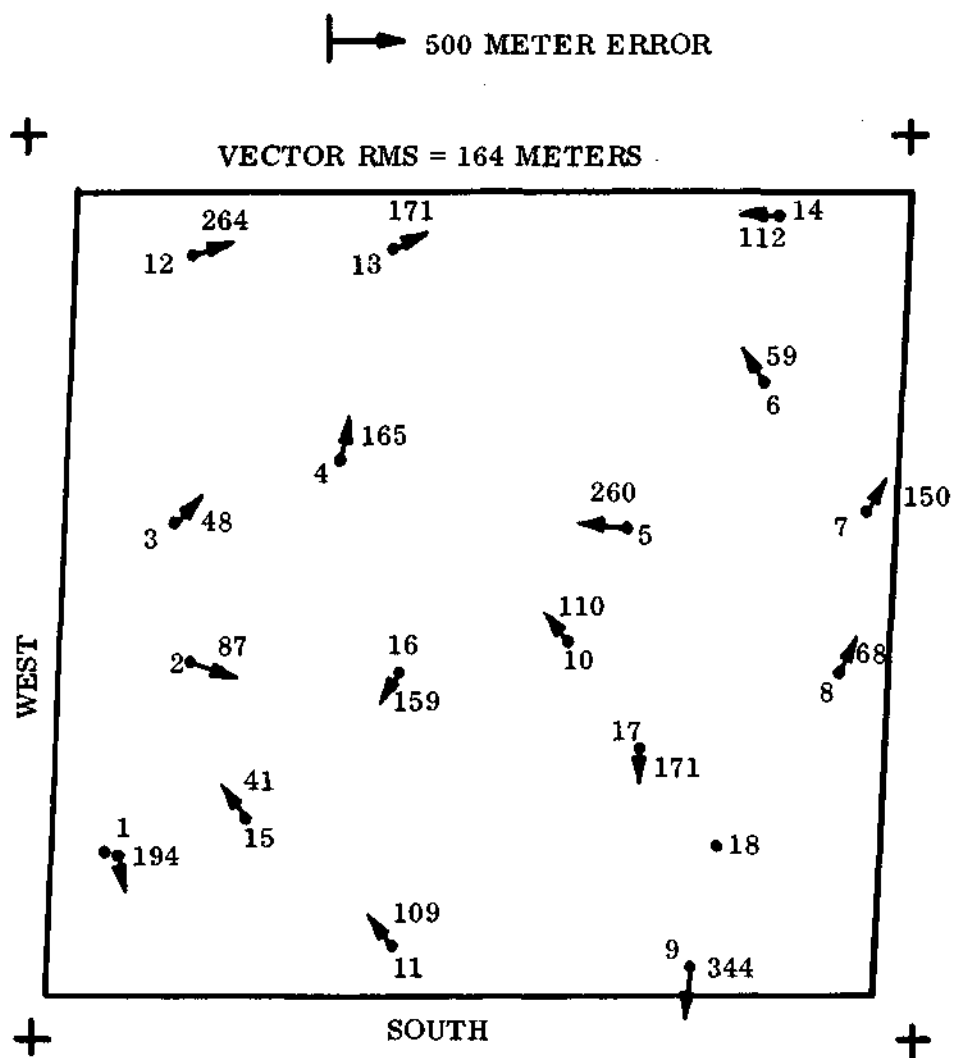


Figure 2. +9.5 In Scene Generated MSS-RBV Mapping Differences

OCT 17 1972

CLASS. LTR.	OPERATION	PROGRAM	SEQUENCE NO.	REV. LTR.
U	1H05	ERTS	240	

PROGRAM INFORMATION REQUEST/RELEASE

USE "C" FOR CLASSIFIED AND "U" FOR UNCLASSIFIED

FROM	TO
W. Guard/S. Schramm ERTS Systems Engineering	Distribution
DATE SENT	DATE INFO. REQUIRED
10/12/72	
PROJECT AND REQ. NO.	REFERENCE DIR. NO.
2A00- 2030	

SUBJECT

ASSESSMENT OF RESOLUTION IN ERTS IMAGERY

INFORMATION REQUESTED/RELEASED

INTRODUCTION

A preliminary investigation utilizing available imagery was undertaken to arrive at some quantitative measure of actual ERTS system resolution. Resolution is related to the ability of an observer to detect and identify fine details in the final imagery. Scenes of several metropolitan areas were visually analyzed with the aid of ground truth data (i.e., small scale maps and aerial photography), to determine the detectability of small objects. Although the scene derived data are necessarily sketchy, they do demonstrate a close agreement with expected performance.

Figures 1 and 2 summarize the trend of measured data toward analytically derived curves of predicted tri-bar resolution as a limit.

PROCEDURE/RESULTS

Of all the available imagery scenes containing large cities provided the best data for resolution assessment because of the abundance of man-made features having physical size near the resolution limit of the ERTS sensors. Natural land formations, agricultural patterns, etc., were clearly visible but were in general too large for resolution assessment purposes. Data from images of Boston, Monterey, Dallas, Spokane, Marseilles, France, and New York City, were used in the study.

Tables 1 and 2 contain a listing, for the RBV and MSS respectively, of all the targets visually analyzed. Accurate target dimensions (W-smallest dimension, L-largest dimension) were determined from ERTS imagery and verified whenever possible by using 1:100,000 street maps and 1:100,000 aerial photography. Target contrast (C) was based on subjective estimates made by the data evaluators. A dash in the table means that the target was known to be there but not resolvable in that particular band. A blank in any column signifies that no data was taken for that case. The data contained in the 3 sections of the table were derived from 70+3, 9.5+3, and 9.5+5 products (from top to bottom).

Figures 1 and 2 provide comparison between analytical predictions of system resolution (tribar) and actually observed resolution for RBV band 2 and MSS band 5, respectively. The solid curves of resolution as a function of contrast for high and low mean radiances were generated by the system resolution models (Ref. 1 and 2), which incorporated latest MTF and noise test data from pre-launch checkout activities. Agreement between predicted and measured tri-bar resolution was established during system performance tests (Ref. 3). The significance of Figures 1 and 2 lies in the agreement between real scene data and expected performance. Note how the data points from tables 1 and 2 tend toward the tri-bar curves as a limit. An X signifies a detectable target of a given size and contrast, while an O means the target was

C-19

PAGE NO.	ATTENTION REQUIREMENTS	
1	COPIES FOR	MASTERS FOR
	<input type="checkbox"/> 1 MO.	<input type="checkbox"/> 1 MO.
	<input type="checkbox"/> 2 MO.	<input type="checkbox"/> 2 MO.
	<input type="checkbox"/> 3 MO.	<input type="checkbox"/> 3 MO.
	<input type="checkbox"/> 4 MO.	<input type="checkbox"/> 4 MO.
	<input type="checkbox"/> 5 MO.	<input type="checkbox"/> 5 MO.
	<input type="checkbox"/> 6 MO.	<input type="checkbox"/> 6 MO.
	<input type="checkbox"/> 7 MO.	<input type="checkbox"/> 7 MO.
	<input type="checkbox"/> 8 MO.	<input type="checkbox"/> 8 MO.
	<input type="checkbox"/> 9 MO.	<input type="checkbox"/> 9 MO.
	<input type="checkbox"/> 10 MO.	<input type="checkbox"/> 10 MO.

known to be present from ground truth, but it was not resolvable.

The best verification of predicted tribar resolution is provided by four sets of three piers each in Boston harbor. The pier structures simulated a tribar quite well in that they appeared as three bright rectangular bars (length to width ratio of about 3:1) of approximately equal width separated by 2 dark bars (water) of about the same width.

Of the four pier sets chosen, two had an average pier and water spacing width of 50 meters (data point 1), one of 80 meters (data point 2), and one of 90 meters (point 3). For the sake of clarification, it should be noted that a pier and water spacing width of 50 meters corresponds to tribar resolution of 100 meters per line pair. These measurements were verified with ground truth data. As predicted by the resolution model, the 80 and 90 meter piers were resolvable in bands 2 and 5, while the 50 meters piers were not. From this it is concluded that for medium contrast targets, the actual observed tribar resolution is slightly better than 80 meters.

Figure 3 is a map of the Boston area at 1:100,000 scale showing the various pier structures present in the harbor. MSS images of Marseilles, France showed similar pier structures in the harbor (see Figure 4, 1:100,000 map). These piers, which represent 100 meters resolution, reinforce the results obtained with the Boston piers.

Attachment 1 (which is not contained in all copies of this PIR, due to costs of reproduction) contains an aerial photograph of the Boston harbor area and an enlargement of similar portions of the 70+3 MSS images taken of the Boston area (orbit 68, 28 July 1972). The scale in all cases is about 1:100,000. The specific pier structures of interest are clearly visible in the aerial photo. In MSS bands 7, 6, and 5, the 80 and 90 meter piers are easily resolved while the 50 meter piers are not. In band 4, the 80 and 90 meter piers are not resolved due to the significant reduction in scene contrast caused by atmospheric haze.

It is interesting to note that the 80 meters piers are not resolved in band 5 when viewing the 70+3 product through either a 40x microscope or a 12x comparator. In the photographic process used to enlarge and copy the harbor area to produce attachment 1, an enhancement in contrast occurred which allowed the 80 meter bars to be resolved.

#### CONCLUSIONS/RECOMMENDATIONS

Observed system resolution appears to agree well with predicted performance.

Some improvement in resolving fine detail can be achieved by photographic processing (i.e., contrast enhancement).

Cross track resolution for the MSS appears to be better than along track, since pier structures broke up where they were parallel to scan lines. Also, it should be noted that no difference in resolution was observed between RBV and MSS data.

Further image evaluation should be performed to more accurately quantify system resolution as a function of ground scene characteristics such as contrast and mean radiance.

#### REFERENCES

1. ERTS Data Users Handbook, Appendix F, System Performance, Revised 18 July 1972.
2. ERTS System Performance Document, February 11, 1972
3. PIR 1H05-ERTS-232, Results of SPT-1, RBV System Resolving Power, S. Schramm, 3 Aug. '72

TABLE 1

Scene/Target	RBV BAND								
	C	$\frac{1}{W}$	L	C	$\frac{2}{W}$	L	C	$\frac{3}{W}$	L
Boston/Piers (50m)	-	-	-	-	-	-	-	-	-
Boston/Piers	-	-	-	Med	80	240	Med	80	240
Boston/Piers	-	-	-	Med	90	337	Med	90	337
Boston/Chelsea River Bridge				Med	168	1347			
Boston/Island				Med	337	1010			
Dallas/New Dam				Hi	337	3030			
Dallas/Highway				Hi	337	16090			
<hr/>									
Monterey/Airport	Med	150	2200	Med	150	2400	Lo	200	2200
<hr/>									
Spokane/Airport	Lo	200	2800	Lo	150	2500	-	-	-
Spokane/3 Fields	-	-	-	Lo	200	800	-	-	-

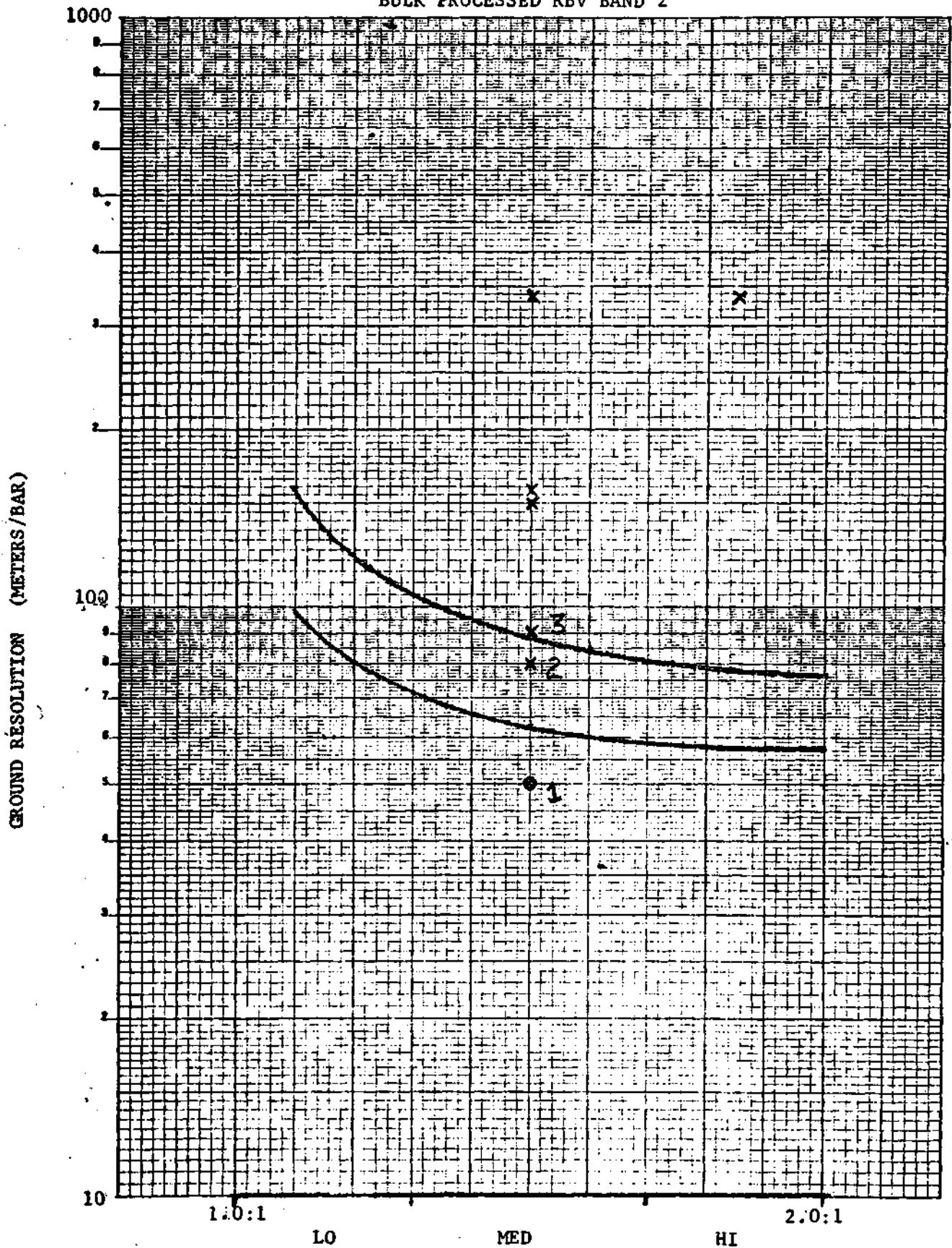


TABLE 2

Scene/Target	MSS BAND											
	C	$\frac{4}{W}$	L	C	$\frac{5}{W}$	L	C	$\frac{6}{W}$	L	C	$\frac{7}{W}$	L
NYC/Air Field	Med	471	3872	Med	505	4040	-	-	-	Lo	337	3704
NYC/Central Park	Lo	875	4040	Lo	842	3872	Med	808	4040	Med	842	4141
NYC/C.P. Lake	-	-	-	Med	673	842	Hi	673	842	Hi	673	842
NYC/Peninsula	Med	269	1683	Hi	337	1683	Hi	337	1683	Hi	337	1683
NYC/Verrazano Narrows Bridge	Lo	168	1683	Med	168	1683	Hi	168	1515	Hi	168	1548
NYC/Laguardia Runway	Lo	337	-	Lo	337	-	Lo	337	-	Lo	337	-
Boston/Piers (50m)	-	-	-	-	-	-	-	-	-	-	-	-
Boston/Piers	-	-	-	Med	80	240	Med	80	240	Hi	80	240
Boston/Piers	-	-	-	Med	90	337	Med	90	337	Hi	90	337
Boston/Chelsea River Bridge				Med	168	1347						
Boston/Island				Med	337	842						
Marseille/Piers	-	-	-				Hi	100	200	Hi	100	200
Monterey/Airport	Med	150	2500	Med	150	2400	-	-	-	-	-	-
Monterey/3 Fields	Lo	200	750	Med	150	750	-	-	-	Lo	250	800
Spokane/Airport	Lo	130	3000	Lo	130	2100	Lo	180	2500	-	-	-
Spokane/3 Fields	Med	180	750	Hi	180	800	-	-	-	Lo	200	850

FIGURE 1

BULK PROCESSED RBV BAND 2



SPACE CONTRAST

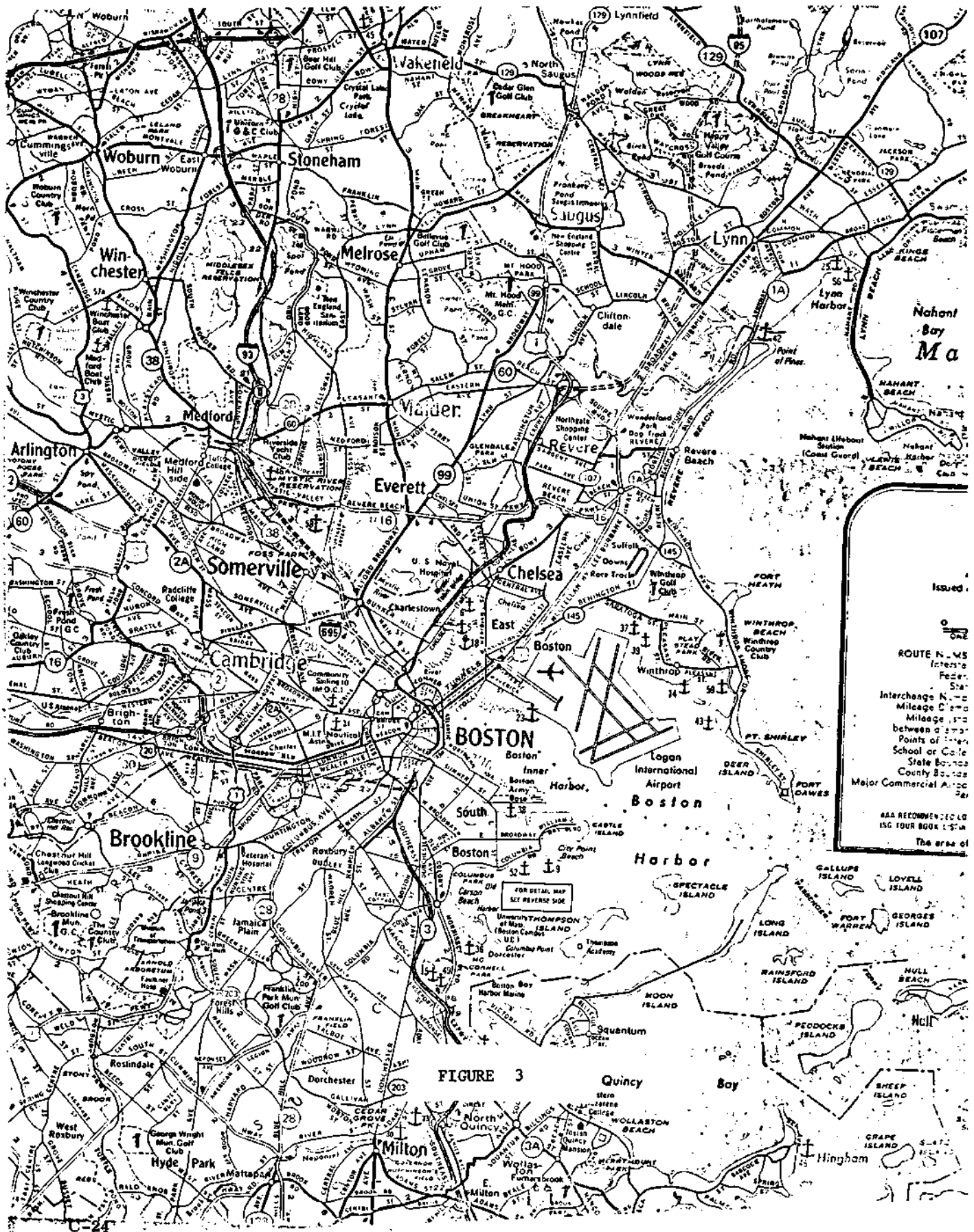
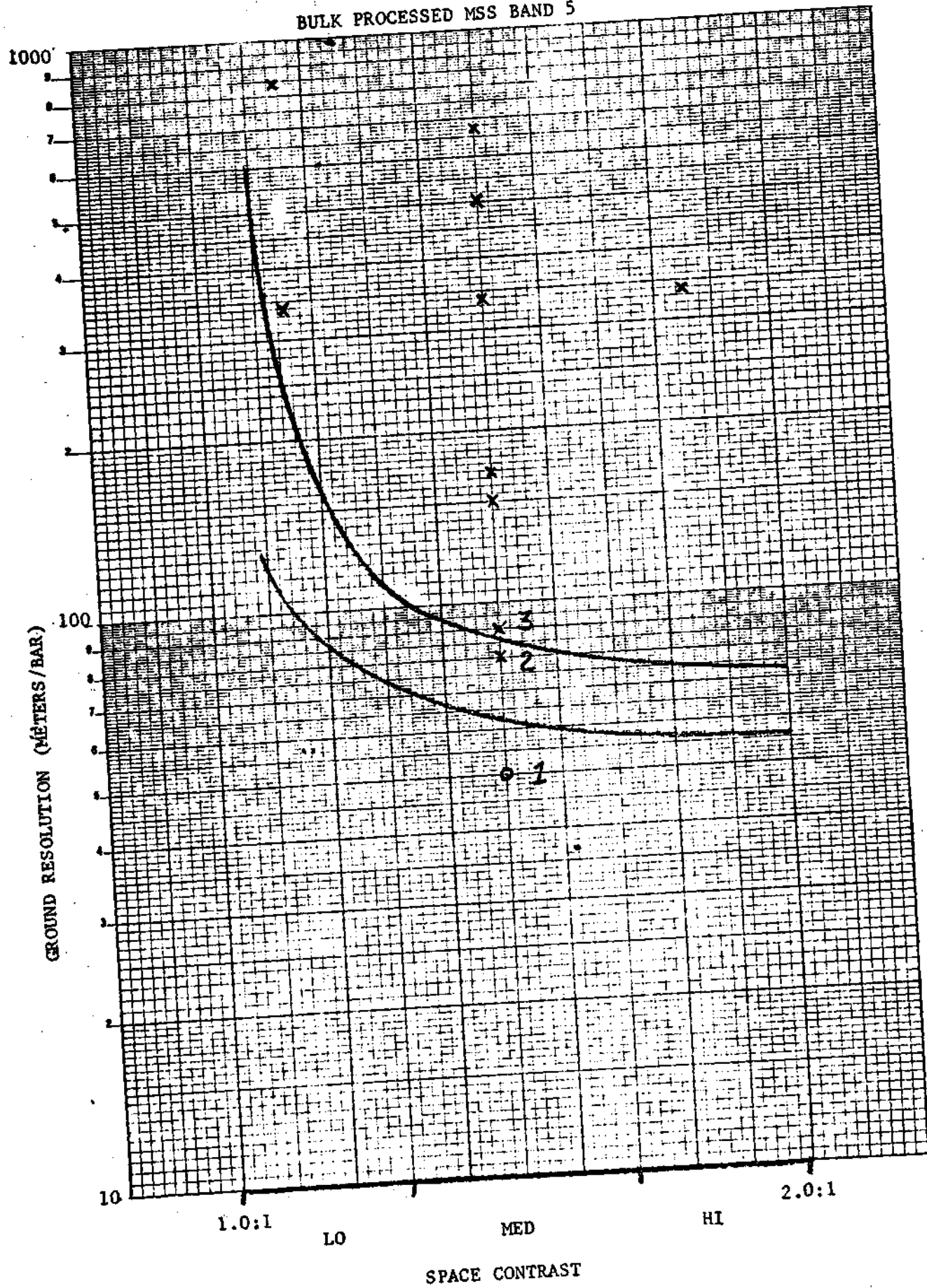


FIGURE 2

BULK PROCESSED MSS BAND 5





**APPENDIX D**  
**ERTS-1 GROUND TRACE REPEAT CYCLE**  
**PREDICTIONS TABLE**

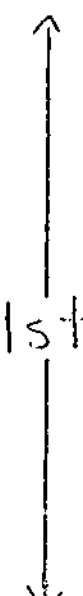

*D-1*

JULY 1972

Date	GMT Day	Flight Day	Spacecraft Orbit	Reference Orbit	Ref Day	Cycle
23	205	0	0-3	150-153	11	0th
24	206	1	4-17	154-167	12	
25	207	2	18-31	168-181	13	
26	208	3	32-45	168-181*	13	
27	209	4	46-59	182-195	14	
28	210	5	60-73	196-209	15	
29	211	6	74-87	210-223	16	
30	212	7	88-101	224-237	17	
31	213	8	102-115	238-251	18	

\*Shift due to initial orbit (prior to orbit adjustments)

AUGUST 1972

DATE	GMT DAY	FLIGHT DAY	SPACECRAFT ORBITS	REFERENCE ORBITS	REF DAY	CYCLE
1	214	9	116-129	1-14	1	
2	215	10	130-143	15-28	2	
3	216	11	144-157	29-42	3	
4	217	12	158-171	43-56	4	
5	218	13	172-185	57-70	5	
6	219	14	186-199	71-84	6	
7	220	15	200-213	85-98	7	
8	221	16	214-226	99-111	8	
9	222	17	227-240	112-125	9	
10	223	18	241-254	126-139	10	
11	224	19	255-268	140-153	11	
12	225	20	269-282	154-167	12	
13	226	21	283-296	168-181	13	
14	227	22	297-310	182-195	14	
15	228	23	311-324	196-209	15	
16	229	24	325-338	210-223	16	
17	230	25	339-352	224-237	17	
18	231	26	353-366	238-251	18	
19	232	27	367-380	1-14	1	
20	233	28	381-394	15-28	2	
21	234	29	395-408	29-42	3	
22	235	30	409-422	43-56	4	
23	236	31	423-436	57-70	5	
24	237	32	437-450	71-84	6	
25	238	33	451-464	85-98	7	
26	239	34	465-478	99-111	8	
27	240	35	479-491	112-125	9	
28	241	36	492-505	126-139	10	
29	242	37	506-519	140-153	11	
30	243	38	520-533	154-167	12	
31	244	39	534-547	168-181	13	



SEPTEMBER 1972

DATE	GMT DAY	FLIGHT DAY	SPACECRAFT ORBITS	REFERENCE ORBITS	REF DAY	CYCLE
1	245	40	548-561	182-195	14	2nd ↓
2	246	41	562-575	196-209	15	
3	247	42	576-589	210-223	16	
4	248	43	590-603	224-237	17	
5	249	44	604-617	238-251	18	
6	250	45	618-631	1-14	1	
7	251	46	632-645	15-28	2	3rd ↑ ↓
8	252	47	646-659	29-42	3	
9	253	48	660-673	43-56	4	
10	254	49	674-687	57-70	5	
11	255	50	688-701	71-84	6	
12	256	51	702-715	85-98	7	
13	257	52	716-728	99-111	8	
14	258	53	729-742	112-125	9	
15	259	54	743-756	126-139	10	
16	260	55	757-770	140-153	11	
17	261	56	771-784	154-167	12	
18	262	57	785-798	168-181	13	
19	263	58	799-812	182-195	14	
20	264	59	813-826	196-209	15	
21	265	60	827-840	210-223	16	
22	266	61	841-854	224-237	17	
23	267	62	855-868	238-251	18	
24	268	63	869-882	1-14	1	4th ↑
25	269	64	883-896	15-28	2	
26	270	65	897-910	29-42	3	
27	271	66	911-924	43-56	4	
28	272	67	925-938	57-70	5	
29	273	68	939-952	71-84	6	
30	274	69	953-966	85-98	7	

OCTOBER 1972

DATE	GMT DAY	FLIGHT DAY	SPACECRAFT ORBITS	REFERENCE ORBITS	REF DAY	CYCLE
1	275	70	967-979	99-111	8	4+h ↓
2	276	71	980-993	112-125	9	
3	277	72	994-1007	126-139	10	
4	278	73	1008-1021	140-153	11	
5	279	74	1022-1035	154-167	12	
6	280	75	1036-1049	168-181	13	
7	281	76	1050-1063	182-195	14	
8	282	77	1064-1077	196-209	15	
9	283	78	1078-1091	210-223	16	
10	284	79	1092-1105	224-237	17	
11	285	80	1106-1119	238-251	18	↑ 5+h ↓
12	286	81	1120-1133	1-14	1	
13	287	82	1134-1147	15-28	2	
14	288	83	1148-1161	29-42	3	
15	289	84	1162-1175	43-56	4	
16	290	85	1176-1189	57-70	5	
17	291	86	1190-1203	71-84	6	
18	292	87	1204-1217	85-98	7	
19	293	88	1218-1230	99-111	8	
20	294	89	1231-1244	112-125	9	
21	295	90	1245-1258	126-139	10	↑ 6+h
22	296	91	1259-1272	140-153	11	
23	297	92	1273-1286	154-167	12	
24	298	93	1287-1300	168-181	13	
25	299	94	1301-1314	182-195	14	
26	300	95	1315-1328	196-209	15	
27	301	96	1329-1342	210-223	16	
28	302	97	1343-1356	224-237	17	
29	303	98	1357-1370	238-251	18	
30	304	99	1371-1384	1-14	1	
31	305	100	1385-1398	15-28	2	

NOVEMBER 1972

DATE	GMT DAY	FLIGHT DAY	SPACECRAFT ORBITS	REFERENCE ORBITS	REF DAY	CYCLE
1	306	101	1399-1412	29-42	3	6th ↓
2	307	102	1413-1426	43-56	4	
3	308	103	1427-1440	57-70	5	
4	309	104	1441-1454	71-84	6	
5	310	105	1455-1468	85-98	7	
6	311	106	1469-1481	99-111	8	
7	312	107	1482-1495	112-125	9	
8	313	108	1496-1509	126-139	10	
9	314	109	1510-1523	140-153	11	
10	315	110	1524-1537	154-167	12	
11	316	111	1538-1551	168-181	13	
12	317	112	1552-1565	182-195	14	
13	318	113	1566-1579	196-209	15	
14	319	114	1580-1593	210-223	16	
15	320	115	1594-1607	224-237	17	
16	321	116	1608-1621	238-251	18	
17	322	117	1622-1635	1-14	1	↑ 7th
18	323	118	1636-1649	15-28	2	
19	324	119	1650-1663	29-42	3	
20	325	120	1664-1677	43-56	4	
21	326	121	1678-1691	57-70	5	
22	327	122	1692-1705	71-84	6	
23	328	123	1706-1719	85-98	7	
24	329	124	1720-1732	99-111	8	
25	330	125	1733-1746	112-125	9	
26	331	126	1747-1760	126-139	10	
27	332	127	1761-1774	140-153	11	
28	333	128	1775-1788	154-167	12	
29	334	129	1789-1802	168-181	13	
30	335	130	1803-1816	182-195	14	

DECEMBER 1972

DATE	GMT DAY	FLIGHT DAY	SPACECRAFT ORBITS	REFERENCE ORBITS	REF DAY	CYCLE
1	336	131	1817-1830	196-209	15	7th ↓
2	337	132	1831-1844	210-223	16	
3	338	133	1845-1858	224-237	17	
4	339	134	1859-1872	238-251	18	8th ↑ ↓
5	340	135	1873-1886	1-14	1	
6	341	136	1887-1900	15-28	2	
7	342	137	1901-1914	29-42	3	
8	343	138	1915-1928	43-56	4	
9	344	139	1929-1942	57-70	5	
10	345	140	1943-1956	71-84	6	
11	346	141	1957-1970	85-98	7	
12	347	142	1971-1983	99-111	8	
13	348	143	1984-1997	112-125	9	
14	349	144	1998-2011	126-139	10	
15	350	145	2012-2025	140-153	11	
16	351	146	2026-2039	154-167	12	
17	352	147	2040-2053	168-181	13	
18	353	148	2054-2067	182-195	14	
19	354	149	2068-2081	196-209	15	
20	355	150	2082-2095	210-223	16	
21	356	151	2096-2109	224-237	17	
22	357	152	2110-2123	238-251	18	9th ↑
23	358	153	2124-2137	1-14	1	
24	359	154	2138-2151	15-28	2	
25	360	155	2152-2165	29-42	3	
26	361	156	2166-2179	43-56	4	
27	362	157	2180-2193	57-70	5	
28	363	158	2194-2207	71-84	6	
29	364	159	2208-2221	85-98	7	
30	365	160	2222-2234	99-111	8	
31	366	161	2235-2248	112-125	9	

JANUARY 1973

DATE	GMT DAY	FLIGHT DAY	SPACECRAFT ORBITS	REFERENCE ORBITS	REF DAY	CYCLE
1	1	162	2249-2262	126-139	10	9th ↓
2	2	163	2263-2276	140-153	11	
3	3	164	2277-2290	154-167	12	
4	4	165	2291-2304	168-181	13	
5	5	166	2305-2318	182-195	14	
6	6	167	2319-2332	196-209	15	
7	7	168	2333-2346	210-223	16	
8	8	169	2347-2360	224-237	17	
9	9	170	2361-2374	238-251	18	
10	10	171	2375-2388	1-14	1	↑ 10th ↓
11	11	172	2389-2402	15-28	2	
12	12	173	2403-2416	29-42	3	
13	13	174	2417-2430	43-56	4	
14	14	175	2431-2444	57-70	5	
15	15	176	2445-2458	71-84	6	
16	16	177	2459-2472	85-98	7	
17	17	178	2473-2485	99-111	8	
18	18	179	2486-2499	112-125	9	
19	19	180	2500-2513	126-139	10	
20	20	181	2514-2527	140-153	11	
21	21	182	2528-2541	154-167	12	
22	22	183	2542-2555	168-181	13	
23	23	184	2556-2569	182-195	14	
24	24	185	2570-2583	196-209	15	
25	25	186	2584-2597	210-223	16	
26	26	187	2598-2611	224-237	17	
27	27	188	2612-2625	238-251	18	
28	28	189	2626-2639	1-14	1	↑ 11th
29	29	190	2640-2653	15-28	2	
30	30	191	2654-2667	29-42	3	
31	31	192	2668-2681	43-56	4	

FEBRUARY 1973

DATE	GMT DAY	FLIGHT DAY	SPACECRAFT ORBITS	REFERENCE ORBITS	REF DAY	CYCLE
1	32	193	2682-2695	57-70	5	11th ↓
2	33	194	2696-2709	71-84	6	
3	34	195	271-2723	85-98	7	
4	35	196	2724-2736	99-111	8	
5	36	197	2737-2750	112-125	9	
6	37	198	2751-2764	126-139	10	
7	38	199	2765-2778	140-153	11	
8	39	200	2779-2792	154-167	12	
9	40	201	2793-2806	168-181	13	
10	41	202	2807-2820	182-195	14	
11	42	203	2821-2834	196-209	15	
12	43	204	2835-2848	210-223	16	
13	44	205	2849-2862	224-237	17	
14	45	206	2863-2876	238-251	18	
15	46	207	2877-2890	1-14	1	
16	47	208	2891-2904	15-28	2	
17	48	209	2905-2918	29-42	3	
18	49	210	2919-2932	43-56	4	
19	50	211	2933-2946	57-70	5	↑ 12th
20	51	212	2947-2960	71-84	6	
21	52	213	2961-2974	85-98	7	
22	53	214	2975-2987	99-111	8	
23	54	215	2988-3001	112-125	9	
24	55	216	3002-3015	126-139	10	
25	56	217	3016-3029	140-153	11	
26	57	218	3030-3043	154-167	12	
27	58	219	3044-3057	168-181	13	
28	59	220	3058-3071	182-195	14	

MARCH 1973

DATE	GMT DAY	FLIGHT DAY	SPACECRAFT ORBITS	REFERENCE ORBITS	REF DAY	CYCLE
1	60	221	3072-3085	196-209	15	12th
2	61	222	3086-3099	210-223	16	↓
3	62	223	3100-3113	224-237	17	
4	63	224	3114-3127	238-251	18	
5	64	225	3128-3141	1-14	1	↑
6	65	226	3142-3155	15-28	2	
7	66	227	3156-3169	29-42	3	
8	67	228	3170-3183	43-56	4	
9	68	229	3184-3197	57-70	5	
10	69	230	3198-3211	71-84	6	
11	70	231	3212-3225	85-98	7	
12	71	232	3226-3238	99-111	8	
13	72	233	3239-3252	112-125	9	
14	73	234	3253-3266	126-139	10	13th
15	74	235	3267-3280	140-153	11	↓
16	75	236	3281-3294	154-167	12	
17	76	237	3295-3308	168-181	13	
18	77	238	3309-3322	182-195	14	
19	78	239	3323-3336	196-209	15	
20	79	240	3337-3350	210-223	16	
21	80	241	3351-3364	224-237	17	
22	81	242	3365-3378	238-251	18	↓
23	82	243	3379-3392	1-14	1	
24	83	244	3393-3406	15-28	2	↑
25	84	245	3407-3420	29-42	3	
26	85	246	3421-3434	43-56	4	
27	86	247	3435-3448	57-70	5	
28	87	248	3449-3462	71-84	6	
29	88	249	3463-3476	85-98	7	
30	89	250	3477-3489	99-111	8	
31	90	251	3490-3503	112-125	9	14th

APRIL 1973

DATE	GMT DAY	FLIGHT DAY	SPACECRAFT ORBITS	REFERENCE ORBITS	REF DAY	CYCLE
1	91	252	3504-3517	126-139	10	14th ↓
2	92	253	3518-3531	140-153	11	
3	93	254	3532-3545	154-167	12	
4	94	255	3546-3559	168-181	13	
5	95	256	3560-3573	182-195	14	
6	96	257	3574-3587	196-209	15	
7	97	258	3588-3601	210-223	16	
8	98	259	3602-3615	224-237	17	
9	99	260	3616-3629	238-251	18	
10	100	261	3630-3643	1-14	1	15th ↑ ↓
11	101	262	3644-3657	15-28	2	
12	102	263	3658-3671	29-42	3	
13	103	264	3672-3685	43-56	4	
14	104	265	3686-3699	57-70	5	
15	105	266	3700-3713	71-84	6	
16	106	267	3714-3727	85-98	7	
17	107	268	3728-3740	99-111	8	
18	108	269	3741-3754	112-125	9	
19	109	270	3755-3768	126-139	10	
20	110	271	3769-3782	140-153	11	
21	111	272	3783-3796	154-167	12	
22	112	273	3797-3810	168-181	13	
23	113	274	3811-3824	182-195	14	
24	114	275	3825-3838	196-209	15	
25	115	276	3839-3852	210-223	16	
26	116	277	3853-3866	224-237	17	
27	117	278	3867-3880	238-251	18	
28	118	279	3881-3894	1-14	1	16th ↑
29	119	280	3895-3908	15-28	2	
30	120	281	3909-3922	29-42	3	



MAY 1973

DATE	GMT DAY	FLIGHT DAY	SPACECRAFT ORBITS	REFERENCE ORBITS	REF DAY	CYCLE
1	121	282	3923-3936	43-56	4	16th ↓
2	122	283	3937-3950	57-70	5	
3	123	284	3951-3964	71-84	6	
4	124	285	3965-3978	85-98	7	
5	125	286	3979-3991	99-111	8	
6	126	287	3992-4005	112-125	9	
7	127	288	4006-4019	126-139	10	
8	128	289	4020-4033	140-153	11	
9	129	290	4034-4047	154-167	12	
10	130	291	4048-4061	168-181	13	
11	131	292	4062-4075	182-195	14	
12	132	293	4076-4089	196-209	15	
13	133	294	4090-4103	210-223	16	
14	134	295	4104-4117	224-237	17	
15	135	296	4118-4131	238-251	18	
16	136	297	4132-4145	1-14	1	
17	137	298	4146-4159	15-28	2	
18	138	299	4160-4173	29-42	3	
19	139	300	4174-4187	43-56	4	↑ 17th
20	140	301	4188-4201	57-70	5	
21	141	302	4202-4215	71-84	6	
22	142	303	4216-4229	85-98	7	
23	143	304	4230-4242	99-111	8	
24	144	305	4243-4256	112-125	9	
25	145	306	4257-4270	126-139	10	
26	146	307	4271-4284	140-153	11	
27	147	308	4285-4298	154-167	12	
28	148	309	4299-4312	168-181	13	
29	149	310	4313-4326	182-195	14	
30	150	311	4327-4340	196-209	15	
31	151	312	4341-4354	210-223	16	

JUNE 1973

DATE	GMT DAY	FLIGHT DAY	SPACECRAFT ORBITS	REFERENCE ORBITS	REF DAY	CYCLE
1	152	313	4355-4368	224-237	17	17+h ↓
2	153	314	4369-4382	238-251	18	
3	154	315	4383-4396	1-14	1	↑
4	155	316	4397-4410	15-28	2	
5	156	317	4411-4424	29-42	3	
6	157	318	4425-4438	43-56	4	
7	158	319	4439-4452	57-70	5	
8	159	320	4453-4466	71-84	6	
9	160	321	4467-4480	85-98	7	
10	161	322	4481-4493	99-111	8	
11	162	323	4494-4507	112-125	9	18+h
12	163	324	4508-4521	126-139	10	
13	164	325	4522-4535	140-153	11	
14	165	326	4536-4549	154-167	12	
15	166	327	4550-4563	168-181	13	
16	167	328	4564-4577	182-195	14	
17	168	329	4578-4591	196-209	15	
18	169	330	4592-4605	210-223	16	
19	170	331	4606-4619	224-237	17	
20	171	332	4620-4633	238-251	18	↓
21	172	333	4634-4647	1-14	1	
22	173	334	4648-4661	15-28	2	↑
23	174	335	4662-4675	29-42	3	
24	175	336	4676-4689	43-56	4	
25	176	337	4690-4703	57-70	5	
26	177	338	4704-4717	71-84	6	
27	178	339	4718-4731	85-98	7	
28	179	340	4732-4744	99-111	8	
29	180	341	4745-4758	112-125	9	
30	181	342	4759-4772	126-139	10	19+h

JULY 1973

DATE	GMT DAY	FLIGHT DAY	SPACECRAFT ORBITS	REFERENCE ORBITS	REF DAY	CYCLE
1	182	343	4773-4786	140-153	11	19+h ↓
2	183	344	4787-4800	154-167	12	
3	184	345	4801-4814	168-181	13	
4	185	346	4815-4828	182-195	14	
5	186	347	4829-4842	196-209	15	
6	187	348	4843-4856	210-223	16	
7	188	349	4857-4870	224-237	17	
8	189	350	4871-4884	238-251	18	
9	190	351	4885-4898	1-14	1	
10	191	352	4899-4912	15-28	2	↑ 20+h ↓
11	192	353	4913-4926	29-42	3	
12	193	354	4927-4940	43-56	4	
13	194	355	4941-4954	57-70	5	
14	195	356	4955-4968	71-84	6	
15	196	357	4969-4982	85-98	7	
16	197	358	4983-4995	99-111	8	
17	198	359	4996-5009	112-125	9	
18	199	360	5010-5023	126-139	10	
19	200	361	5024-5037	140-153	11	
20	201	362	5038-5051	154-167	12	
21	202	363	5052-5065	168-181	13	
22	203	364	5066-5079	182-195	14	
23	204	365	5080-5093	196-209	15	
24	205	366	5094-5107	210-223	16	
25	206	367	5108-5121	224-237	17	
26	207	368	5122-5135	238-251	18	